ARSENIC SPECIATION BY HIGH PERFORMANCE LIQUID CHROMATOGRAPHY INDUCTIVELY COUPLED PLASMA MASS SPECTROMETRY AND CAPILLARY ELECTROPHORESIS INDUCTIVELY COUPLED PLASMA MASS SPECTROMETRY

By

RUIXUE CHEN

A DISSERTATION PRESENTED TO THE GRADUATE SCHOOL OF THE
UNIVERSITY OF FLORIDA IN PARTIAL FULFILLMENT OF THE
REQUIREMENTS FOR THE DEGREE OF
DOCTOR OF PHILOSOPHY

UNIVERSITY OF FLORIDA

2003

This dissertation is dedicated to my parents, Yongzheng Chen and Zhiying Wang, my husband, Chenglong Yang, and my son, Edward B. Yang.

ACKNOWLEDGMENTS

Many individuals have contributed to the work in this dissertation. First, I would like to thank and respect my advisor, Dr. James D. Winefordner, for his full supervision and continuous support on my research. It is a wonderful experience to work in Dr. Winefordner's research group: He provided me with new insights and new ways to look at a problem. I would also like to thank Dr. Benjamin W. Smith for his competent scientific suggestions, productive discussion and extensive knowledge in my daily research as well as his great encouragement on multiple research projects.

I would also like to take the opportunity to thank all the members in Dr. Winefordner's research group for their discussion and friendship during my study here. Special thank go to Paige Eagan for her help. I would also like to thank Dr. Willard W. Harrison and all the members in Dr. Harrison's research group for their helpful discussions. I express my appreciation to Steve Miles and Larry Hartley in the electronic shop for their support with ICP-MS; to Dr. David Powell for his help with capillary electrophoresis; to Dr. Kathryn Williams and Dr. Oleg Matveev for their help with high performance liquid chromatography. I would also like to thank Dr. Lena Ma, Dr. Mike S. Tu and Gina Kertulis, who have been involved in part of this research, for their support and helpful discussion.

I am grateful for the chemistry teaching award, its support and encouragement are far beyond the financial meaning itself.

A special word of gratitude goes to my family. Many many thanks go to my parents for their everlasting love and continuous encouragement in my whole life. Their selfless support helped me get through all of the difficulties and made me happy all the time.

I owe special thanks to my husband for his constant love, boundless support and encouragement in my life. His insightful suggestions and helpful discussions contribute a lot to my graduate research. I honor all three of you with this dissertation.

TABLE OF CONTENTS

ACKNOWLEDGEMENTS iii

ABSTRACT viii

CHAPTERS

1 INTRODUCTION 1

The Goal of the Research 1
Overview of the Research 3

2 BACKGROUND 5

Inductively Coupled Plasma Mass spectrometry (ICP-MS) 5
The Principle of ICP-MS Technique 5
Sample Introduction System 7
Inductively Coupled Plasma 13
ICP-MS Sampling Interface and Ion Focusing System 14
Mass Analyzer 15
Detector and Data Acquisition 16
Capillary Electrophoresis (CE) 17
High Performance Liquid Chromatography (HPLC) 22

3 ELEMENTAL SPECIATION AND ARSENIC OVERVIEW 27

Elemental Speciation 27
Arsenic Overview 28
Chemical and Physical Property of Arsenic 28
Arsenic Toxicity and Health Effects 29
Arsenic Occurrence 32

4 EXPERIMENTAL 34

Chemicals and Reagents 34
Instrumentation 36
Capillary Electrophoresis (CE) 36
High Performance Liquid Chromatography (HPLC) 37
Inductively Coupled Plasma mass Spectrometry (ICP-MS) 37
Analytical Procedures 39

        CE-ICP-MS 39
        HPLC-ICP-MS 40

5 CE-ICP-MS INSTRUMENT DESIGN 43

    Capillary Electrophoresis Inductively Coupled Plasma Mass Spectrometry (CE-ICP-MS) Overview 43
    Concentric Nebulizer Design 46
        Modified Meinhard Concentric Nebulizer 46
        Optimum Capillary Tip Position 48
    CE-ICP-MS Interface Design 51
    CE-ICP-MS Instrument Setup 58
        CE Sampling Volume 58
        Laminar Flow Effect 62

6 ARSENIC SPECIATION BY CE-ICP-MS 66

    ICP-MS Parameters Selection 66
        Make Up Sheath Flow Rate 66
        Nebulizer Gas Flow Rate 68
        Ion Lens Settings 70
        Arsenic Detection Limit of VG PQII ICP-MS 73
    Sample Transport Efficiency Discussion 73
        ICP-MS Efficiency Discussion 73
        Different Data Acquisition Mode Efficiency Comparison 79
        ICP-MS and CE-ICP-MS Efficiency Comparison 79
    CE Parameters Selection 83
        CE Capillary Length and Size, High Voltage, Buffer Concentration and pH Selection 83
        Analyte Transport Efficiency in CE 85
    Determination of Selenium Compounds by CE-ICP-MS 85
    Determination of Arsenic Compounds by CE-ICP-MS 90
    Conclusion 97

7 HPLC-ICP-MS INSTRUMENT SETUP 98

    High Performance Liquid Chromatography Inductively Coupled Plasma Mass Spectrometry (HPLC-ICP-MS) Overview 98
    HPLC-ICP-MS Instrument Setup 105
    HPLC Parameter Optimization 105
        Elution Peak Identification 105
        Effect of Equilibrated Time and Ion Paring Reagent Concentration 109
        Effect of Methanol Concentration 112
        Effect of Phosphate Buffer Concentration 115
        Effect of Phosphate Buffer pH 117
        Effect of Mobile Phase Flow Rate 119

Gradient Elution 119
Spectroscopic Interference 121
New Column and Old Column Comparison 123
Characteristics of HPLC-ICP-MS Method 123

8 HPLC-ICP-MS APPLICATIONS 129

Human Urine 129
Natural Water Reference Material 134
Analysis of Arsenic Species in Chinese Brake Fern 136
Chinese Brake Fern Root Exudate 138
Chinese brake fern cultivation and root exudate collection 138
Chinese brake fern roots treated with different levels As(V) solutions 139
HPLC-ICP-MS and GFAAS method comparison 139
Chinese brake fern roots treated with 15 ppm As(III), DMA, MMA, or As(V) solutions 143
Chinese Brake Fern Xylem Sap 147
Chinese brake fern xylem sap collection 147
Chinese brake fern treated with 10 ppm or 50 ppm DMA or MMA solutions and xylem sap sample analysis 147

9 CONCLUSIONS AND FUTURE WORKS 152

Conclusions 152
Future Directions 153

APPENDIX 155

REFERENCES 157

BIOGRAPHICAL SKETCH 163

Abstract of Dissertation Presented to the Graduate School
of the University of Florida in Partial Fulfillment of the
Requirements for the Degree of Doctor of Philosophy

ARSENIC SPECIATION BY HIGH PERFORMANCE LIQUID CHROMATOGRAPHY INDUCTIVELY COUPLED PLASMA MASS SPECTROMETRY AND CAPILLARY ELECTROPHORESIS INDUCTIVELY COUPLED PLASMA MASS SPECTROMETRY

By

Ruixue Chen

May, 2003

Chairman: Prof. James D. Winefordner
Major Department: Chemistry

Arsenic contamination has been a global problem. Thousands of people suffer from chronic toxicity effects from the surrounding arsenic contaminated soil, ground water, and various foods. Identification and quantification of individual arsenic forms are important to appropriately measure the arsenic toxicity, environmental impact, and health risk related to arsenic exposure. Coupling either capillary electrophoresis (CE) or high performance liquid chromatography (HPLC) to inductively coupled plasma mass spectrometry (ICP-MS) is a powerful technique for trace elemental speciation analysis in various sample matrices. This hyphenated technique combines the high separation efficiency of CE and HPLC with the high elemental sensitivity and selectivity of ICP-MS. In addition, HPLC is more suitable to couple with ICP-MS due to the compatible liquid flow rate of HPLC.

A modified concentric Meinhard nebulizer and interface were developed and used for coupling CE with ICP-MS. This interface is inexpensive, easy to handle, and universally applicable. The parameters that influence both separation efficiency and the detection limit were investigated.

An ion-pair reverse phase HPLC-ICP-MS method of separation and determination of arsenite (As(III)), dimethyl arsenic acid (DMA), monomethyl arsenic (MMA), and arsenate (As(V)) was studied. The separation was performed on a C18 column with hexadecyltrimethyl ammonium bromide (CTAB), ammonium phosphate buffer and methanol as mobile phase. This HPLC-ICP-MS method was validated by determing the arsenic species in urine standard reference material (SRM) 2670 and applied to Chinese brake fern, an arsenic hyperaccumulating plant. The speciation information can help to better understand the mechanisms of arsenic accumulation, translocation and detoxification in Chinese brake fern.

CHAPTER 1
INTRODUCTION

The Goal of the Research

Elemental speciation analysis has become increasingly important in the environmental, biological, geological, and medical fields. This is due to the fact that behavior of a given element is critically dependent on its actual chemical form. The physiological, toxicological, and biological effects also depend on the species of the individual element.

Capillary electrophoresis (CE) has been a powerful analytical technique for the separation of a variety of analytes, ranging from small inorganic and organic ions to large biomolecules. It has the advantage of simple instrument set-up, quick and efficient separation, and relatively low cost. Inductively coupled plasma mass spectrometry (ICP-MS) provides rapid multi-element analysis of environmental, biological, and geological samples with detection limit at parts per trillion level. CE-ICP-MS system has the advantages of small sample volume, minimal buffer consumption, low detection limit, direct species identification, and quantification. Therefore, CE-ICP-MS combines the high separation efficiency of CE and the high selectivity and sensitivity of ICP-MS, making it a powerful analytical technique for trace elemental speciation in various sample matrices. However, CE-ICP-MS still has some drawbacks including the requirement of a special interface for ICP-MS sample introduction, CE buffer interference, low liquid flow rate, and laminar flow effect.

Compared with CE-ICP-MS, high performance liquid chromatography (HPLC) is more suitable to couple with ICP-MS. This is because the liquid flow rate of HPLC, which is typically 1.0 mL/min, is more agreeable to the ICP-MS nebulizer sample uptake rate (0.5 – 1.0 mL/min). Therefore, a HPLC–ICP-MS system combines the separation potential of HPLC and the superior sensitivity and selectivity of ICP-MS. In addition, the simple coupling of HPLC with ICP-MS makes it the most widely used technique for elemental speciation in various sample matrices. However, HPLC still cannot satisfy the entire requirement for routine analysis due to its lengthy experimental runs, adverse organic solvent effects on the plasma, and relatively expensive instrumentation. Therefore, CE-ICP-MS is a useful complementary technique for HPLC-ICP-MS.

Arsenic contamination has been a global problem. Thousands of people suffer from chronic toxicity effects from the surrounding arsenic contaminated soil, ground water, and various foods. For example, approximately 35 to 77 million people out of a population of 125 million in Bangladesh are at the risk of being exposed to arsenic in their drinking water [1]. Identification and quantification of individual arsenic forms are important to measure appropriately the arsenic toxicity, environmental impact, and health risk related to arsenic exposure.

The Chinese brake fern (*Pteris vittata L.)* has recently been discovered as an arsenic hyperaccumulating fern plant [2]. The Chinese brake fern can effectively extract large amounts of arsenic from the soil into its fronds in a short time. Since this plant is also hardy, versatile, and fast-growing, it holds great potential to clean up commercially and cheaply thousands of soil and water sites which were contaminated by arsenic from natural or anthropogenic activities all around the world. Knowing only the total arsenic concentration in the fronds is insufficient to evaluate fully the environmental impact of Chinese brake fern. The arsenic speciation information helps to better understand the mechanisms of arsenic accumulation and transformation in Chinese brake fern.

The goal of this research was to develop a reliable and robust analytical method for routine arsenic speciation in a variety of samples in a single run. The HPLC-ICP-MS method can also be widely applied to determine various elemental species in environmental, biological, geological, and medical fields.

Overview of the Research

In this research, a modified concentric Meinhard nebulizer and an interface were developed and used for coupling CE to ICP-MS. This interface has several notable features. The interface was placed outside and operated independently of the nebulizer. It was flexible and could be connected to various types of nebulizers. It was easy to operate and inexpensive. The parameters that influenced both separation efficiency and detection limit have been investigated. This CE-ICP-MS system has been used to analyze arsenite (As(III)) and arsenate (As(V)) in a laboratory created sample.

Ion-pair reverse phase HPLC-ICP-MS was employed to determine arsenite (As(III)), dimethyl arsenic acid (DMA), monomethyl arsenic (MMA), and arsenate (As(V)) in various sample matrices. The choices of HPLC separation conditions were based on the selection and optimization of ion-pairing reagent concentration, buffer concentration, methanol concentration, pH, and mobile phase flow rate. The organic solvent and flow rate effects as well as spectroscopic interferences were also considered for ICP-MS detection. Despite the fact that there are numerous publications on arsenic speciation recently, there is still no commercial standard reference material (SRM) available with certified concentrations of individual arsenic species. This method was validated by determing the arsenic species present in SRM 2670 (Total metal in freeze-dried urine) from NIST (National Institute of Standards and Technology) and compared with the results reported by other research groups.

This optimized ion-pair HPLC-ICP-MS method was applied to determine arsenic species in Chinese brake fern (*Pteris vittata L.*), an arsenic hyperaccumulating plant. The speciation information can help to better understand the mechanisms of arsenic accumulation, translocation, and detoxification in Chinese brake fern.

CHAPTER 2
BACKGROUND

Inductively Coupled Plasma Mass spectrometry (ICP-MS)

Inductively coupled plasma mass spectrometry (ICP-MS) was commercially introduced in 1983. It has become the most sensitive and selective technique for the determination of metals, and it is a standard method for rapid multi-elemental analysis of diverse biological, environmental, and geological samples [3]. Compared with another rapid multi-element analysis technique, such as inductively coupled plasma atomic emission spectrometry (ICP-AES), ICP-MS provides a superior detection limit at single parts per trillion or below, less spectral interference, and the capability of isotope ratio analysis. The major problems of ICP-MS are the high cost and the complexity of the technique. The former includes high initial instrumentation and operation costs. Additionally, the ICP-MS instrument requires a well-trained person to operate and maintain it because of its complexity.

The Principles of ICP-MS Technique

The principles of ICP-MS technique are briefly summarized below. Figure 2-1 is a schematic diagram of the VG plasma quadrupole ICP-MS system used in this work [4]. Generally, liquid samples are injected into the sample introduction system by a peristaltic pump. Then the liquid sample is dispersed into an aerosol by the sample introduction system, which consists of a nebulizer and a spray chamber. Aerosol samples are carried into the core of the plasma by a carrier gas. The radio frequency field produces a high

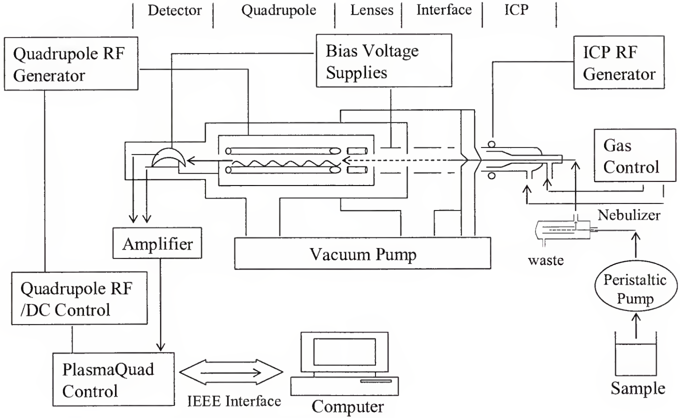

Figure 2-1. Schematic of Inductively Coupled Plasma Mass Spectrometry (ICP-MS).

temperature plasma. When aerosol samples travel through the different heating zones of the plasma torch, the liquid aerosols are first dried into solid particles. As the solid particles move further, they are vaporized into gaseous species. Next, the gaseous sample travels to the analytical zone of the plasma, where the temperature is about 6000-7000 K, and it is atomized into ground-state atoms. Finally, the atoms collide with the energetic argon electrons which produce excited ions. The ions emerge from the plasma region and enter the interface region of the mass spectrometer; the interface includes the sample cone and the skimmer cone. The ions pass through the small orifice of the cones into the reduced pressure regions. Then, the positive ions are extracted and focused into a linear path by a series of electrostatic lenses and directed into a quadrupole mass analyzer. Only ions of the selected mass-to-charge ratio are transmitted into the ion detector. The ions are then collected and amplified as an electron pulse by the electron multiplier assembly. This pulse is transferred into a microprocessor controlled multi-channel scaler (MCS) data acquisition system. Finally, acquired data are transmitted and stored into a computer by the PlasmaQuad program. The primary ICP-MS components are the sample introduction system, inductively coupled plasma, sampling interface, ion lenses, mass analyzer, and ion detector and data acquisition system. A brief review of these components will be presented.

Sample Introduction System

The ICP-MS requires the sample in a form that can be introduced into the torch by a carrier gas, which is usually argon. The sample form can be a gas, a vapor, or a fine aerosol of droplets or solid particles. Several techniques have been employed to transport gas, liquid, and solid samples into ICP-MS.

For solid sample introduction, these techniques include electrothermal vaporization (ETV), laser ablation (LA), arc and spark ablation, slurry nebulization, and direct sample insertion (DSI) [5]. Among these techniques, LA-ICP-MS and ETV-ICP-MS are the most popular techniques [6, 7]. ETV-ICP-MS can be used for both liquid and solid sample introduction, and can also be a pre-concentration device for liquid sample. ETV-ICP-MS has advantages of selective sample volatilization, less matrix interference, and lower detection limit. The major disadvantages of ETV-ICP-MS are the requirement of sample homogeneity and small sample size (10 mg or less). When LA-ICP-MS is compared with other solid analysis techniques such as glow discharge mass spectrometry, X-ray fluorescence, laser microprobe mass spectrometry, and secondary ion mass spectrometry, it has the benefits of sampling various solids or powders such as conducting and non-conducting inorganic and organic materials. It also possesses great precision and accuracy. However, the lack of suitable solid standards limits LA-ICP-MS application.

For gas sample introduction, common techniques include hydride generation (HG), direct gaseous sample introduction, gas chromatography (GC), and supercritical fluid chromatography (SFC). HG-ICP-MS plays an important role in the analysis of toxic elements, especially arsenic and selenium, due to their ability to form volatile hydride compounds [8]. Gas chromatography is a good source to introduce volatile organic, inorganic, and organo-metallic compounds into the ICP-MS; but use of argon for ICP limits the sensitivity for certain elements [9]. Supercritical fluid chromatography is included in gas sample introduction methods because the fluid is converted to gas when it exits the column and enters the plasma. To analyze nonvolatile, high molecular weight and thermally labile compounds, SFC-ICP-MS is a complementary technique for GC-ICP-MS. It is important to note that unstable transfer line temperatures may cause peak broadening and degrade the SFC-ICP-MS resolution [10]. Without a traditional nebulizer and spray chamber, gas sample introduction can be achieved into the ICP with near 100% transfer efficiency. However, most samples naturally exist as liquids or solids. Additionally, many liquid and solid samples are difficult to convert into gaseous forms.

Liquid sample introduction is a significant aspect of ICP-MS instrumentation. A number of sample introduction modes have been used for the introduction of liquid samples, including the concentric and cross-flow nebulizer, direct injection nebulizer (DIN), ultrasonic nebulizer (USN), micro-concentric nebulizer (MCN), high efficiency nebulizer (HEN), oscillating capillary nebulizer (OCN), direct injection high efficiency nebulizer (DIHEN), thermal spray nebulizer, glass frit nebulizer as well as hydride generation (HG) and electrothermal vaporization (ETV). All of these liquid sample introduction methods involve generation of a fine aerosol from the liquid sample.

Standard components of liquid sample introduction systems include a peristaltic pump, nebulizer, and spray chamber. The peristaltic pump is a small pump with several rollers that rotate at the same speed. Therefore, a constant liquid flow is introduced *via* the peristaltic pump into the nebulizer. The pump speed and the size of the pump tubing affect the liquid sample solution uptake rate. The sample uptake rate in this research is approximately 0.5 – 1.0 ml/min for the concentric nebulizer.

The most commonly used nebulizers for ICP-MS are concentric, cross-flow, and ultrasonic types. They are usually made from glass, but other materials have also been used for some special purposes. A Meinhard concentric nebulizer is used in the present research; the sample solution is carried by high velocity gas flow through a capillary tube, resulting in the production of a droplet spray at the open end of the nebulizer nozzle. Sample solution uptake rate, capillary inner diameter and wall thickness, nebulizer operating pressure and nebulizer nozzle configuration determine the sample aerosol quality. Figure 2-2 shows a typical Meinhard concentric nebulizer. The Meinhard TR series concentric nebulizer (Meinhard Glass Products, Golden, CO) capillary inner diameter is around 0.22 – 0.32 mm. The annular separation at nozzle is around 0.02 mm [11]. In this research, the flow rate of nebulizer carrier gas, usually argon, is approximately 0.60 – 0.80 L/min, and corresponding nebulizer gas pressure is approximately 15 – 40 psi. The concentric nebulizer is primarily used in ICP-MS because of its stability, simplicity, and relatively low cost. However, the concentric nebulizer has drawbacks of low analyte transport efficiency at 1-2%, high sample uptake rate at 1-2 mL/min, and clogging problems because of the small orifice.

Compared with the concentric nebulizer, the cross-flow nebulizer is used for heavy matrix samples [12]. This nebulizer has two capillary tubes, which are set at right angles to each other in a polytetrafluoroethylene (PTFE) body. A sample solution is injected into one capillary tube while argon gas is directed into the other capillary tube, making the gas flow vertical to the liquid flow. The liquid flow is then broken into an aerosol at the capillary tip aided by the high-speed argon gas flow. The argon gas flow rate is approximately 0.5 - 1.0 L/min and the sample uptake rate is approximately 1 – 3 mL/min. In comparison with a concentric nebulizer, the cross-flow nebulizer has inferior efficiency and precision.

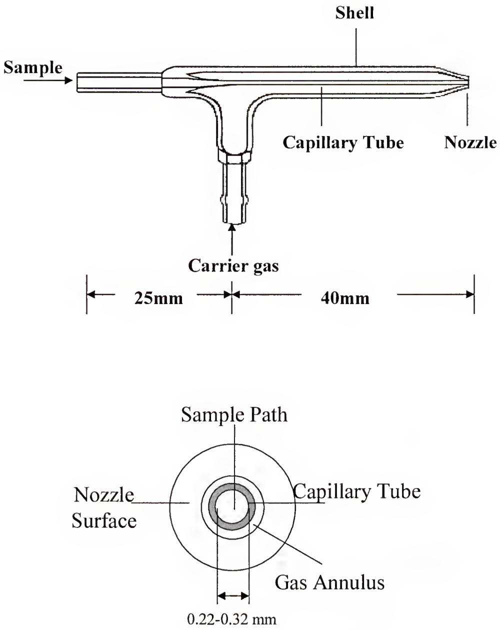

Figure 2-2. Schematic of a typical Meinhard concentric nebulizer [11].

In addition to the concentric and cross-flow nebulizer, the ultrasonic nebulizer is used for heavy matrix samples and exhibits high transport efficiency around 20% [13]. The sample solution is injected onto the surface of a piezoelectric transducer by argon carrier gas. An ultrasonic generator produces longitudinal waves, which travel perpendicularly from the surface of the piezoelectric crystal to the liquid-gas interface. The liquid is broken into an aerosol by the amplitude of the ultrasonic wave. The sample uptake rate is approximately 1-3 mL/min. Disadvantages of the ultrasonic nebulizer include high cost, low precision, and long washout time.

The concentric, cross-flow, and ultrasonic nebulizers are used for relatively large volumes of sample solution at flow rates of approximately 1- 3 mL/min. When the sample solution is hazardous or expensive and the volume is limited, a microflow nebulizer such as the direct injection nebulizer (DIN) is used [14]. The typical direct injection nebulizer design involves the installation of a microconcentric pneumatic nebulizer into the ICP-MS torch without the spray chamber. Therefore, the sample solution can be transformed into an aerosol at flow rates between 10 μL /min to 100 μL/ min while maintaining almost 100% aerosol transport efficiency to the plasma. The direct injection nebulizer also has advantages of low dead volume (< 2 μl), short washout time, and good precision. Compared with the concentric nebulizer, the direct injection nebulizer is more expensive and complicated.

In addition to the concentric, cross-flow, ultrasonic, and direct injection nebulizers mentioned above, other nebulizers such as microconcentric, high efficiency, oscillating capillary, and direct injection high efficiency nebulizer have also been used in CE-ICP-MS system.

There are two common types of spray chambers used in ICP-MS, the double pass and the cyclonic spray chambers. The spray chamber is used to prevent large droplets from entering the plasma and to limit the total aerosol transport rate (typically less than 10 μl of aqueous aerosol/min). In this research, a Scott double pass spray chamber (Precision Glassblowing, Centennial, CO) is used to introduce small aerosol droplets (around 10 μm diameter) into the ICP. Large droplets fall into the spray chamber drain by gravity and are pumped away by a peristaltic pump. The spray chamber is cooled to 2-5 °C to reduce the introduction of solvent into the plasma, thereby decreasing polyatomic interference due to oxygen and keeping the temperature stability.

Inductively Coupled Plasma

Atmospheric pressure inductively coupled plasma (ICP) transfer the sample aerosol droplet into ions. The ICP system includes a radio frequency generator, torch box, and gas control panel. In this research, the radio frequency generator (Henry Radio, USA) is a freestanding unit and can generate up to 2000 W at a frequency of 27 MHz. The torch is mounted horizontally in the center of the RF coil and located approximately 10-14 mm from the plasma sampling interface. Argon gas is introduced into the torch by three concentric tubes. When argon gas is flowing through the torch, the tesla coil produces a potential high enough to overcome the dielectric resistance of the gas and a high voltage spark is applied to the gas. The spark seeds the argon gas with energetic electrons and an inductively coupled plasma is formed. The radio frequency current through the coil creates an electromagnetic field at the top of the torch. The ICP is sustained by this high electromagnetic field and argon gas in the torch. The three concentric tubes are denoted as outer tube, middle tube, and sample injector tube.

Cooling gas between the outer and middle tubes prevents the outer tube of the torch from overheating; the flow rate is approximately 12-15 L/min. Auxiliary gas between the middle and sample injector tubes affects the shape of the plasma; the flow rate is approximately 0- 0.8 L/min. Nebulizer argon in the injector tube carries sample aerosol droplets from the spray chamber and punches a channel through the center of the plasma; the flow rate is approximately 0.6-0.8 mL/min at a relative nebulizer gas pressure of 15-30 psi. The sample aerosol droplets travel through the various plasma regions at different temperatures ranging from 6200 K to 8000 K [15]. At first, a sample aerosol droplet is desolvated to a solid particle. Secondly, the solid particle is vaporized to a gaseous species. Then, the gas is atomized to ground-state atoms. Finally, atoms collide with energetic argon electrons and are ionized to ions. The ions emerge from the ICP and are directed into the ICP-MS sampling interface.

ICP-MS Sampling Interface and Ion Focusing System

Analyte ions from the ICP are directed through an interface region and focused *via* an ion optics system into the mass analyzer chamber. A key part of ICP-MS instrumentation is the interface region. In this research, the interface region includes a sample cone with an orifice diameter of 1.0 mm and skimmer cone with an orifice diameter of with 0.75 mm. Both are made from pure nickel, which has good endurance with corrosive liquids and good thermal conductively. The sampling depth, which is the distance between the tip of the sample cone and the nearest turn of the load coil, is 12 mm. Ions are transferred constantly and efficiently from the atmospheric plasma to the expansion chamber, which is maintained at 2 mbar by an E1M18 single stage rotary pump (5.5 L/s) (BOC Edwards, Wilmington, MA), behind the sample cone. The conditions of the sample and skimmer cones affect the instrument sensitivity and the formation of polyatomic species. In order to eliminate an electrical discharge from ICP radio frequency interference, a copper-beryllium contact strip on the expansion chamber front plate is used to provide a good earth return path between the interface region and the plasma torch box.

Positively charged analyte ions are focused by the lens system and transported from the interface region to the mass analyzer. The particulates, photons, and neutral species are stopped from entering the mass analyzer by the lens system. Such species are undesirable because they can increase background noise and cause signal instability. In this research, the ion focusing system is made of a series of axially symmetric electrostatic lens, which include extraction lens, collector and photon stop, L1, L2, differential apertures, L3, L4, and a quadrupole entrance aperture. Voltages are applied to these lenses. First, the positively charged ions are pulled to the lens stack by the negative voltage on the extraction lens and the negatively charged species are repelled while the neutral species diffuse away from the system axis to the intermediate diffusion pump. Second, the particulates, photons, and neutral species are physically blocked by the on-axis photon stop on the collector, while the positively charged ions around the photon stop are focused through the differential aperture by L1 and L2. Finally, the analyte ions are refocused by L3 and L4 and transmitted through the quadrupole entrance aperture to the mass analyzer.

Mass Analyzer

There are four different types of mass analyzers used in the ICP-MS: quadrupole, time-of-flight, magnetic sector, and ion trap. Currently, quadrupole-based systems are installed in almost 90% of the ICP-MS instrument. The quadrupole mass analyzer separates the analyte ions of interest from other ions on the basis of mass to charge ratio (m/z). The analyte ions of interest pass through the middle of quadrupole rods to the detector, while the other ions are ejected from the quadrupole. In this research, the 12-12S quadrupole system includes analyzer, radio frequency generator, quadrupole control unit, power control unit, and remote power supply unit. The quadrupole consists of four electrically conducting parallel hyperbolic rods (12 mm diameter, 230 mm long, molybdenum) located in a square array. Opposite rods are connected together with a particular direct current (DC) and radio frequency (RF) applied to the rods. One pair of rods has an applied potential of $\Phi(t) = U + V \cos(2\pi ft)$ (U is the DC voltage, V is the peak amplitude of the RF voltage at frequency f); the other pair of rods has the same applied potential but the opposite sign. An appropriate amplitude of the potential results only in the transmission of ions of a particular mass to charge through the rod assembly. The ability of the transmission and separation is determined by certain parameters including RF voltage, DC voltage, frequency of quadrupole power supply, shape-diameter-length of the rods, operating vacuum, and mass to charge ratio of the ions.

Detector and Data Acquisition

Analyte ions that emerge from the mass analyzer are converted to electrical pulses by the detector, and then the electrical pulses are counted into memory channels and transferred to the computer data system by a multi-channel scaler (MCS). In this research, the detector is a channeltron electron multiplier and is operated under the pulsed counting mode for trace metal analysis. A typical high voltage, which ranged from –3000 V to –3500 V, is applied to the multiplier to attract the positive ion. First, a positive ion hits the surface of the electron multiplier, and one or more secondary electrons are ejected. These secondary electrons strike another section of the surface and more secondary electrons are emitted. After repeating this process millions of times, a discrete pulse that contains 10^7 to 10^8 electrons for every import ion leaves the base of the multiplier channel and enters a very fast preamplifier. The pulse voltage is around 50 mV to 100 mV and 10 ns wide. Second, the pulse from the preamplifier is passed to a discriminator and counter printed circuit board (PCB) of the PlasmaQuad control unit. The dead time of the detector system ranges from 10 to 25 ns with this ICP-MS. The pulse is gated into a counter for a selected dwell time. The counter contents are processed by the microprocessor and stored in the acquisition memory. Finally, the acquisition memory contents are transferred through the IEEE interface to the computer and are shown as mass peaks or time peaks. The continuous scan mode is used for quality analysis, and the peak jump mode is used for quantitative analysis.

For CE-ICP-MS and HPLC-ICP-MS, time resolved acquisition (TRA) software is used to acquire electropherogram and chromatogram data. VG data files are stored and exported as ASCII files. Data analysis is performed with Microsoft Excel or Origin for peak information.

Capillary Electrophoresis (CE)

Capillary electrophoresis (CE), commercially introduced in the late 1980s, can separate complex mixtures of charged and uncharged species quickly and efficiently in a single run. Also, it has the advantages of simple instrument set-up and relatively low cost. Therefore, CE has been a powerful analytical technique for the separation of a variety of analytes ranging from small inorganic and organic ions (e.g. selenite and selenate) to large biomolecules (e.g. proteins and nucleic acids). Capillary electrophoresis can also be effectively used to separate different metal ions, and the separation is usually faster and requires much less sample (a few nanoliters) [16, 17]. Capillary electrophoresis is more suitable than the other chromatographic methods for elemental speciation owing to the lack of stationary phase and wide pH range well within the stability region of many species. The stationary and mobile phase may interact with the labile species resulting in biasing the original distribution of elemental species. However, CE has analyte-wall interaction and sample may be lost due to trapping by the inner wall of the capillary. Compared with HPLC, CE is a relative clean technique and has less environmental impact and health risk. This is because CE uses only small amounts of organic solvent in the buffer solution or even no organic solvent at all. However, CE still has problems such as sample injection, lack of precision, and unreliability.

As shown in Figure 2-3, the typical CE experiment set-up consists of four major parts: a capillary, a high voltage supply, buffer, and a detector. The high voltage (10-30 kV) direct current (DC) power supply is connected to two platinum electrodes and inserted into the buffer containers. Likewise, the capillary (20-300 μm ID) is filled with buffer solution and dipped into the buffer containers. The high voltage is applied to the capillary to separate the ions, which move at different speeds depending on their size and charge. A sample solution (10-100 nl) is injected from the positive end of the capillary. Anions are attracted by the anode and move to the positive end. Neutrals are not attracted by either anode or cathode. Cations are attracted by the cathode and toward the

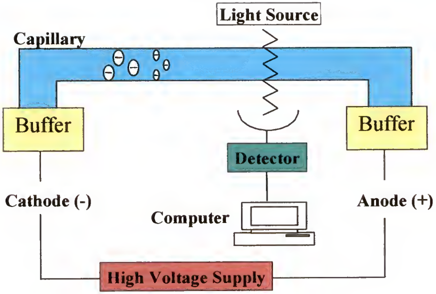

Figure 2-3. Schematic of typical capillary electrophoresis.

negative end, where detection occurs. However, all of the species will pass through the detector by the electroosmotic flow (EOF) and arrive at the negative end of the capillary at different elution times. Elution has the following sequence: cations elute first; neutral elute secondly; anions elute lastly at all. EOF flow is the result of the double layer at the silanol / buffer interface. For pH values higher than about 3, the negatively charged silanol groups (SiO^-) on the surface of the capillary are equilibrated by the positive ions from the buffer. When applying a high voltage, the positive ions in the diffusion region will move towards the cathode and produce the EOF flow from anode to cathode.

The development of highly sensitive and selective detectors for CE has been one of the most important and challenging prerequisites for the growth of CE. On-column UV and fluorescence detectors have been widely used. However, the sensitivity of these detectors are usually between 10^{-5} and 10^{-6} M. Some other detection methods such as mass spectrometry, laser induced fluorescence, chemiluminescence, electrochemical method, and laser Raman spectroscopy have been employed to provide more sensitive and selective detection of the analyte separated by CE [18]. However, these detectors are not suitable for the determination of metal ions subsequent to CE separation due to a lack of adequate sensitivity and selectivity.

Element-selective detectors, including inductively coupled plasma atomic emission spectrometry (ICP-AES) and mass spectrometry (ICP-MS), microwave induced plasma (MIP) AES and MS, graphite furnace atomic absorption spectrometry (GFAAS), and electrochemical techniques, have been used in combination with separation techniques [19]. Among these techniques, the high selectivity and sensitivity of ICP-MS makes it the most suitable instrument for speciation analysis. The advantages of ICP-MS as a CE detector are listed below: low detection limits of this hyphenated system (<1 μg/L); direct element information and element quantification; all buffer systems fit well to the detector; and species identification *via* migration times. Therefore, ICP-MS as a CE detector provides a powerful tool for elemental speciation analysis.

In principle, CE separation is based on the migration of ions in a strong electric field. The separation of free metal ions is related to their equivalent ionic conductance. Many divalent metals, such as Cu^{2+}, Fe^{2+}, and Mg^{2+}, are difficult to separate because their equivalent ionic conductances are similar. Capillary electrophoresis cannot separate mixtures of ions with similar mobility, such as lanthanides, unless an additional separation mechanism is used. If ICP-MS is used as an element selective detector, there is no need to separate different +2 or +3 ions containing different elements by adding complexing ligands to the sample. Therefore, CE-ICP-MS maintains the original sample species.

Electrospray ionization (ESI) source is widely used as an interface for capillary electrophoresis and mass spectrometry. CE-ESI-MS is very popular in the bioanalytical field. CE-ESI-MS can perform direct detection and quantification of species, but it is not suitable to identify bound metals because electrospray is a soft ionization technique [20, 21]. When CE-ESI-MS is applied to elemental species analysis, some problems have been reported. Since only volatile buffers are appropriate for the ESI-process, elemental information is achieved indirectly by the characteristic isotope pattern. This presents possible losses of species information due to gas phase intra-molecular charge transfer and detection limits are strongly compound dependent. For ICP-MS, the temperature of the plasma is about 6000-8000 K, so that the sample solution is almost entirely dissociated to ions in the plasma. Therefore, ICP-MS is almost independent of sample matrices for quantitation analysis, and CE-ICP-MS is a useful complementary technique to CE-ESI-MS.

CE-ICP-MS system has the advantages of small sample volume (10-100 nl), minimal buffer consumption (< 20 ml per day), low detection limits (around 1 ppb (μg/L)), direct elemental information, and element quantification and species identification *via* migration times. Therefore, CE-ICP-MS combines the separation potential of CE and the superior elemental sensitivity and selectivity of ICP-MS, making it a powerful analytical technique for the elemental speciation in various sample matrices.

However, CE-ICP-MS still has disadvantages including the requirement of a special interface for ICP-MS sample introduction, CE buffer interference, low liquid flow rate and laminar flow due to suction from the nebulizer gas.

High Performance Liquid Chromatography (HPLC)

A variety of separation techniques have been used for speciation analysis, including supercritical fluid chromatography (SFC), capillary electrophoresis (CE) and gas chromatography (GC). Among them, high performance liquid chromatography (HPLC) is the most widely used separation technique since it was developed in the 1970s. The reasons of its popularity are high sensitivity and high accuracy. Both CE and HPLC require little sample pretreatment and small sample volumes (microliter or even less). Therefore, HPLC can be used as a powerful analytical technique to separate certain organic or inorganic compounds, or to purify target compounds from other compounds or contaminants in variety fields of science and industry [22, 23].

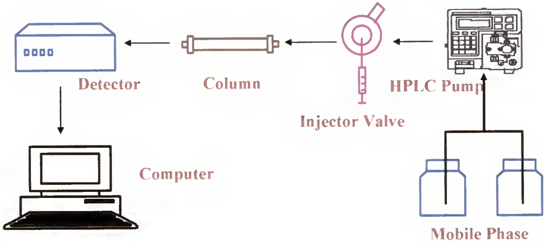

Figure 2-4. Diagram of typical High Performance Liquid Chromatography.

As shown in Figure 2-4, a typical HPLC experiment set-up consists of five major parts: mobile phase, pump, injector valve, column, and detector. The mobile phase acts as a carrier liquid for the sample solution. Composition of the mobile phase can be altered to achieve better separation efficiency. The two major mobile phase introduction systems include isocratic elution (a single solvent of constant composition) and gradient elution (two or more solvents of different polarity). The sample solution is injected into the mobile phase through an injector valve. The volume of the sample injection loop ranges from 5 μl to 500 μl. The pump pushes the mobile phase to continuously flow through the column (stationary phase), which is packed with 3 μm to 50 μm particle. The flow rate ranges from 0.1 to 10 mL/min and the corresponding pump pressure can be up to 6000 psi (pounds per square inch). The columns are commonly made from smooth bore stainless steel tubing and packed with porous particles. The length of the column ranges from 10 cm to 30 cm and the inner diameter ranges from 4 mm to 10 mm with common particle sizes of 3 μm, 5 μm and 10 μm. Among them, the 5 μm particle size column is the most routine column due to its high separation efficiency and moderate operating pressure requirement. The column contains various types of stationary phases, such as normal phase, reverse phase, ion exchange, size exclusion, affinity and adsorption packing. The chemical interaction of the mobile phase and the sample with the stationary phase, determines the separation efficiency and the migration sequence of the species in the sample. Species pass through the detector at different retention times.

The common detector of HPLC is the UV-Vis absorbance and refractive index detector. Similarly as CE-ICP-MS, HPLC-ICP-MS combines the powers of high separation efficiency of HPLC with the high selectivity and sensitivity of ICP-MS.

HPLC-ICP-MS has the ability to perform real time analysis on separating species of interest. HPLC-ICP-MS also has multi-element capability and high detection power.

Compared with CE-ICP-MS, HPLC is more easily coupled with ICP-MS. This is because the liquid flow rate of HPLC, which is typically in the range of 0.1-10 mL/min, is consistent with the requirement of the ICP-MS nebulizer sample uptake rate (0.5-1.0 mL/min). The coupling technique of HPLC-ICP-MS is simple and just needs a short Teflon tube of small diameter to connect the HPLC column to the ICP-MS nebulizer.

However, HPLC still cannot satisfy the entire requirement for routine analysis due to the equilibrate time, organic solvent effect on the plasma and the relative expense. It usually takes half an hour to two hour to wash and equilibrate the column. The organic solvent, which is introduced with the mobile phase, may adhere to the inner wall of the spray chamber and affect the signal stability or change the loading of the plasma affecting the sensitivity. Because of the need for high-pressure, HPLC equipment is more expensive than the other chromatographic instruments. Columns used in HPLC are also expensive (at least $240 each) in comparison to capillaries used in CE (less than $10 per meter). Furthermore, the amount of organic solvent, which is used in HPLC, cannot be neglected. For example, methanol is introduced by the HPLC pump at a flow rate of about 1 mL/min. First, 60% v/v methanol equilibrates the column for 10 minutes, and then 2% v/v methanol is introduced with the mobile phase for a 360-minute experiment; finally 100% methanol is used to rinse the column for 10 minutes. Most of this methanol transfers through the column to the nebulizer of ICP-MS and finally to the waste bottle. Therefore, the total methanol waste solution will be about 23 mL each day and 8.5 L per year. The vaporizable methanol is harmful to human health, too. Contacting methanol with skin and eye can poison people even causing blindness [24]. Thus, the environmental impact and health risk of the organic solvent is another drawback of the HPLC technique.

CHAPTER 3
ELEMENTAL SPECIATION AND ARSENIC OVERVIEW

Elemental Speciation

Elemental speciation is the identification and quantification of the species of an element. Traditional trace elemental analysis focuses on the total content of a specific element in a sample. Today, elemental speciation analysis has become increasingly important in the environmental, biological, geological and medicinal fields. It is due to the behavior of a given element which is critically dependent on its actual chemical form. The physiological, toxicological and biological effects also depend on the species of the individual element, including different bonding forms or oxidation states [25]. For example, Cr (III) at trace level is an essential nutrient for humans; however, Cr (VI), which is sometimes used as an algaecide, is toxic to humans [26]. Therefore, the determination of the concentration of specific chemical forms, such as organic Cr (VI) instead of the total chromium is important to explain the biochemical behavior or assessment of the potential danger to organisms. The adsorption and transportation of pollutants from toxic waste sites and agricultural runoff are also species dependent. Thus, elemental speciation has been an important analytical technique for determination of toxicity of selected elements, studies of biogeochemical cycles of chemical compounds, technological process control, examination of occupational exposure, and clinical analysis. Considerable research has been done recently to determine the species of some elements such as Al, As, Cd, Cr, Fe, I, Hg, Se, Sn, P, Pb, Pt, Sb, etc [27]. Nevertheless analytical instruments still need to be improved to achieve high separation efficiencies and low detection limits. Additionally appropriate sequential extraction methods need to be developed to obtain more arsenic from real-world sample.

Arsenic Overview

Arsenic is the 20th element in abundance in the earth's crust, is widely present in the natural environment, and is produced from human activity. Arsenic is a well-known poison and the toxicity and bioavailability of its compounds are strongly dependent on the chemical forms. Humans can be senselessly exposed to arsenic through food, contaminated soil, plants and atmosphere. Knowing the chemical form of an individual arsenic compound is essential to a reliable assessment of health risk. Despite the numerous publications for arsenic speciation in the past few years, there are still some limitations in the current analytical methods. Therefore, arsenic is a huge concern in environmental and human health fields and there remains the need to develop an analytical method to efficiently and simultaneously determine arsenic species.

Chemical and Physical Property of Arsenic

Arsenic (As) is a metalloid element which is located in the fourth period and Group V of the periodic table. The atomic number of arsenic is 33 and the corresponding atomic mass of arsenic is 74.92160 g/mol. When considering mass spectrometry, arsenic has only one stable isotope, ^{75}As, with an abundance of 100%. In atomic emission spectrometry, the most sensitive atomic spectral lines of arsenic are at 189.0 nm, 193.7 nm, 197.3 nm and 228.8 nm. Elemental arsenic exists as a gray or metallic or yellow crystal. The gray form represents the ordinary, semi-metallic solid arsenic [28]. The physical properties of arsenic are listed in Table 3-1. Inorganic arsenic compounds can be arsenic hydrides, halides, oxides, acids and sulfides. Arsenic combined with carbon and hydrogen is called organic arsenic. The typical organic and inorganic arsenic compounds in arsenic speciation analysis, are listed in Table 3-2. Arsenic can be presented in valence states of –3, 0, +3 and +5. The –3 and 0 valence states rarely exist. Arsenite (As(III)) and arsenate (As(V)) are the main valence states of arsenic compounds in environmental and biological systems.

Arsenic Toxicity and Health Effects

Arsenic and its compounds are well known poisons. The ancient Chinese, Egyptians and Greek discovered their toxic property centuries ago. The toxicity of arsenic compounds varies dramatically with their chemical forms of arsenic. The toxicity of arsenic compounds, which are based on the median lethal dose values (LD_{50}) in rats, is shown in Table 3-3 [29]. The order of decreasing toxicity of arsenic compounds are as follows: arsenic hydride > arsenite > arsenate > arsenic trioxide > dimethyl arsenic acid > monomethyl arsenic acid > arsenocholine > arsenobetaine > Trimethyl arsine oxide. Accordingly, both inorganic and organic arsenic compounds are very toxic to humans, but inorganic arsenic compounds tend to be more toxic than organic arsenic, and As(III) is more toxic than As(V). Therefore, identification and quantification of individual arsenic forms are important to appropriately measure the arsenic toxicity, environmental impact, and health risk related to arsenic exposure.

Most inorganic and organic arsenic compounds are white or colorless powders. They have low vapor pressure so that they have no smell, and also no special taste. Thus, the potential problems become more dangerous since people cannot determine if arsenic

Table 3-1. Arsenic physical properties [28].

Electron configuration	$[Ar]3d^{10}4s^{2}4p^{3}$	Electronegativity	2.18
Density	5.727 g/cm^{3}	Covalent radius	120 pm
Melting point	817 °C (28 atm)	Atomic volume	13.1 cm^{3}/mol
Boiling point	613 °C sublime	Heat capacity	0.329 J/g K
Crystal form	Rhombohedral	Thermal conductivity	50.2 w/ mK
1st Ionization potential	9.815 eV	2nd ionization potential	18.633 eV

Table 3-2. Typical arsenic compounds in the environment and biological system [28].

Arsenic Compound	Formula
Sodium arsenite, As(III)	$NaAsO_2$
Sodium arsenate, As(V)	Na_2HAsO_4
Dimethyl arsenic acid sodium salt, (DMA)	$(CH_3)_2AsO_2Na$
Disodium methyl arsenate, (MMA)	$CH_3AsO_3Na_2$
Arsenocholine, (AC)	$(CH_3)_3AsCH_2CH_2OH$
Arsenobetaine, (AB)	$(CH_3)_3AsCH_2COOH$
Trimethyl arsine oxide, (TMAO)	$(CH_3)_3AsO$
Arsine	AsH_3
Arsenolipids, (AsL)	$(CH_3)_3AsCH_2CHOHCOOH$
Arsenosugars, (AsS) *	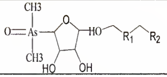

*R_1 = OH, R_2 = OH (giant clams and algae); R_1 = OH, R_2 = SO_3H (Brown algae); R_1 = NH_2, R_2 = SO_3H (Brown algae); R_1= OH, R_2 = $O_3POCH_2CH(OH)CH_2OH$ (Green algae)

Table 3-3. LD_{50} of arsenic compounds in rats/mouse [29].

Arsenic compounds	LD_{50} (mg/kg body weight)	Animal / Administration
Sodium arsenite	4.5	Rat / intraperitoneal
Sodium arsenate	14-18	Rat / intraperitoneal
Arsenic trioxide	35	Mouse / oral
Dimethyl arsenic acid	1200	Mouse / oral
Monomethyl arsenic acid	1800	Mouse / oral
Arsenocholine	6500	Mouse / oral
Arsenobetaine	10000	Mouse / oral
Trimethyl arsine oxide	10600	Mouse / oral

is present in the air, water, soil, and even food. Acute exposure can cause sever abdominal pain and even death.

Chronic health risks include non-cancer effects (e.g. diabetes) and cancer effects (e.g. bladder cancer). People can be exposed to arsenic by eating food, drinking water, breathing air, or skin contact with soil or water. Furthermore, children can be exposed to arsenic by eating dirt. Inorganic arsenic, which is ingested as arsenate, will be reduced to arsenite. Then arsenite changes to monomethyl arsenic acid, and finally to dimethyl arsinic acid. Arsenobetaine is the main arsenic species that humans ingest from food. It is so stable that it does not change to another form. Compared with other arsenic species, arsenobetaine is less toxic and can be discharged quickly from the body. This may be the reason that people are not be poisoned when they eat a lot of fish and shellfish. However, the ingestion of arsenosugar-containing food will increase the concentration of dimethyl arsenic acid in urine [30]. This is due to the metabolism of arsenosugar, which are present in seaweed. Conversion of arsenic species in the body still needs further research.

Arsenic Occurrence

Inorganic arsenic occurs naturally in soil and minerals; therefore, it may seep into air, water, plants and animals. Arsenic compounds were widely used as a component of herbicides, pesticides and fungicides. Additionally, 90% of all arsenic produced is used as a preservative for wood to make it resistant to rot and decay. Arsenic compounds are also used in the glass making, semiconductor, pigment, and pharmaceutical fields. Thus, arsenic may be released into the environment by use and disposal of industrial arsenic products and affect human health. Arsenic contamination has been a global problem. Thousands of people suffer from toxicity effects from chronic exposure by arsenic contaminated soil, ground water, and even food. Even in Gainesville, the wooden equipment and top 8 inches of soil were removed from several playgrounds because high arsenic levels were found nearby [31]. The contamination was a result of the arsenic leaching into the surrounding soils from the Chromated Copper Arsenic (CCA) treated wood. It is a potential risk to the children who play in the dirt and sometimes may unintentionally ingest the contaminated soil. Therefore, Environmental Protection Agency (EPA) has a limit of 10 mg/kg for arsenic in soil. In January 2001, EPA published a new standard to require public water supplies to reduce arsenic in drinking water from 50 ppb to 10 ppb by 2006. Occupational Safety and Health Administration (OSHA) has a permissible exposure limit (PEL) of 10 $\mu g/m^3$ averaged over an-eight-hour for airborne arsenic in various workplaces that use inorganic arsenic [32]. Arsenic contamination is difficult to treat because arsenic cannot be destroyed. Since the toxicity and mobility of arsenic highly depends on the actual arsenic form, effective and long-term arsenic treatment needs a highly efficient and sensitive arsenic speciation method. The goal of this research is to find a reliable and robust analytical method for arsenic speciation in a single run.

CHAPTER 4
EXPERIMENTAL

Chemicals and Reagents

The chemicals and reagents used in this research were listed in Table 4-1.

Table 4-1. The chemicals and reagents list.

Name	CAS number*	Manufacturer
Ammonium phosphate, dibasic	CAS 7783-28-0	Aldrich, Milwaukee, WI
Ammonium dihydrogen phosphate	CAS 7722-76-1	Aldrich, Milwaukee, WI
Dimethylarsinic acid, sodium salt, DMA	CAS124-65-2	Supelco, Bellefonte, PA
Disodium methyl arsenate, MMA	CAS 144-21-8	Supelco, Bellefonte, PA
Hexadecyltrimethyl ammonium bromide, CTAB	CAS 57-09-0	Sigma, St. Louis, MO
Methanol, HPLC grade	CAS 67-56-1	Fisher, Fair Lawn, NJ
mili-Q water, 18.2 MΩ distilled		Milipore, Molsheim, France
NaOH		Fisher, Fair Lawn, NJ
Nitric acid, Optima	CAS 7697-37-2	Fisher, Fair Lawn, NJ
Sodium arsenite	CAS 7784-46-5	MCIB, East Rutherford, NJ
Sodium arsenate	CAS 10048-95-0	Sigma, St.Louis, MO
Sodium borate	CAS 1303-96-4	Fisher, Fair Lawn, NJ
Sodium phosphate, dibasic, heptahydrate	CAS 7782-85-6	Fisher Biotech
Sodium phosphate, monobasic	CAS 10049-21-5	Fisher, Fair Lawn, NJ
Sodium selenite	CAS10102-18-8	Sigma, St.Louis, MO
Sodium selenate	CAS13410-01-0	Sigma, St.Louis, MO
Tetradecyltrimethyl ammonium bromide	CAS 1119-97-7	Sigma, St.Louis, MO

*CAS- Chemical Abstracts Service

The stock solution (1000 ppm of As) of arsenite (As(III)), arsenate (As(V)), and DMA were prepared separately by dissolving 0.1734 g $NaAsO_2$, 0.4164 g $Na_2HAsO_4 \cdot 7H_2O$, and 0.2133 g $C_2H_6AsO_2Na$ into 100 mL milli-Q water. The stock solution (100 ppm of As) of MMA was prepared by dissolving 0.0389 g $CH_3AsNa_2O_3 \cdot 6H_2O$ into 100 mL milli-Q water. The stock solution (1000 ppm of Se) of selenite and selenate were prepared by dissolving 0.222 g Na_2SeO_3 and 0.242 g Na_2SeO_4 into 100 mL milli-Q water. All stock solutions were stored in refrigerator at 4 °C.

The buffer solutions of HPLC-ICP-MS were prepared by dissolving 2.1166 g $NH_4H_2PO_4$ and 0.2133 g $(NH_4)_2HPO_4$ into 1 L milli-Q water for 20 mM ammonium phosphate buffer, or other appropriate weights to obtain required concentrations. The pH of the buffer solutions was adjusted to 6.0 by drop wise addition of diluted phosphoric acid or ammonium hydroxide. The ion pair reagent, hexadecyltrimethyl ammonium bromide (CTAB), was prepared by directly adding an adequate amount of $C_{19}H_{42}BrN$ to 1L buffer solutions to produce 1 mM, 5 mM and 10 mM concentrations (e.g. 3.6445 g for 10 mM CTAB solution). The mobile phase was mixed 98% v/v 20 mM ammonium phosphate buffer and 10 mM CTAB solution with 2% v/v methanol by HPLC pump.

The buffer solutions for CE-ICP-MS required mixing 7.62 g $Na_2B_4O_7 \cdot 10H_2O$ and 0.336 g $C_{17}H_{38}NBr$ into 1 L milli-Q water to make 20 mM sodium borate buffer for selenium at pH 9.5, or 6.20 g $NaH_2PO_4 \cdot H_2O$ and 1.34 g $Na_2HPO_4 \cdot 7H_2O$ to 1 L milli-Q water to make 50 mM sodium phosphate buffer for arsenic at pH 6.0. 1 mM tetradecyl trimethyl ammonium bromide (TTAB) was added to borate buffer as an osmotic flow modifier to reverse the EOF flow direction to anode.

Working solutions of arsenic and selenium were prepared daily by appropriate dilution from the stock solutions with milli-Q water. All solutions and mobile phases were filtered through 0.45 μm Teflon filter (Gelman Instrument Company, Ann Arbor, MI). The mobile phases were degassed using an ultrasonic bath for 20 minutes and also a helium sparge for 10 minutes before starting the chromatography.

Instrumentation

Capillary Electrophoresis (CE)

A capillary electrophoresis (Dionex, Sunnyvale, CA) and its UV detector were modified for coupling with the ICP-MS. The capillary (Polymicro Technologies, Phoenix, AZ) was a fused-silica capillary of dimensions 375 μm outer diameter, 75 μm inner diameter, and 80 cm length. No separate cooling system was applied to the capillary, but the temperature of the laboratory was kept constant at 25 °C by the air conditioning system. The inlet end of the capillary was connected to the positive potential of the power supply and the outer end was grounded. There were three injection modes: gravity, electrokinetic and hydrodynamic. Gravity injection was achieved by using the height difference between the two ends of the capillary. Electrokinetic injection was accomplished by applying the potential difference. Hydrodynamic injection was obtained by applying the pressure difference. Among them, electrokinetic injection was the preferable injection method for elemental speciation due to better separation resolution for a longer injection duration. The sample solution was injected electrokinetically from a 500 μL microcentrifuge sample vial (Eppendorf, Westbury, NY). The control voltage range was from 0 to 30 kV in 10 V increments and the current was from 0 to 1000 μA in 1 μA increments. The voltage can be switched to positive or negative polarity.

High Performance Liquid Chromatography (HPLC)

The chromatography system consisted of a SpectraSYSTEM P2000 Binary gradient pump (Thermo separation production Inc., Fremont, CA), an Auzx 210 injector valve with a 20 μL loop and a Haisil 100 (Higgins analytical Inc., Mountain View, CA) C18 column with 150 mm × 4.6 mm i.d. × 5 μm particles. The sample solution was injected with a 250 μL syringe (SGE international, Victoria, Australia).

Inductively Coupled Plasma Mass Spectrometry (ICP-MS)

A VG Plasma Quadrupole II (VG Elemental, Winsford, Cheshire, UK) ICP-MS was used. The ICP-MS was computer controlled (Dell Dimension XPS 4100, Dell, TX, USA) and VG instrument control software (Plasma Quad, Version 4.30, VG elemental 1996) was operated under the OS/2 (IBM, USA) system. The liquid sample was injected by a peristaltic pump (Rainin, Woburn, MA) to a Meinhard TR-30-A concentric nebulizer (Precision glassblowing, Englewood, CO). After nebulization, sample was transported to the ICP torch through a spray chamber held at 5 °C. Ion transport was aided by sample and skimmer cones which were made from purity nickel. Ions were detected by an electron multiplier (Detector technique, inc., Palmer, MA) after passing through the quadrupole. The ICP-MS data acquisitions during the CE-ICP-MS or HPLC-ICP-MS analyses were performed in a time resolved acquisition (TRA) mode. The scanning mode was used to optimize the ICP-MS working conditions. The ICP-MS system was optimized using the ^{115}In signal from a 1-ppm Indium solution. The ICP-MS operating conditions are summarized in Table 4-2.

Table 4-2. Typical ICP-MS operating conditions.

RF power	1350 W
Reflected power	10 W
Coolant gas flow rate	13.5 L/min
Auxiliary gas flow rate	0.95 L/min
Nebulizer gas flow rate	0.880 L/min
Nebulizer pressure	40 psi
Sampler cone orifice	1.00 mm, Ni
Skimmer cone orifice	0.70 mm, Ni
Detector mode	pulsing counting
Pulse counting discrimination	20
Analyzer pressure	5×10^{-7} mbar
Resolution setting	3.00 (normal)
Data acquisition parameters for arsenic sample	
Dwell time (pulsing counting)	640 μs
Channels/amu	19
Time/Sweeps	0.5 s
Default dwell	365 ms
Points/peak	3

Analytical Procedures

CE-ICP-MS

A new capillary was conditioned by flushing with 1 M NaOH for 30 minutes, followed by rinsing with milli-Q water for 20 minutes. This conditioning procedure assured the capillary surface was uniformly charged. Daily, the capillary was flushed with 0.1 M NaOH for 5 minutes, rinsed with milli-Q water for 5 minutes, and equilibrated with a buffer solution for 10 minutes. Between each run, the capillary was flushed with buffer solution for 5 minutes to ensure reproducible migration times. All the solutions were drawn into the capillary by self-aspiration. After the CE capillary was conditioned, the ICP-MS was turned on and rinsed by injecting 1% nitric acid for 5 minutes followed by milli-Q water for 10 minutes to remove any remaining acidic solution.

CE-ICP-MS experiment was conducted using the following procedure. First, the needle of a syringe (SGE international, Victoria, Australia) was connected to a Teflon tube and a conditioned capillary was inserted into the tube. The syringe, full of buffer, forces the injected solution through the capillary to remove air bubbles. Effort to prevent air bubbles is reported in literature [32], and is done by turning off the nebulizer gas during sample injection. However, this method has the risk of extinguishing the plasma and affecting signal stability. The syringe method used in this current study, worked efficiently and safely for CE-ICP-MS. The capillary was immersed into an arsenic sample vial, and the sample was introduced by electrokinetic injection (0.3 minutes at 15 kV). The injection volume was approximately 0.63 μL.

After sample introduction, the capillary was submerged in a 50 mM sodium phosphate buffer solution for the duration of the separation period. Concurrently, the time resolved acquisition software was initiated to acquire the electropherogram data. Separation was performed at a voltage of 20 kV with an approximate current of 56 μA. The sample solution moved through the capillary inlet, the interface of the CE-ICP-MS, and the nebulizer of the ICP-MS, respectively. The nebulizer carrier argon gas was usually set at 0.7 mL/min for CE-ICP-MS analysis. A make-up sheath flow was introduced at a flow rate of 0.23 mL/min by the peristaltic pump. It is this flow rate which carried the arsenic sample continuously through the spray chamber to the ICP torch. The temperature range of the torch was from 6000 K to 8000 K. Upon exiting the torch, arsenic ions travel through the sample cone, skimmer cone, and electronic lens system to quadrupole mass analyzer. The quadrupole mass analyzer was constantly scanned at m/z 75 for arsenic analysis. Ions of different chemical form arrived the electron multiplier at different time.

Finally, data was acquired and evaluated by the VG instrument control software. Before the CE and ICP-MS were turned off, the CE capillary was regenerated by rinsing with buffer solution for 10 minutes and the ICP-MS was cleaned by injecting 1% nitric acid for 10 minutes followed by milli-Q water for another 10 minutes.

HPLC-ICP-MS

For the first stage of HPLC-ICP-MS analysis, milli-Q water, 100% methanol, and phosphate buffer solutions were sparged by helium for 10 minutes as a degassing procedure. The HPLC was then turned on, the relieve valve was opened, and solutions were purged about 3 minutes at a flow rate of 3 mL/min. This purging procedure removed residual air bubbles and any previous solvents from the intake lines. After closing the relieve valve, the HPLC pump was set at a flow rate of 1.65 mL/min with 40% v/v milli-Q water and 60% v/v pure methanol for 10 minutes. The corresponding pump pressure was approximately 600 – 1000 psi. The actual flow rate at the end of the column was determined to be 1.0 mL/min which corresponded to a 1.65 mL/min setting of the HPLC pump. Using this information, the HPLC pump was then set at a flow rate of 1.65 mL/min with 98% v/v phosphate buffer, CTAB, and 2% v/v pure methanol for the remaining analysis. The reverse phase C18 column was equilibrated with this ion pair reagent for 80 minutes. The organic waste solution was directly discarded into the waste bottle from the column exit.

Next, the ICP-MS was turned on when the HPLC was ready. The ICP-MS was rinsed by injecting 1% nitric acid for 5 minutes followed by milli-Q water for 10 minutes to remove leftover acidic solution. The instrument was tuned daily with 100 ppb arsenic solution to achieve the same ICP-MS sensitivity with optimized lens voltage and torch position. The HPLC column was connected to the ICP-MS nebulizer by a Teflon tube.

At this point in the analysis, the injector valve was turned to the load position and the 250 μL syringe, filled with arsenic sample, was inserted into injector port. Contents of the syringe flushed and filled the 20 μL injection loop with excess sample going to a waste line. The injector valve was then turned back to the inject position. At the same time, the time resolved analysis computer program was initiated to acquire the chromatogram data. During this period, the arsenic sample traveled through the column carried by the mobile phase. The arsenic sample moved through the column exit at a flow rate of 1.0 mL/min to the ICP-MS nebulizer. Nebulizer carrier argon gas flow rate was usually set at 0.880 mL/min. Details concerning sample transportation and detection were provided previously in the discussion on CE-ICP-MS. Finally, data was acquired by the VG instrument control software and exported to Microsoft Excel (Microsoft Corporation) where integration and quantification were carried out.

Before the HPLC and ICP-MS were turned off, the HPLC column was regenerated by rinsing with 40% v/v water and 60% v/v methanol for 10 minutes, and 100% methanol for another 10 minutes. As stated before, the ICP-MS was cleaned by injecting 1% v/v nitric acid for 10 minutes followed by milli-Q water for an additional 10 minutes.

CHAPTER 5
CE-ICP-MS INSTRUMENT DESIGN

Capillary Electrophoresis Inductively Coupled Plasma Mass Spectrometry (CE-ICP-MS) Overview

The separation potential of CE, the superior element-selective detection capability of ICP-MS, and the diversity of potential applications bring CE-ICP-MS into central focus when considering elemental speciation. In 1995, Olesik and co-workers first published interfacing CE with ICP-MS and demonstrated that CE-ICP-MS could be used to speciate metals at parts-per-billion levels in aqueous solutions [33]. Since that time, a number of papers describing various interfaces and applications have been published. Some representative interface designs and applications are summarized in Table 5-1 [14, 33-57].

The key to successful coupling of CE to ICP-MS is the interface. The requirements for interfacing both instruments involve completing the electrical circuit from the CE, optimizing the nebulization efficiency, mass transport into the ICP-MS, and (in combination with capillary dimensions) reduction of suction flow through the capillary to minimize band broadening. Several approaches have been described that work along these strategies. A modified concentric Meinhard nebulizer and interface was developed and used for coupling CE and ICP-MS. This interface has several notable features. The interface is placed outside and independent of the nebulizers. It is flexible, low cost, easy to operate, and could be connected to various types of nebulizer. The parameters that influence both separation efficiency and detection limit have been

Table 5-1. Interface designs and applications of CE-ICP-MS.

Interface	Analyte	Buffer	Reference
Modified Meinhard nebulizer	Sn (II), Sn (IV)	0.04 M NaCl electrolyte, pH7.0	Olesik *et al.* 1995 [33]
Modified Meinhard nebulizer	MT-1, MT-2	20 mM Tris-HCl, pH7.1	Lu *et al.* 1995 [34]
Modified Meinhard nebulizer	Se (IV), Se (VI)	200 mM Phosphate buffer, pH6.0	Michalke & Schramel 1997 [35]
Modified Meinhard nebulizer	La compounds	20 mM ammonium acetate, ph7.0	Majidi & Miller-Ihli 1998 [36]
Modified Meinhard nebulizer	Hg compounds	20 mM tetraborate decahydrate, pH9.3	Rocha *et al.* 2000 [37]
Meinhard high efficiency Nebulizer (HEN)	K^+,Y^{3+}, Co^{2+}, Cr^{3+}, Li^+	2.7 mM $CaCl_2$, pH5.9	Kinzer *et al.* 1996 [38]
Meinhard high efficiency Nebulizer (HEN)	12 lanthanides	4 mM HIBA, 5 mM UV cat1, pH4.2	Sutton *et al.* 1998 [39]
Meinhard high efficiency Nebulizer (HEN)	Cr compounds	5 mM $LaCl_3$, pH5	Stewart & Olesik 2000 [40]
Meinhard high efficiency Nebulizer (HG-HEN)*	As(III), As(V), MMA, DMA, Ge	20 mM potassium hydrogen phthalate-20 mM boric acid, pH 9.03	Magnuson *et al.* 1997 [41]
Microconcentric nebulizer (MCN)	TML, TEL		Tangen *et al.* 1997 [42]
Microconcentric nebulizer (MCN)	MT1, MT2	20 mM tris/ HCl, pH7.8	Taylor *et al.* 1998 [43]
Microconcentric nebulizer (MCN)	As(III), As(V), MMA, DMA, AsB, AsC	20 mM borate, pH9.4	Holderbeke *et al.* 1999 [44]
Microconcentric nebulizer (MCN)	As(III), As(V), MMA, DMA, AsB, AsC	20 mM borate, pH9.3	Schaumloffel & Prange 1999 [45]
Microconcentric nebulizer (MCN)	As(III), As(V), MMA, DMA, AsB	4.4 mM sodium chromate, pH8.2	Day *et al.* 2000 [46]

Table 5-1. Continued.

Interface	Analyte	Buffer	Reference
Microconcentric nebulizer (MCN)	Hg(II), CH_3Hg, C_2H_5Hg	50 mM $NaHCO_3$ / Na_2CO_3, pH11	Lee & Jiang 2000 [47]
Direct injection nebulizer (DIN)	As(III), As(V), MMA, DMA	0.75 mM hexamethonium hydroxide, pH7.7	Liu *et al.* 1995 [14]
Direct injection nebulizer (DIN)	Cr(III), Cr(V), Cd(II)	6.5 mM HIBA, 5.0 mM UV cat1	Tangen *et al.* 1998 [48]
Direct injection high efficiency nebulizer (DIHEN)	Se(IV), Se(VI), selenocystine, selenomethionine	25 mM nitric acid and 0.5 mM cetyltrimethyl ammonium hydroxide, pH9.25	Bendahl *et al.* 2000 [49]
Cross flow nebulizer	MT-1, MT-2	50 mM tris, pH9.0	Baker & Miler-Ihli 1999 [50]
Ultrasonic nebulizer	MT-1, MT-2	20 mM tris/HCl, pH7.8	Lu & Barnes 1996 [51]
Oscillating capillary nebulizer (OCN)	As(III), As(V), DMA	4.2 mM sodium tetraborate, pH4.2	Kirlew & Caruso 1998 [52]
Oscillating capillary nebulizer (OCN) sol-gel fritted capillary	MT1, Ferritin	15 mM tris (hydroxy-methy) aminomethane, pH 6.8	B'Hymer *et al.* 1999 [53]
Muliticapillary parallel	Cs, Ba, Mn, La	20 mM ammonium acetate, pH6.5	Majidi *et a*l. 1999 [54]
High efficiency cross-flow micronebulizer (HECFMN)	Cr^{3+}, $Cr_2O_7^{2-}$	20 mM CH_3COONa, pH 7.2	Li *et al.* 2001 [55]
Meinhard, Babington type, high efficiency (HEN)	MT1, MT2	70 mM Tris/HCl, pH7.5 and 5% MeOH	Alvarez-Llamas *et al.* 2001 [56,57]

*HG-Hydride Generation

studied. The CE-ICP-MS system has been used to measure Se (IV) and Se (VI), As(III) and As(V).

Concentric Nebulizer Design

Modified Meinhard Concentric Nebulizer

For coupling CE to ICP-MS, no commercial nebulizers are available that work well at the relatively low flow typical of CE. The challenge is to achieve effective introduction of microflow from the CE to the ICP-MS without excessive band broadening, while maintaining a complete electrical circuit. A number of sample introduction modes have been used for the interfacing of CE and ICP-MS. These include the modified Meinhard nebulizer, the high efficiency nebulizer (HEN), the microconcentric nebulizer (MCN), the direct injection nebulizer (DIN), direct injection high efficiency nebulizer (DIHEN), the cross-flow nebulizer, and the ultrasonic nebulizer (USN), the oscillating capillary nebulizer. Additionally there is hydride generation with the reaction manifold and gas-liquid separator situated after the CE column. Compared with the nebulizers mentioned above, the Meinhard concentric nebulizer has advantages of simplicity and low cost.

In this research, a modified Meinhard concentric was designed to meet the requirements of CE-ICP-MS hyphenation. Three different nebulizers have been modified from the commercial Meinhard concentric nebulizers. For the first design, a glass capillary with an inner diameter of 0.40 mm and an outer diameter of 0.75 mm (A-M systems, Inc., Carlosborg, WA) replaced the inner tube of the original nebulizer. Additionally, the nebulizer nozzle was rebuilt to fit the glass capillary. For the second

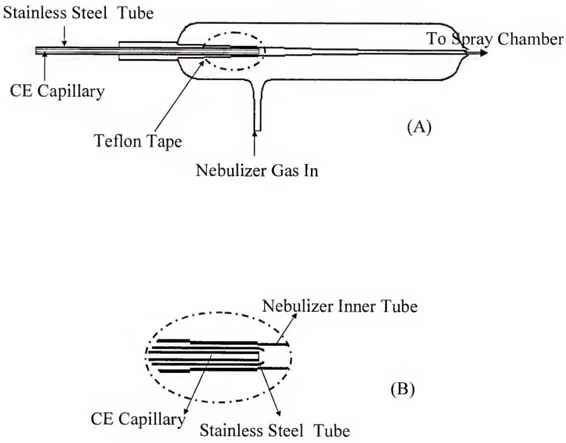

Figure 5-1. (A) Schematic of modified concentric nebulizer and (B) Expanded region (dashed).

design, the nozzle was kept as is, but the inner tube of the nebulizer was replaced by a stainless steel capillary with an inner diameter of 0.40 mm and an outer diameter of 0.72 mm and inserted into the central tube of the interface. For the third design, all parts of the commercial concentric nebulizer were kept as is with the addition of a stainless steel capillary. The capillary consisted of an inner diameter of 400 μm and an outer diameter of 720 μm, and was inserted into the inner tube of the glass concentric nebulizer end. As shown in the Figure 5-1, the CE fused silica capillary with an inner diameter of 75 μm and an outer diameter of 375 μm was inserted into the stainless steel capillary. Teflon tape was placed in the front section of the stainless steel tube to protect the nebulizer inner glass tube, but care was still taken not to push the CE capillary and stainless steel capillary too far into the nebulizer because the fine glass of the nebulizer inner tube was easy to break. The stainless steel capillary at the end of the nebulizer was inserted into a Teflon tube with a 0.80 mm inner diameter and a 1.80 mm outer diameter. Then the whole thing (stainless steel capillary and Teflon tube) was wrapped with Teflon tape and fitted to the nebulizer end with 2.31 mm inner diameter and 3.94 mm outer diameter to reduce the dead volume. These three modified Meinhard nebulizer designs were tested with standard solutions. When the results were compared with the commercial concentric nebulizer data, a mixed success was evident. The signals of the first and second designs decreased by approximately 4 times, compared to the commercial configuration. The third design worked well and the signal was comparable to the commercial nebulizer.

Optimum Capillary Tip Position

Special care was focused on the stainless steel capillary tip and the possibility of an exact and optimized positioning of the fused-silica capillary end with the argon gas

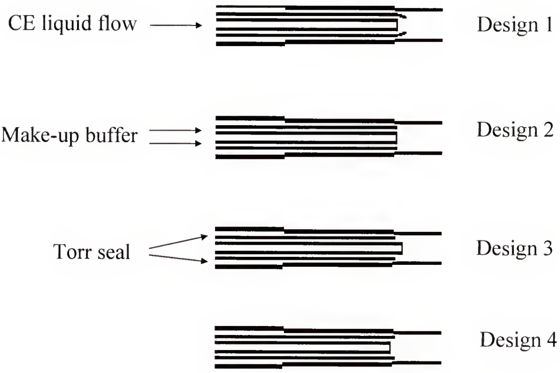

Figure 5-2. The configuration of the capillary tip.

stream. This was done to minimize dead volume and facilitate high nebulization efficiency. The stainless steel outlet tip should be minimized in order to decrease the laminar flow. The make-up buffer solution introduced into the stainless steel capillary was mixed with the CE eluent at the tip of the CE capillary. Thus, the ion signal increased slightly if the capillary was placed further inside the capillary because the sample solution was less diluted by the make-up buffer solution. However, this positioning increased the chance of introducing air bubbles into the capillary due to nebulizer suction. The electronic connection with the ground platinum electrode was formed at this point, too. The make-up buffer solution, platinum ground electrode and the stainless steel capillary provided an electrical contact at the end of the CE capillary. The capillary tip and stainless steel capillary tip position also affected the stability of CE current.

In this research, four different interface configurations were tested and shown in Figure 5-2. In design 1, the tip of the CE capillary was withdrawn about 1 mm relative to the stainless steel capillary tip. The outer diameter of the stainless steel tip was smaller than the inner diameter of the nebulizer capillary. This design worked well and had very stable CE current. The make-up sheath flow was used to create a backpressure in the tip so that the laminar flow could be controlled. In design 2 and 3, the CE current was not as stable as design 1. Design 4 was found to work well for the CE current. However, laminar flow had a negative effect on CE resolution compared to design 1. Therefore, Design 1 was used in this research.

CE-ICP-MS Interface Design

Since Olesik and co-workers reported first CE-ICP-MS system in 1995, a number of subsequent CE-ICP-MS publications have focused on the interface design. However, there are still no commercially available interfaces specifically designed for coupling CE to ICP-MS. The interface design published by Olesik *et al.* involved a CE capillary coated with silver paint to facilitate electric contact completing the electrophoresis circuit. This silver coated capillary was inserted into the center tube of a Meinhard concentric nebulizer for introduction to the ICP-MS [33]. The silver paint could cause silver contamination and a large diameter capillary had to be used to insure sufficient flow rate. Kinzer and Olesik used a high efficiency nebulizer (HEN) and an open conical spray chamber to improve aerosol transport efficiency up to 20% [38]. Advantages of the HEN interface include less internal liquid dead volume (0.2 µl) and a lower sheath flow rate required to reduce laminar flow effect. The HEN interface has a few disadvantages including its fragility and high cost in comparison to a concentric nebulizer. Tangen *et al.* used a microconcentric nebulizer (MCN-100) interface to obtain a stable spray and improve analyte transport efficiency to 20-30% at low flow rates (10-150 µL/min) [42]. The MCN interface has a problem with clogging and long wash-out times. Also, the MCN interface cannot be used for quantitative analysis because of less robustness and reliability. Baker and Miller-Ihli used a cross flow nebulizer interface due to its simplicity and high resistance to clogging. However, the sensitivity of the cross flow nebulizer interface was poor [50]. Lu and Barnes used an interface based on an ultrasonic nebulizer (USN) to eliminate laminar flow due to the eliminated need for suction [51]. The USN can also improve sample transport efficiency resulting from the production of dense aerosols containing small droplets. The USN has the drawback of high cost and high background noise level in comparison with a concentric nebulizer. Kirlew and Caruso used an oscillating capillary nebulizer (OCN) interface with sample transport efficiency approaching 100% at flow rate as low as 1 μL/min [52]. The signal output of the OCN was lower than that of concentric nebulizer. Magnuson *et al.* used a CE interface incorporated with hydride generation (HG) for arsenic speciation [41]. Large amounts of arsenic analyte were injected to improve the detection limit without significant peak broadening. However, samples which HG can be applied are limit and the chloride may cause interference at m/z 75 for arsenic.

When using a pneumatic nebulizer and interface system to couple CE with ICP-MS, the major problem is that the suction effect generated by the nebulizer can cause the forming of laminar flow through the capillary. Laminar flow broadens the peak and thus decreases the CE resolution. Increasing the sample flow rate in CE or the make-up sheath flow rate to the ICP-MS can overcome this problem. At the same time, loss of CE resolution or ICP-MS aerosol transfer efficiency needs to be considered in CE-ICP-MS system. Liu and Lopez-Avila *et al.* used a direct injection nebulizer (DIN) interface with no spray chamber, introducing liquid sample directly into the central tube of the ICP torch [14]. The DIN interface improved peak shape and sensitivity because there was no laminar flow during CE separation. Compared to the concentric nebulizer interface, the advantages of the DIN interface included low detection limit due to 100% sample transport efficiency into the ICP torch, low sample flow rate (10-100 μL/min), reduced peak broadening due to small dead volume (< 2 μL), and short rinse time with minimum memory effect. However, the DIN interface was expensive and difficult to use. It is also possible that the ICP-MS plasma could be unstable, or even extinguished, as the CE high voltage is initiated. Due to the short distance between the CE platinum electrode terminus and the ICP-MS radio frequency (RF) coil, the high voltage used for CE interferes with the ICP-MS plasma RF supply.

Generally, the diameter of a typical CE capillary is smaller than 100 μm, and the flow rate is only several hundred nL/min to several μL/min. Conversely, the sample uptake rate of ICP-MS is several mL/min. Therefore, when combining CE with ICP-MS, the make-up solution (CE buffer) is always used to compensate for the flow rate difference between CE and ICP-MS. However, introduction of the make-up solution in the interface causes dilution of the sample and thus decreases the sensitivity of the method. Majidi *et al.* used multi-capillary parallel CE to couple with ICP-MS [54]. Several individual capillaries with identical internal diameters and lengths were put in a loose bundle, and then the capillary terminal end was placed into a cross flow nebulizer. This interface design allowed more sample loading and improves the overall sensitivity and analyte detection limit without decreasing the separation efficiency. Although applying multi-capillary CE can increase the flow rate of CE to match ICP-MS flow rate, this method makes the interface more complicated due to lack of a uniform individual capillary. Even though the capillaries of the CE have the same length and conditions, the currents that pass through the capillaries are not equal and the analyte does not reach the ICP-MS at the same time. Therefore, the resolution of the CE is decreased due to the difficulty in controlling the CE separation process.

In this research, an interface for Meinhard concentric nebulizer was designed as shown in Figure 5-3. A successful interface union required low dead volume, high

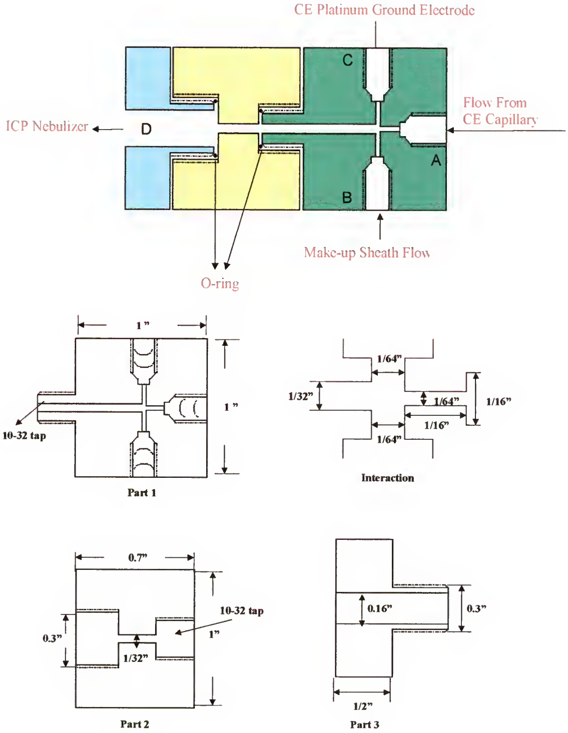

Figure 5-3. The schematic of CE-ICP-MS interface.

aerosol transport efficiency, and electrical connection to the end of the CE capillary. When a pneumatic nebulizer is used for aerosol generation, the effect of laminar flow on CE separation needs to be considered. This interface was made from 3 pieces of polymethyl methacrylate block and the whole size was 2.0 inch × 1.0 inch × 0.5 inch. It had a four-way connector that accommodated: A.) CE capillary inlet; B.) Make-up sheath flow inlet; C.) Electrical connector; and D.) Nebulizer. Due to the small CE sample injection volume, the dead volume needs to be as small as possible. The place where dead volume may exist is between the CE capillary ends that are inside of the interface and inside the nebulizer. In order to decrease the dead volume of the interface, the diameter of the connector must be as close as possible to the outside of the capillary or the platinum electrode. The interface consisted of three holes (A, B and C) with a diameter of 1/64 inch. The inner diameter of the connector (D) for the nebulizer was 0.15 inch. This interface was placed outside of the nebulizer and acted as an independent entity. The design was more flexible and could be connected to a variety of nebulizers.

Since CE involves the application of 5 to 30 kV high voltages across the capillary, an electrical connection to the end of the CE capillary is required. Typically one end of the fused-silica capillary, located inside the CE, was connected to the negative or positive high voltage through the buffer; the other end, within the interface, was connected to the platinum electrode with the ground potential through the buffer. The make-up buffer solution, platinum ground electrode, and the stainless steel capillary provided a continuous and stable electrical contact at the end of the CE capillary so that the complete electrophoresis circuit can be established.

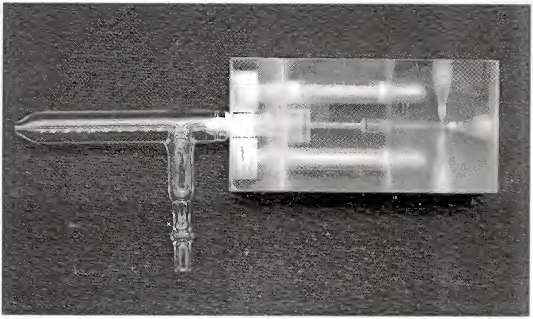

Figure 5-4. The photo of CE-ICP-MS nebulizer and interface system.

The small amount of sample volume (typically 5 to 150 nL) appropriate for CE requires a high transport efficiency of aerosol into the ICP-MS. Unfortunately, the typical ICP-MS transport efficiency is 1-2% when the sample consumption rate is 1 mL/min. The turbulent coalescence of small drops with large drops may result in loss of aerosol as it travels through the spray chamber. Even with 100% transport efficiency, the amount of sample aerosol introduced into the ICP will be less than that for a typical ICP-MS. However, when the sample uptake rate is decreased, the aerosol drop number density in the spray chamber lowers and the probability for drop-drop collisions likewise decrease. Therefore, the decrease in collision is far less than the decrease in sample flow rate compared to typical ICP-MS with a 1 mL/min sample consumption rate. This research investigated several ways to improve the sensitivity of CE-ICP-MS. For example, large injection volumes can be obtained by mixing the sample solution from the CE capillary and the make-up sheath flow (buffer solution) from a peristaltic pump; however, it diluted the sample solution and decreased the resolution. Another way to improve the sensitivity was to increase the electrokinetic injection sample volume by increasing the electrokinetic injection time. However, this approach was species and sample conductivity dependent, which complicated quantitative analysis. Also, increasing the electrokinetic injection sample volume negatively affected electrophoretic resolution.

As shown in Figure 5-4, the modified Meinhard concentric nebulizer is coupled to the interface. This modified Meinhard concentric nebulizer and interface can be easily installed, removed, and used in combination with different models of ICP mass spectrometers. The notable features of this interface were low cost, easy-to-handle and universally applicability.

CE-ICP-MS Instrument Setup

After the modified Meinhard concentric nebulizer and interface design was finished, it was used to hyphenate CE to ICP-MS as shown in Figure 5-5. The details of CE and ICP-MS instrumentation have been previously discussed in chapter 4. Parameters such as injection volume and laminar flow, which influence both separation efficiencies and detection limits, must be considered and are presented in the following sections.

CE Sampling Volume

It is very important to determine the CE sampling volume in a CE-ICP-MS system; but this is not easy due to capillary electrophoresis is an analytical technique based on micrometer level. Only a few nanoliters to microliters volume samples can be loaded on the capillary. A regular capillary can only contain a small portion of analyte in order to avoid excessive band broadening. Mei *et al.* calculated the sample volume by measuring sampling time or weighing the sample [18]. This method is inaccurate because of weighing scale limitation. Michalke *et al.* calculated the sample volume by purging sample from the capillary into outlet buffer and measuring selenium concentration by ETV-ICP-MS [58]. This method was complicated. In this research, the CE sampling volume is determined based on a calculation and experimental result.

The volume of the capillary in microliter, $V_{capillary}$, is calculated as the volume of a cylinder by Equation 5-1: [16]

$$V_{capillary} = \pi d^2 L/4 * 10^{-5} \qquad (5\text{-}1)$$

where L is the capillary length in centimeter and d is the capillary inner diameter in micrometer. Thus, the volume of a capillary with a length of 80 cm and an inner diameter of 75 μm is about 3.53 μL.

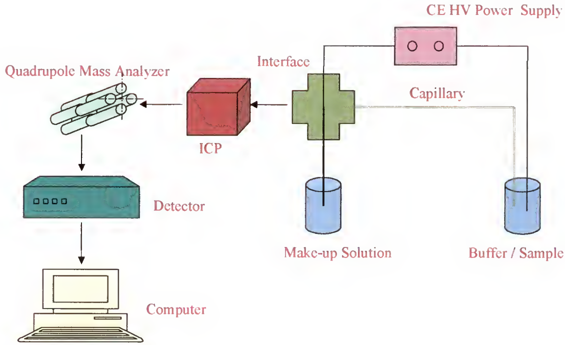

Figure 5-5. The schematic of CE-ICP-MS system.

The sample injection mode, in this research, is electrokinetic injection. The electrokinetic injection volume , V_{inject} is estimated by Equation 5-2:

$$V_{inject} = \frac{E_{inject}}{E_{separate}} \times \frac{t_{inject}}{t_{retention}} \times V_{capillary} \qquad (5\text{-}2)$$

where E_{inject} is the injection potential in volt, $E_{separate}$ is the separation potential in volt, t_{inject} is injection time in second, and $t_{retention}$ is the analyte retention time in second. The time from nebulizer to detector is so small that it can be considered negligible. Thus, for a sample that is electrokineticly injected for 18 s at –15 kV and separated for 180 s at –20 kV, the injection volume with the above capillary would be 0.26 μL.

The sampling volume, V_{sample}, can also be determined directly by CE-ICP-MS. For this research, a 40 ppm arsenic sample (20 ppm arsenite and 20 ppm arsenate) was electro-injected for about 18 s at –15 kV. After injection, the sample was pushed by a syringe (SGE international, Victoria, Australia) and immediately transferred to the capillary outlet. The sample was introduced to the ICP-MS with make-up buffer solution and time resolved acquisition was used to acquire data. The total CE peak area of the 40 ppm arsenic sample injected from CE was 31971 counts. Next, flow injection was used to introduce 134 μL of 400 ppb arsenic sample by the injection valve. The sodium phosphate buffer was injected continuously to the ICP-MS when the arsenic sample was not being injected. Time resolved acquisition was used to acquire data as shown in Figure 5-6. The average counts of the 400 ppb of 134 μL arsenic sample was 203400 counts as shown in Table 5-1.

Table 5-1. The signal of 400 ppb arsenic solutions.

File No.	As 400 ppb1	As 400 ppb2	As 400 ppb4	Average
Signal (counts)	208515	198635	203052	203400

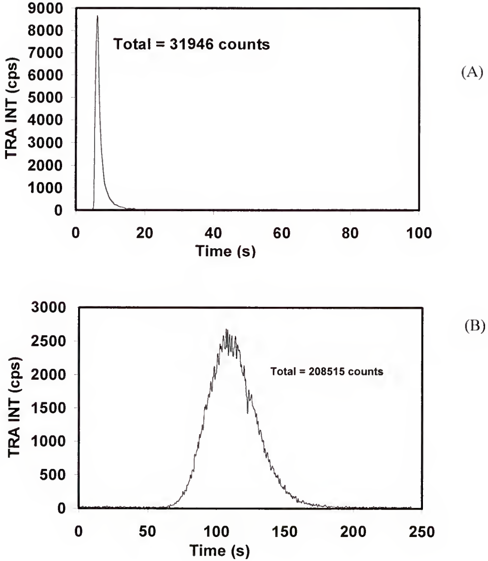

Figure 5-6. ICP-MS TRA signal observed when (A) Electro-injection 40 ppm arsenic solution from CE; (B) Flow injection 400 ppb arsenic solution from ICP-MS.

Then, the CE injection sampling volume, V_{sample}, can be calculated based on Equation 5-3:

$$V_{sample} = \frac{C_{ICP-MS}}{C_{CE}} \times \frac{S_{CE}}{S_{ICP-MS}} \times V_{ICP-MS} \qquad (5\text{-}3)$$

where C_{CE} is the concentration of sample from the CE in ppm, C_{ICP-MS} is the concentration of sample from the ICP-MS in ppm, S_{CE} is the TRA signal for CE injection in counts, S_{ICP-MS} is the TRA signal for flow injection in counts, and V_{ICP-MS} is the flow injection volume in microliter. Thus, the CE sample volume based on the above experiment was 0.21 μL. Comparing with the injection volume of 0.26 μL based on the theory, the CE sample volume is a little bit less. This is possibly due to analyte ions were adhered to the CE capillary either by chemical absorption to the walls or by being trapped in the electrical double layer near the capillary wall.

Laminar Flow Effect

Laminar flow is normally considered undesirable in capillary electrophoresis. Ion migration and electroosmotic flow (EOF) produce nearly flat flow profiles across the capillary because it originates from the capillary wall. As shown in Figure 5-7, laminar flow produces a parabola flow profile that exhibits higher flow in the center of the capillary than near the walls. This results in band broadening and a decrease in the electrophoretic resolution. However, if there is sufficient and positive laminar flow toward the electrophoresis capillary exit, positive, neutral, and negative species can be detected from a single injection. Therefore, sometimes laminar flow can be used for speciation analysis of free metal positives, neutrals, and negatively charged metal-ligand complexes from a single injection by CE-ICP-MS.

Cross-Sectional Flow Profile Due to Electroosmotic Flow

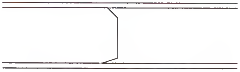

Cross-Sectional Flow Profile Due to Laminar Flow

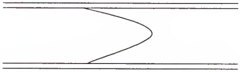

Figure 5-7. The profile of EOF and laminar flow.

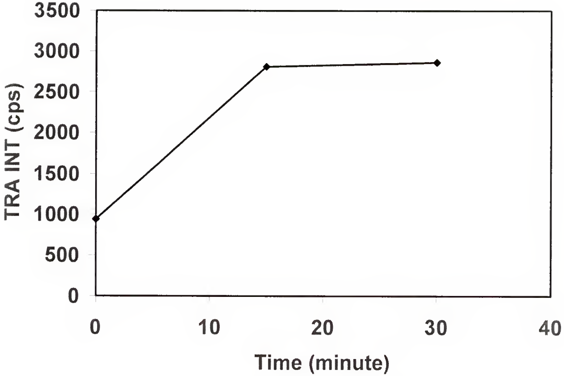

Figure 5-8. Laminar flow effect in CE-ICP-MS.

In a CE-ICP-MS system, the rapidly flowing gas that exits through the annular tip of a pneumatic nebulizer produces a suction, which can induce laminar flow in the CE capillary. The presence of laminar flow can be proved by the following method. First, mili-Q water was used to wash the CE-ICP-MS system for 20 minutes. Secondly, the capillary was immersed into a sample vial with 1 ppm indium solution for 30 minutes at no applied potential. There were no any other injections such as gravity or electrokinetic or hydrodynamic injection. The make up mili-Q water was constantly introduced into the ICP-MS. Finally, the CE-ICP-MS system was washed by mili-Q again. If there was no laminar flow, the signal after 15 minutes will be almost same as the mili-Q water at m/z 115, which is indium mass to charge ratio. If the laminar flow effect was vigorous, the indium solution in the sample vial will decrease quickly and the signal will increase significantly at m/z 115. As shown in Figure 5-8, the signal after 15 minutes increased slightly from the start point and it remained constant after 30 minutes. Therefore, laminar flow was present in this CE-ICP-MS system and the effect was not serious.

In this research, make-up sheath flow was introduced to overcome the suction effect so that laminar flow was not introduced in the capillary. The make-up sheath flow rate and nebulizer gas flow rate will be discussed in Chapter 6.

CHAPTER 6
ARSENIC SPECIATION BY CE-ICP-MS

ICP-MS Parameters Selection

The variable parameters that affect ICP-MS sensitivity include nebulizer gas flow, make-up solution flow rate, torch position, and ion lens settings.

Make Up Sheath Flow Rate

The make-up sheath flow was introduced through the interface into the ICP-MS to have a complete electrophoresis circuit and decrease the laminar flow effect. If the make up sheath flow rate is too high, it will dilute the sample solution from the CE significantly. This would cause a decrease of aerosol quality, resulting in a reduction of analyte signal intensity. Similarly, if the make up flow rate is too low, it will decrease the ICP-MS sensitivity because of lower aerosol transport efficiency and difficulty forming aerosol particles. Additionally a low flow rate cannot minimize the nebulizer suction to overcome the laminar flow effect, which decreases CE separation resolution. Therefore, the choice of make up liquid flow rate was a compromise between the CE separation resolution and ICP-MS sensitivity. Figure 6-1 describes the relationship between make up sheath flow rate and ICP-MS signal. A 1 ppm indium solution was injected as the make-up sheath flow. The 1 ppm indium solution signal increased as the make up solution flow rate increased. However, the system efficiency (signal vs flow rate) exhibited a rise followed by a decrease. As shown in Figure 6-1(B), when the make up flow rate was approximately 0.28 mL/min, the system efficiency was optimized. The sample flow rate

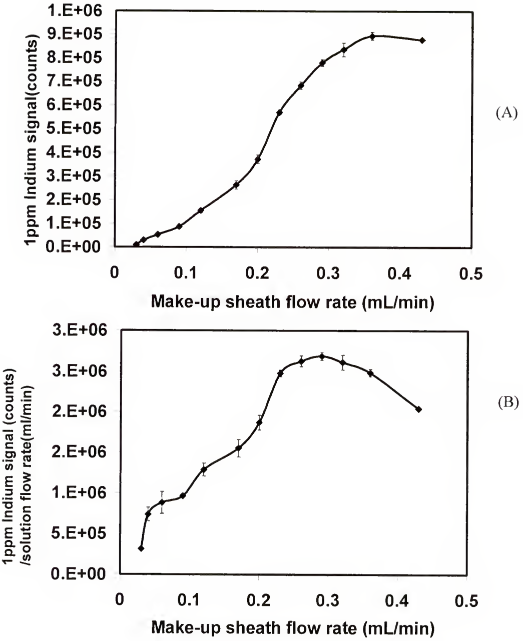

Figure 6-1. Make up sheath flow rate test by using 1 ppm Indium solution at m/z 115. (A) the relationship of make up sheath flow rate with Indium signal; (B) the relationship of make up sheath flow rate with Indium signal verse solution flow rate.

in CE capillary in microliter per minute, v, can be calculated with Equation 6-1:

$$v = V_{inject} / t_m \qquad (6\text{-}1)$$

where V_{inject} is sample injection volume in microliter, and t_m is sample migration time in minute.

As discussed in Chapter 5, the sample injection volume was 0.21 μL. The typical migration time for As(III) was 3 minutes. Thus the sample flow rate in CE capillary was 0.07 μL/min. This means the sample flow rate increased 3285 times from the CE to the ICP-MS in the present CE-ICP-MS system.

Nebulizer Gas Flow Rate

The nebulizer gas flow rate can affect signal sensitivity, migration time and separation resolution of CE-ICP-MS system. Among them, optimization of the nebulizer gas flow for maximum sensitivity is most important. If the nebulizer gas flow rate is too low (e.g. less than 0.5 L/min), the generation and transport efficiency of a fine aerosol into the ICP will be low, even not sufficient to punch a channel through the plasma torch. If the nebulizer flow rate is too high (e.g. more than 1.1 L/min), the amount of analyte ions produced in the torch is decreased because the plasma temperatures are decreased by the introduction of too much liquid aerosol. In this research, the nebulizer gas flow rate was tested with a 1 ppm indium solution. As shown in Figure 6-2, when the nebulizer argon gas flow rate was about 1 L/min, the highest signal of 8.7×10^5 at mass 115 was reached with a corresponding nebulizer pressure of 28 psi (pounds per inch). This optimum nebulizer gas flow rate and corresponding nebulizer pressure can vary with different nebulizer designs and different positions of fused-silica capillary and stainless steel capillary. The higher nebulizer flow rate can also reduce the spray chamber wash

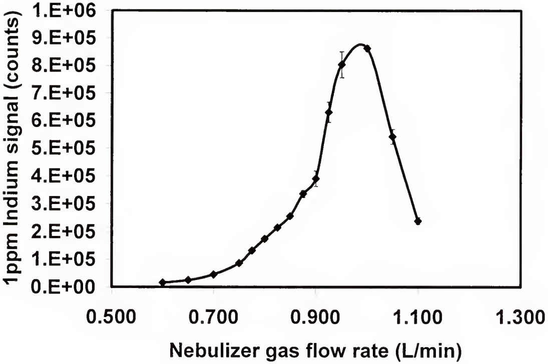

Figure 6-2. Modified Meinhard concentric nebulizer gas flow rate test.

out time to improve the sensitivity. The effect of nebulizer flow rate to migration time and separation is complex. Usually, higher nebulizer flow rate can decrease migration time, making separation quick and efficient. However, there is the possibility of decreasing migration time to the point that resolution is sacrificed. Higher nebulizer flow rate can also increase laminar flow effect due to increase suction from the nebulizer. Therefore, a nebulizer flow rate of 0.8 L/min was chosen in some of the experiments for better CE separation resolution and ICP-MS sensitivity.

Ion lens Settings

The torch position and ion lens settings need to be optimized to achieve better ICP-MS sensitivity and resolution. Considering this CE-ICP-MS system, mass spectrum's peak shape and peak height depend on torch position and voltage applied to ions lens, in conjunction with previously mentioned nebulizer gas flow rate, solution flow rate, auxiliary gas flow rate, and cooling gas flow rate. The torch was positioned by adjusting the end of the auxiliary tube 3 mm behind the load coil. The front and back level was set at 5 mm, and the up and down level was set at 7.3 mm by the knob. At this position, the center of plasma channel resided exactly at the center of the sample cone orifice. The ion lens settings varied with the torch position, and the mass analyzer radio frequency voltage. Generally, the optimum ion lens settings were determined by using 1 ppm indium solution and watching the signal change in time resolved acquisition mode. At the optimum condition, a typical indium peak is shown in Figure 6-3. Indium has an isotope at m/z 113 and m/z 115. If only arsenic is detected, the ion lenses settings can be specially adjusted to obtain the optimum arsenic peaks as shown in Figure 6-4. Arsenic has 100% abundance at m/z 75. The typical ion lens settings are shown in Table 6-1.

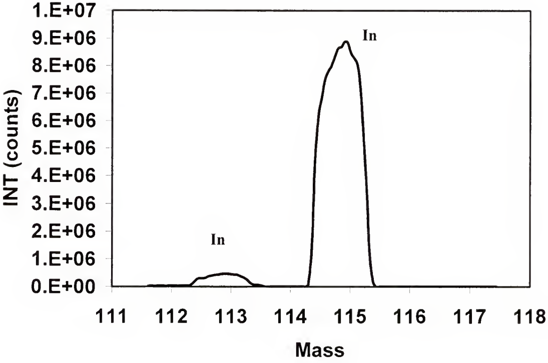

Figure 6-3. Typical indium mass spectrum of ICP-MS.

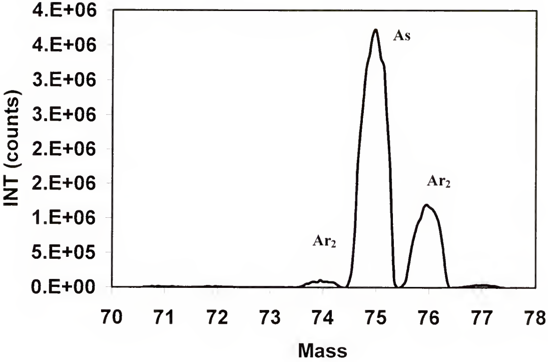

Figure 6-4. Typical arsenic mass spectrum of ICP-MS.

Table 6-1. Typical ion lens relative settings. (not actual voltage)

Extraction	L1	L3	FP
1.00	8.00	5.50	8.00
Collector	L2	L4	PB
7.70	5.40	3.80	6.00

Arsenic Detection Limit of VG PQII ICP-MS

After the ICP-MS parameters have been optimized, the arsenic detection limit of this VG Plasmaquad II ICP-MS was defined as the concentration that produced a signal equal to three times the standard deviation of the background noise (3σ) divided by the slope of the response curve for arsenic. The arsenic curve was based on mili-Q water, 1 ppb, 5 ppb, 10 ppb, 100 ppb and 500 ppb arsenic standard solution and corresponding signal. The arsenic detection limit calibration curve is shown in Figure 6-5. In the present research, the detection limit of arsenic was 1.3 ppb of VG ICP-MS.

Sample Transport Efficiency Discussion

ICP-MS Efficiency Discussion

As discussed in Chapter 2, liquid sample is changed to aerosol by the sample introduction system (nebulizer and spray chamber), and the aerosol is converted to solid particle, gaseous species, the ground-state atom, and finally the excited ion in the torch. The ion passes through the interface region (sample cone and skimmer cone) into the reduced pressure regions, and travels through electrostatic lenses into the quadrupole mass analyzer. Finally, the ion is detected and processed by the data acquisition system. Following these procedures, the sample transport efficiency of VG ICP-MS was

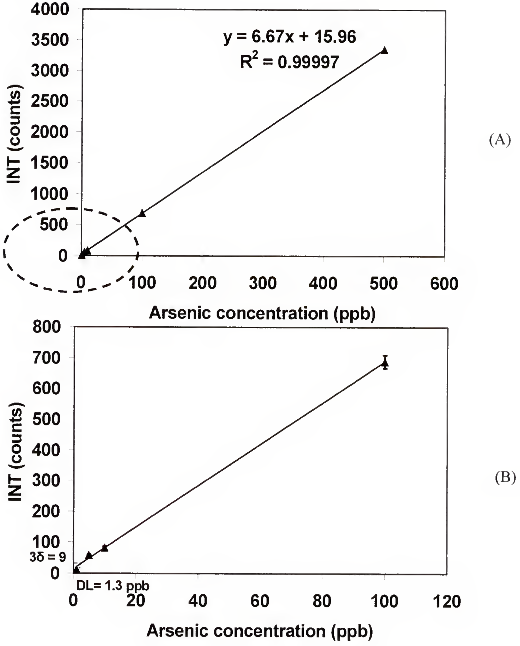

Figure 6-5. (A) Arsenic detection limit calibration curve and (B) Expanded region (dashed).

determined. The typical aerosol generation efficiency of the concentric nebulizer and Scott type spray chamber is approximately 1% in most ICP-MS instruments. Ideally, the remaining aerosol particles are transformed 100% to analyte ions. Only about 1% of the analyte ions can pass through the sample and skimmer cone. The efficiencies of the ion lens system and mass analyzer are estimated to be 10%, separately. The duty factor of pulsing counting data acquisition is estimated to be 10%, as well. Taking all these efficiencies into account, the overall analyte ion loss factor is approximated to be 10^7 to 10^8 for a typical ICP-MS [59, 60]. The losses of current VG ICP-MS with quadrupole mass analyzer is shown in Figure 6-6. The loss factor is calculated with Equation 6-2:

$$\text{Loss factor} = S_{\text{ICP-MS}} / N \qquad (6\text{-}2)$$

where $S_{\text{ICP-MS}}$ is ICP-MS signal in count, and N is the number of analyte atom in atom. The number of analyte atom with continuous injection of ICP-MS is calculated with Equation 6-3:

$$N = C \times v \times N_0 / M \qquad (6\text{-}3)$$

where C is the analyte concentration in g/mL, v is the analyte flow rate in mL/s, M is the analyte molecule weight in g/mol, and N_0 is the Avogadro constant 6.022×10^{23} atoms/mol.

For the VG ICP-MS in this research, 400 ppb arsenic was continuously injected at a flow rate of 0.313 mL/min into the nebulizer. Thus the initial flow rate of atoms was 1.67×10^{13} atoms/s. The ICP-MS signal of this 400 ppb arsenic was 659537 counts per second (cps) as shown in Figure 6-7. The ICP-MS signal to sample introduction ratio was 3.9×10^{-8} count per atom. Therefore, the analyte atom loss factor of this VG ICP-MS was approximately 2.5×10^7 for arsenic.

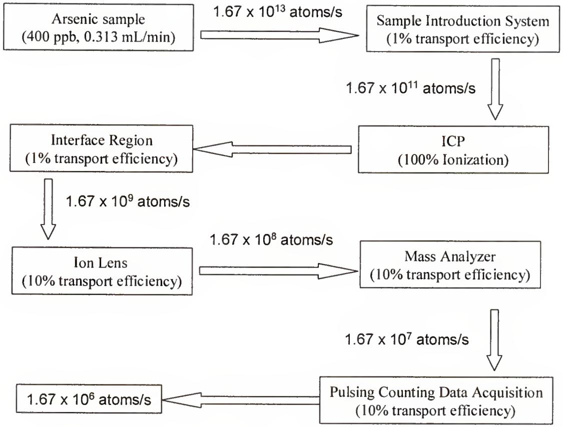

Figure 6-6. Block diagram of losses in VG ICP-MS (Quadrupole) instrument [59, 60].

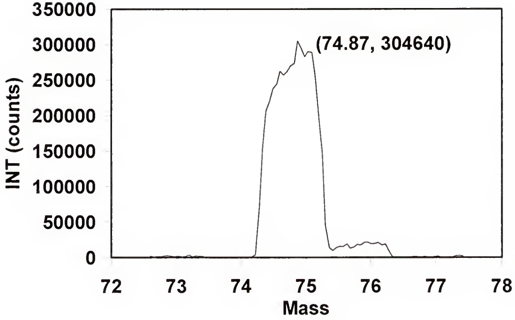

Figure 6-7. The peak of 400 ppb arsenic with continuous injection at flow rate 0.313 mL/min.

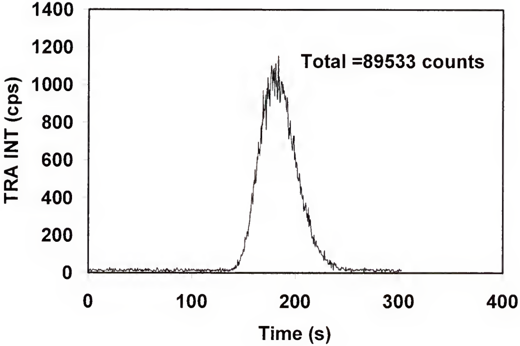

Figure 6-8. The peak area of 400 ppb arsenic with 134 μL injection by flow injection.

Different Data Acquisition Mode Efficiency Comparison

The ion loss factor, 2.5×10^7, is based on the continual sample injection with scanning mode processing. When using the flow injection valve to inject 134 μL of 400 ppb arsenic, the signal was 89533 counts by the time resolved acquisition mode, as shown in Figure 6-8. The number of analyte atom with flow injection of ICP-MS is calculated with Equation 6-4:

$$N = C \times V \times N_0 / M \qquad (6\text{-}4)$$

where C is the analyte concentration in g/mL, V is the analyte injection volume in mL, M is the analyte molecule weight in g/mol, and N_0 is the Avogadro constant 6.022×10^{23} atoms/mol.

The initial analyte sample of 134 μL of 400 ppb arsenic contained 4.3×10^{14} atoms. Thus the ICP-MS signal to sample introduction ratio was 2.1×10^{-10} counts per atom. The corresponding factor of analyte atom loss of this VG ICP-MS was 4.8×10^9. Therefore, the analyte transport efficiency of flow injection and TRA mode was 100 times worse than the continual sample injection and scanning mode.

ICP-MS and CE-ICP-MS Efficiency Comparison

As discussed in Chapter 5, the sample volume introduced by CE electrokinetic injection 18 seconds at –18 kV was 0.21 μL. In this research, 0.21 μL of 40 ppm arsenic (20 ppm arsenite and 20 ppm arsenate) solution was injected and the electrophoresis peak was about 50 seconds wide. Thus approximately 0.084 ng of As(III) or As(V) were introduced into the ICP-MS per second during the peak. In comparison with the continual sample injection rate of 0.203 mL/min for 20 ppm arsenic solution, approximately 67.7 ng of arsenic (either As(III) or As(V)) was introduced into the ICP-MS per second.

Therefore, the analyte introduced for CE-ICP-MS per second was about 800 times less than the typical ICP-MS. If considering the dead volume of the interface between the CE and ICP-MS instrumentation, the amount of analyte introduced from the CE into the ICP-MS was even less. Therefore, the detection limit of CE-ICP-MS is around hundred times worse than traditional ICP-MS. This is the largest drawback of CE-ICP-MS when compared to HPLC-ICP-MS. As discussed in Chapter 5, in order to increase the amount of analyte into the ICP-MS, a number of groups have tried different methods to increase the sample injection volume for CE.

The sample transport efficiency of CE-ICP-MS is similar to the flow injection and time resolved acquisition mode. For example, in the ideal condition, 0.21 μL of 40 ppm arsenic (20 ppm arsenite and 20 ppm arsenate) solution was introduced directly into the ICP-MS by a syringe so that there was almost no sample loss in the capillary. The initial analyte sample of arsenic contained 6.8×10^{13} atoms and the peak height was 25207 counts as shown in Figure 6-9. Thus, the analyte atom loss factor of this CE-ICP-MS was 2.7×10^{9} for arsenic analysis.

For typical arsenic speciation conditions, 0.21 μL of 20 ppm arsenite and arsenate mixture was injected from the CE to the ICP-MS. Thus, the initial analyte atoms number of As(III) and As(V) were 3.4×10^{13} atoms each. The peak area of As(III) was 5576 counts and As(V) was 5495 counts as shown in Figure 6-10. Thus, the analyte atom loss factor was 6.1×10^{9} for As(III) and 6.2×10^{9} for As(V). Therefore, the sample transport efficiency of As(III) and As(V) in this CE-ICP-MS system is nearly equivalent.

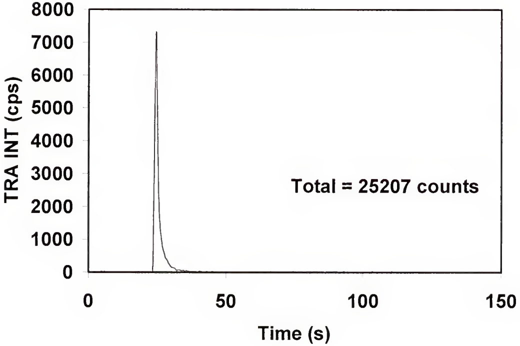

Figure 6-9. Arsenic sample pressed directly into the ICP-MS with syringe.

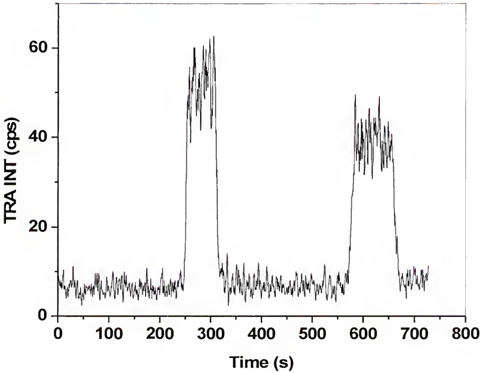

Figure 6-10. Arsenic sample transfers to the ICP-MS with CE separation.

CE Parameters Selection

When using CE for arsenic speciation, a major requirement is that the species should not be altered by the CE separation conditions. The sensitivity and separation efficiency of CE-ICP-MS should also be considered. The sensitivity of CE-ICP-MS also depends on the sample injection volume from the CE. The parameters, which affect CE-ICP-MS separation efficiency and cause band broadening, include laminar flow, long capillary length and low buffer concentration. Therefore, parameters of CE such as capillary length, high voltage, and concentration and pH of CE buffer are very important for achieving arsenic speciation by CE-ICP-MS.

CE Capillary Length and Size, High Voltage, Buffer Concentration and pH Selection

The typical CE capillary inner diameter ranges from 25 to 100 μm. For a CE-ICP-MS system, a small inner diameter capillary has less laminar flow effect due to less suction from nebulizer, which improves resolution. However the injection volume of small inner diameter capillary is limited. Large inner diameter capillary can be used in CE-ICP-MS system to increase sample-loading volume and to further improve sensitivity. However, the joule heating effect of a big inner diameter capillary should not be overlooked. Because the heat in this capillary cannot be effectively dissipated through the capillary wall causing convection related band broadening. Joule heating can also reduce sensitivity due to the increasing of baseline noise. Therefore, the standard 75 μm capillary was used in this research for CE-ICP-MS.

For the CE-UV system, the length of the capillary was about 60 cm. When CE was hyphenated to the ICP-MS, the capillary length was extended because of extra distance between the CE and ICP-MS. The longer the capillary, the more sample loss inside the capillary and the more band broadening effects due to the longer separation period. Therefore, the length of the capillary should be as short as possible and in this research it was about 80 cm.

The typical CE separation voltage ranges from 10 to 30 kV. Generally, high separation voltage is used due to its advantages of reducing retention time and sharpening peak width. Thus, high voltage can improve CE-ICP-MS resolution as long as joule heating caused by increasing voltage is not significant. Therefore, 20 kV was chosen to separate arsenic species. In this research, a positive voltage was applied and the anions moved toward the cathode because of electroosmotic flow (EOF). The EOF flow was from anode to cathode and the EOF could be more than an order great than the electrophoretic mobility. Therefore, As(III) (pKa = 9.3) moved to the cathode first by EOF flow and anionic As(V) (pKa1 = 2.3) moved to the cathode next at a flow rate of electroosmotic flow rate minus electrophoretic flow rate.

The typical CE buffer pH ranges between 2 and 10 for elemental speciation. If it is too acidic, As(III) might be oxidized to As(V), which is important to keep in mind for speciation analysis. If pH is above 10, the strong base may react with silanol and damage the positive coated capillary wall. Therefore, a pH 6 was the adequate pH for the sodium phosphate buffer of arsenic speciation. Low buffer concentrations may cause band broadening because of longer separation time. High buffer concentrations have a lesser chance to cause band broadening, as long as the increasing current does not cause apparent joule heating effect. Therefore, the buffer concentration used in this research was 50 mM sodium phosphate.

Analyte Transport Efficiency in CE

As discussed in section 6.1.5, 0.21 μL of 20 ppm arsenite and arsenate mixture was injected from the CE to the ICP-MS. The peak area of As(III) was 5576 counts and As(V) was 5495 counts. Thus the total peak area of arsenic was 11071 counts. In contrast, the same 0.21 μL of 40 ppm arsenic (20 ppm arsenite and 20 ppm arsenate) solution was injected but directly transferred into the ICP-MS by a syringe. The total peak area of arsenic was 25207 counts. This means half of the analyte was lost in the capillary. It is important to note that it takes 3 minutes for As(V) to arrive at the ICP-MS detector with CE separation condition, but only 0.4 minute or less by the pressure of the syringe and with no separation. So, less time in the capillary and fast flow rate results in less sample trapping by the capillary, less joule heating, less dilution, and less dead volume effects.

Determination of Selenium Compounds by CE-ICP-MS

After CE parameters and ICP-MS parameters were optimized, this CE-ICP-MS system was first applied to selenium speciation. Selenium is an essential trace element and an intake at low level is required for adequate nutrition. However, at high levels, it produces toxic symptoms. The toxicity of selenium is dependent on the actual species. So, instead of using high toxic arsenic compounds, selenium is a good candidate to test the CE-ICP-MS system.

Selenium has six natural isotopes at mass 74, 76, 77, 78, 80 and 82 with the corresponding abundances of 0.87%, 9.02%, 7.58%, 23.53%, 49.82% and 9.19%, respectively [28]. Selenium detection limit of this VG ICP-MS was determined by three methods including ^{76}Se, ^{78}Se and time resolved analysis data acquisition mode. The detection limit calibration curves are shown in Figure 6-11. The detection limit is defined here as a signal equal to three times the standard deviation of the background noise (3σ) divided by the slope of the response curve for selenium. The selenium detection limit was 0.027 ppm based on the peak height of ^{76}Se, 0.011 ppm based on the peak height of ^{78}Se, and 0.083 ppm based on the peak area of selenium.

As described in Chapter 4, the selenium sample was made from 40 ppm sodium selenite and sodium selenate. The buffer was 20 mM sodium borate, at pH 9.5. The electropherogram of selenium species is shown in Figure 6-12. In this plot, Se (VI) was represented by the first peak and Se (IV) by the second peak. The selenium detection limit was 0.53 ppm for Se (VI) and 0.46 ppm for Se (IV) by CE-ICP-MS. The detection limit was defined here as a signal equal to three times the standard deviation of the background noise (3σ) divided by the slope of the selenium net signal intensity to concentration.

Longer capillaries were used to connect the CE with the ICP-MS. As shown in Figure 6-13, the longer the capillary length, the longer the migration time. Capillary length of 127 cm, 96 cm, and 87 cm were evaluated and corresponded to migration time of 400 s, 350 s, and 285 s, respectively. Therefore, the length of capillary was reduced as much as possible to save a considerable amount of separation time in this research.

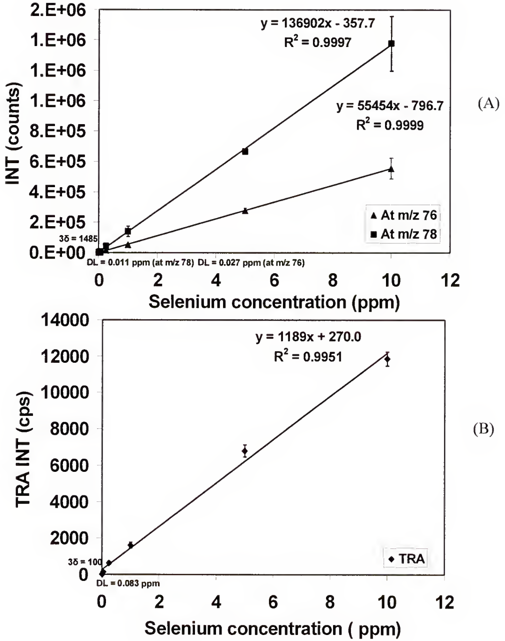

Figure 6-11. Selenium detection limit determination. (A) Selenium detection limit based on m/z 76 and m/z 78; (B) Selenium detection limit based on TRA data.

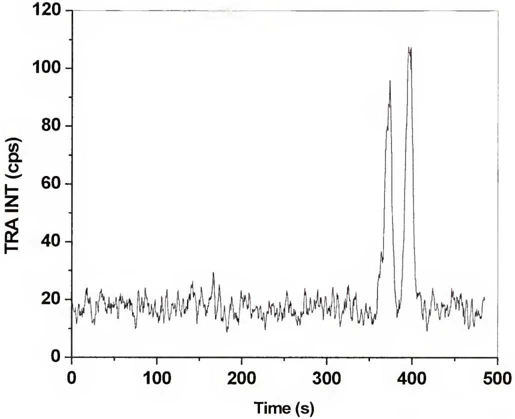

Figure 6-12. A typical electropherogram of selenium species by CE-ICP-MS. The first peak was Se (VI) and the second peak was Se (IV).

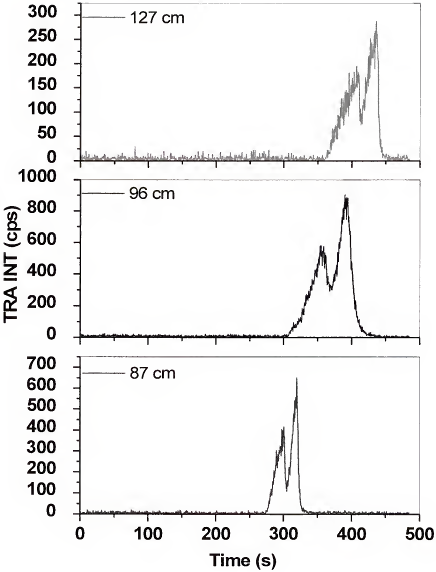

Figure 6-13. The comparison of migration times at different capillary lengths.

Determination of Arsenic Compounds by CE-ICP-MS

As described in Chapter 4, the arsenic sample contains 20 ppm sodium arsenite and sodium arsenate. The buffer was 50 mM sodium phosphate, at pH 6.0. The electropherogram of arsenic species is shown in Figure 6-14, which As(III) as the first peak and As(V) as the second peak. The arsenic detection limit was 0.12 ppm for As(III) and 0.06 ppm for As(V). The detection limit is defined here as a signal equal to three times the standard deviation of the background noise (3σ) divided by the slope of the arsenic net signal intensity to concentration.

The stability of the CE-ICP-MS system was examined by three continuously sample injection as shown in Figure 6-15. The peak height, peak area, peak width, and migration times of As(V) and As(III) were shown in Table 6-4. The peak height is the net signal intensity. The peak area, A, in count, is calculated with Equation 6-5:

$$A = \mathrm{Sum}\ (I) - I_b * N \qquad (6\text{-}5)$$

where Sum (I) the sum of signal intensity of every peak point in count, I_b is the average background intensity in count, and N is number of points of analyte peak.

The signal to noise ratio, detection limit, and signal precision value were calculated based on the peak height. Resolution, R, is calculated with Equation 6-6 [16]:

$$R = 2\ (t_{As(V)} - t_{As(III)}) / (W_{As(V)} + W_{As(III)}) \qquad (6\text{-}6)$$

where $t_{As(V)}$ is the migration time of As(V) in second, $t_{As(III)}$ is the migration time of As(III) in second, $W_{As(V)}$ is the peak width of As(V) at baseline in second, and $W_{As(III)}$ is the peak width of As(III) at baseline in second.

The peak efficiency, which is defined as the number of theoretical plates, N, is calculated with Equation 6-7:

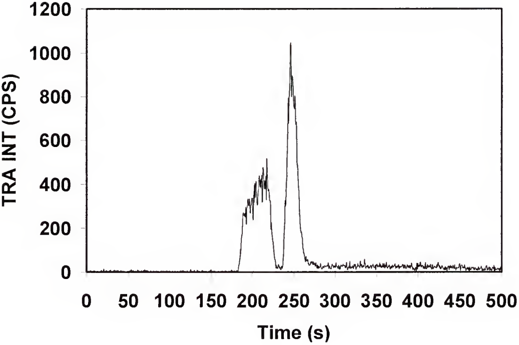

Figure 6-14. A typical electropherogram of arsenic species by CE-ICP-MS. The first peak was As(III) and the second peak was As(V).

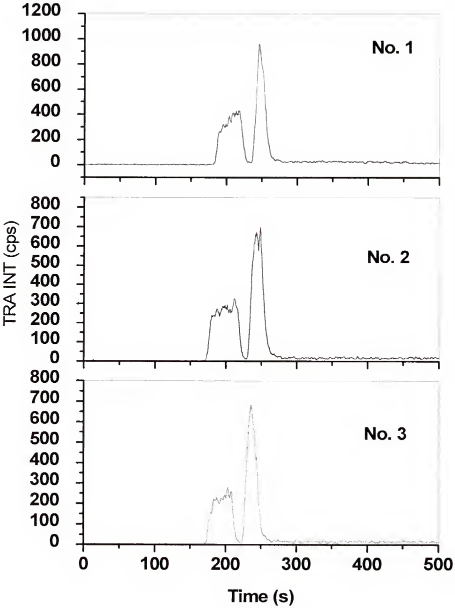

Figure 6-15. The comparison of three continuous arsenic speciation by CE-ICP-MS.

$$N = 5.54\,(t_m / W_h)^2 \qquad (6\text{-}7)$$

where, t_m is the migration time in second, and W_h is the peak width at half of the peak height in second.

Peak asymmetry, AS, is calculated with Equation 6-8:

$$AS = B / A \qquad (6\text{-}8)$$

where A is the distance from the peak front to the center of the peak at 10% of the peak height, in second, and B is the distance from the peak tail to the center of the peak at 10% of the peak height, in second.

The signal to noise ratio (S/N), resolution, peak efficiency, and peak asymmetry of As(III) and As(V) are shown in Table 6-3. The signal to noise ratio was calculated based on peak height. Therefore, the peak efficiency ranged from 225-850 theoretical plates, the peak asymmetry ranged from 0.3-1.7, and the resolution was 1.24 in this CE-ICP-MS system.

As shown in Figure 6-16, three arsenic samples were continuously injected by the CE under the same conditions and introduced into the ICP-MS by a syringe. The peak height, peak area, peak width, and peak asymmetry were shown in Table 6-4. The peak height is the net signal intensity. The peak area is calculated based on Equation 6-5.

The reproducibility of the electropherogram in Table 6-4 was better than that in Table 6-2. This indicates that CE is the major cause of loss for reproducibility and sensitivity in CE-ICP-MS system. It is largely due to the surface silica change during injection and flushing period. In the future, this research will focus on improving the efficiency of CE and ICP-MS hyphenation.

Table 6-2. As(III) and As(V) peak height, peak area, peak width and migration time comparison for CE-ICP-MS of three different trials.

		Peak height (cps)	Peak area (counts)	Peak width (s)	Migration time (s)
No. 1	As(III)	511	25921	50	217
	As(V)	1044	25552	36	246
No. 2	As(III)	379	23119	55	212
	As(V)	759	23620	39	247
No. 3	As(III)	281	15714	49	204
	As(V)	731	20412	39	234
RSD	As(III)	30%	24%	6%	3%
	As(V)	21%	11%	4%	3%

Table 6-3. As(III) and As(V) signal to noise ratio, resolution, peak efficiency and peak asymmetry comparison for CE-ICP-MS of three different trials.

		Signal to noise ratio (S/N)	Peak efficiency (N)	Peak asymmetry (AS)	Resolution (R)
No. 1	As(III)	193	332	0.34	0.68
	As(V)	395	2770	1.7	
No. 2	As(III)	151	172	0.30	0.74
	As(V)	302	1320	0.87	
No. 3	As(III)	112	274	0.5	0.67
	As(V)	290	2106	1.6	
RSD	As(III)	27%	31%	28%	4%
	As(V)	17%	35%	33%	

Table 6-4. Arsenic peak height, peak area, peak width and peak asymmetry comparison for CE-ICP-MS without CE separation.

	Peak height (cps)	Peak area (counts)	Peak width (s)	Peak asymmetry (AS)
No. 1	14193	44082	10	2
No. 2	13507	43561	10	2
No. 3	15533	44218	10	2
RSD	7%	0.8%	0	0

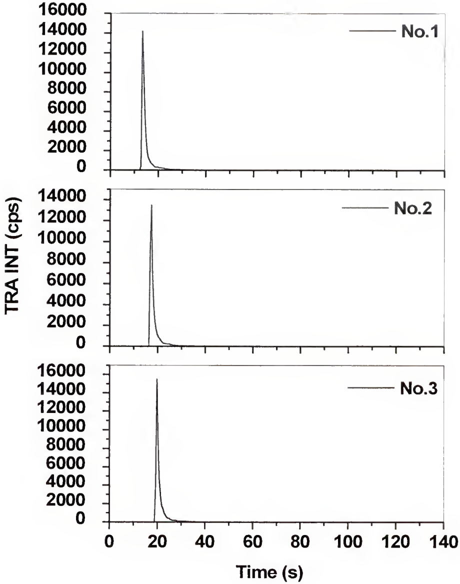

Figure 6-16. Comparison of three continuous arsenic sample injections by CE-ICP-MS without CE separation.

Conclusion

CE-ICP-MS combines the separation potential of CE and the superior elemental sensitivity and selectivity of ICP-MS. However, CE-ICP-MS has disadvantages including low liquid flow rate ranging from several hundred nL/min to several μL/min, and the requirement of a special interface for ICP-MS sample introduction. Compared with CE-ICP-MS, HPLC is more suitable coupled with ICP-MS. This is because the liquid flow rate of HPLC, which is 1 mL/min typically in the range of 0.1-10 mL/min, is consistent with the requirement of the ICP-MS nebulizer sample uptake rate (0.5-1.0 mL/min). The coupling technique of HPLC-ICP-MS is simple and just needs a short Teflon tube of small diameter to connect the end of the HPLC column to the ICP-MS nebulizer. Therefore, HPLC-ICP-MS is the most widely used technique for elemental speciation in various sample matrices, and CE-ICP-MS is a useful complementary technique for HPLC-ICP-MS.

CHAPTER 7
HPLC-ICP-MS INSTRUMENT SETUP

High Performance Liquid Chromatography Inductively Coupled Plasma Mass Spectrometry (HPLC-ICP-MS) Overview

HPLC-ICP-MS combines the high sensitivity and selectivity of ICP-MS and the separation power of HPLC. In the past 10 years, HPLC-ICP-MS has been widely applied to elemental speciation analysis, including the elements of As, Cd, Cr, Au, Pb, I ,Fe, Hg, Se, Te, Sb, Sn, V, Pt, etc. From 1986 [61] to the present, over 100 papers have been published about arsenic speciation by HPLC-ICP-MS. Three different separation methods have been employed to separate arsenic species, which include ion exchange, reverse phase ion-pair and size exclusion chromatography. A number of research groups are currently attempting to design a suitable HPLC method for efficient separation of arsenic species, and transportation from the column to an ICP-MS. Table 7-1 summaries some recent and representative arsenic speciation methods by ion-exchange HPLC-ICP-MS [8, 62-87].

Traditionally, ion exchange chromatography is widely used to separate arsenic compounds. However, ion exchange chromatography has drawbacks such as lower efficiency and short column lifetime in comparison with reverse phase chromatography. Most of all, it can't separate both ionized and non-ionized solutes at the same time. Reverse phase liquid chromatography is the most popular LC separation mode due to its high separation efficiency, good sample loading tolerance, and ability to separate a broad range of different polarity samples. Reverse phase ion-pair chromatography has been develop to routinely separate both non-ionic and ionic compounds in a signal run using the same column. However, the use of ion pairing reagent introduces additional solute-solvent interaction. Table 7-2 summaries some recent and representative arsenic speciation methods by reverse phase ion-pair HPLC-ICP-MS [88-96]. Ion pairing reagents, including tetrabutyl ammonium hydroxide (TBAH) [90, 93, 96], tetrabutyl ammonium phosphate (TBAP) [94], sodium pentanesulfonate [91], methanesulfonic acid, and propanesulfonate acid [92], have been used by other research groups.

In this research, an ion-pair reverse phase high performance liquid chromatography (HPLC) combined with an inductively coupled plasma mass spectrometry (ICP-MS) was employed to determine arsenite (As(III)), dimethyl arsenic acid (DMA), monomethyl arsenic (MMA), and arsenate (As(V)) in various sample matrices. The goal of this research was to develop a reliable and robust analytical method for routine arsenic speciation in a single run. The separation was performed on a silicon based reverse phase column (Haisil 100) by using a mobile phase containing 10 mM hexadecyltrimethyl ammonium bromide (CTAB) as the ion-pairing reagent, 20 mM ammonium phosphate buffer, and 2% methanol at pH 6.0.

Table 7-1. Applications of HPLC-ICP-MS (ion exchange) for arsenic speciation.

Analyte	Column	Mobile Phase	Sample	Reference
As(III),DMA As(V), MMA	Hamilton PRP X 100 150x4.1mm, 20 µl	30mM H_3PO_4, pH 6	Wool	Raab *et al.* 2002 [62]
As(III), AB, As(V), AC DMA, MMA	Shodex 100x7.6 mm, 20 µl	15 mM citric acid, pH2.0	Body fluid	Suzuki *et al.* 2002 [63]
As(III), As(V), MMA	TSKgel 300x7.8 mm, 200 µl	Diluted HNO_3 at pH 2.0	Sea water	Nakazato *et al.*2002 [8]
As(III), AB, As(V), AC, DMA, MMA	Hamilton PRP X 100 150 x 4.1mm, 50 µl	Gradient 15-50mM $(NH_4)_2CO_3$ pH 8.5	Lobster tissue	Brisbin *et al.* 2002 [64]
As(III), MMA, As(V), DMA	Hamilton PRP X 100 250 x 4.1mm, 10 µl	30mM H_3PO_4, pH 6	Rice plant	Abedin *et al.* 2002 [65]
AsB ,As(III), As(V), DMA, MMA	Hamilton PRP X 100 250 x 4.6mm, Supelcosil SCX 250x4.6 mm	20mM acetic acid and ammonium acetate, 20mM pyridine	Kidney	McSheehy *et al.* 2002 [66]
As(III), As(V), DMA, MMA	Hamilton PRP X-100 250x4.1mm, 25 or 100µl	10 mM $NH_4H_2PO_4$ – NH_4NO_3, pH 6.2, 1.0 mL/min	Freeze-dried apple	Caruso *et al.* 2001 [67]
AB ,As(III), As(V), DMA, MMA	IonPack As11, 250x4mm, 200 µl	NaOH, pH12.7	Ground water, soil	Vassileva *et al.* 2001 [68]
AB ,As(III), As(V), DMA, MMA	Waters IC-Pak anion HR 75x4.6 mm Dinoex AS7 & AG7 150x4.6 mm Hamilton PRP X-100 150x4.6 mm	10mM NH_4HCO_3 12.5 mM HNO_3 10 mM $NH_4H_2PO_4$	Rice	Heitkemper *et al.* 2001 [69]
As(III), As(V), DMA, MMA	Hamilton PRP X-100,150x4.1mm,10 µm, 20 µl	10mM H_3PO_4, pH 6	Soil	Yehl *et al.* 2001[70]
As(III), AB As(V), DMA, MMA	IonPack As14, 250 x 4mm	tartaric acid, ammonia, ammonium hydrogen carbonate	Urine, fish soil	Lindeman *et al.*2000 [71]
As(III), As(V), DMA, MMA	IonPack As11, 250x4mm, 100 µl	2mM NaOH-50mM NaOH, 1mL/min	Soil	Bissen & Frimmel 2000 [72]

Table 7-1. Continued.

Analyte	Column	Mobile Phase	Sample	Reference
As(III), AB, As(V), AC,DMA, MMA, TMAO, TMI	Hamilton PRP X100 250x4.1mm, 100 µl Supelcosil SCX 250x4.6mm, 5µm	30mM $NH_4H_2PO_4$ pH 6, 1.5 mL/min 20mM Pyridine, pH 2.5, 1.5 mL/min	Oyster	Chatterje 2000 [73]
As(III), As(V), DMA, MMA	Hamilton PRP X100, 250x4.1mm, 200 µl	25 mM $NH_4H_2PO_4$ and pH 5.8, 1.1 mL/min	Biota tissue	Gomez-Ariza *et al.* 2000 [74]
arsenosugar	Hamilton PRP-X100, 250 x 4.1mm, 20 µl Zorbax 300 SCX, 150 x 4.6mm,5µm	20 mM $NH_4H_2PO_4$ pH 5.6, 1.5 mL/min 20mM Pyridine, pH 2.2, 1.5 mL/min	Algal	Madsen *et al.* 2000 [75]
As(III), AB As(V),DMA, MMA	Gel Pack GI-IC-A15 150x 4.6mm, 100 µl	0.38g/L Phosphate pH10.75, 1 mL/min	Urine	Samanta *et al.* 2000 [76]
As(III), AB, As(V),DMA, MMA, AC, TMAO,TMA	IonPack As 7, 250 x 4mm, 200 µl	Gradient 0.1,0.4 or 0.5 mM HNO_3-50mM HNO_3, 0.05 mM SOS, 0.25mM SDS, 0.05mM BDSA, 1mL/min	dogfish Mushroom	Londesborough *et al.* 1999 [77]
As(III), As(V)	Dinoex AS4A 250x4 mm, 100 µl	1mM $NaHCO_3$, 4mM Na_2CO_3	Coal Fly ash	Jackson & Miller 1998 [78]
As(III), As(V), DMA, MMA	Supelcosil LC SAX 250x 4.6 mm, 5 µm, 100 µl	30 mM ammonium phosphate, pH 5.1	Urine	Kavanagh *et al.* 1998 [79]
As(III), AB, As(V), AC, DMA,MMA, TMAO, TMA	Supelcosil LC SAX 1 250x 4.6 mm, 5 µm Supelcosil LC-SCX, 250x4.6mm, 5 µm 100 µl	20 mM phosphate pH 4.16 20 mM pyridine pH 3.0	Earth-worm	Geiszinger *et al.* 1998 [80]
As(III), AB, AC, As(V), DMA,MMA, TMAO, TMA	Supelcosil LC SAX 1 250x 4.6 mm, 5 µm Supelcosil LC-SCX, 250x4.6mm, 5 µm 100 µl	20 mM phosphate pH 5.1 20 mM pyridine pH 3.0	Dog fish muscle	Goessler *et al.*1998 [81]

Table 7-1. Continued.

Analyte	Column	Mobile Phase	Sample	Reference
As(III), AB, As(V), AC DMA,MMA	Waters IC-Pak Anion HR 75x4.6 mm	10 mM phosphate pH 6.0	Mung bean seedlings	Broeck *et al.* 1998 [82]
As(III), As(V), DMA, MMA	Hamilton PRP-X100, 250x4.1mm, 10 μm, 20 μl	10 mM $NH_4H_2PO_4$-$(NH_4)_2HPO_4$ and 3% MeOH, pH 7.0, 100 mM $(NH_4)_2HPO_4$ and 3% MeOH, pH 8.5	Soil sediment	Thomas *et al.* 1997 [83]
As(III), AC As(V), AB, DMA, MMA	Anion exchange 125 x 4mm, 7-10 μm SAX, 175μl	1mM -50mM K_2SO_4, pH 10.5, 1.5 mL/min	Fishes	Branch *et al.* 1994 [84]
As(III), AB, AC, As(V), DMA,MMA, TMAO, TMA	Hamilton PRP-X100, 250x4.1mm, 10 μm, 20 μl	10 mM $NH_4H_2PO_4$-$(NH_4)_2HPO_4$ and 2% acetonitrile, pH 6.5, 100 mM $(NH_4)_2HPO_4$, pH 6.95	Fish, sediment	Demesm-ay *et al.* 1994 [85]
As(III), As(V), DMA, MMA	Ionosphere-C, 100x3mm Ion 120,125x4.6 mm 100 μl	20mM pyridinium pH 2.65 100mM NH_4HCO_3 pH 10.3	Seafood	Larsen *et al.* 1993 [86]
As(III), As(V), DMA, MMA	Wescan Anion/R-IC, 250x4.1mm, 100μl	50mM carbonate pH7.5 2% propan-1-ol	Urine Club soda Wine	Sheppard *et al.* 1992 [87]

Table 7-2. Applications of reverse phase and ion-pair HPLC-ICP-MS for arsenic speciation.

Analyte	Column	Mobile Phase	Sample	Reference
As(V), AB DMA,MMA, AC, As(V) arsenosugar	Intersil ODS-2 250x 4.6mm,5μm 100 μl	4mM Malonic acid, 0.75 mL/min	Algae	McSheehy *et al.* 2001 [88]
As(III), AB, As(V), DMA,MMA, AsSugD, AsSugB	Intersil ODS-2 250x 4.6mm,5μm 100 μl	4mM Malonic acid, 0.75 mL/min	Oyster	McSheehy *et al.* 2001 [89]
As(III), As(V), DMA,MMA, ASA, 4-OH	Discovery C18 150 x 2.1mm, 4 μm, 1 μl	5,10 or 15 mM tetrabutylammonium hydroxide (TBAH) pH5.2-7.0, 0.7mL/min	Wine	Wangkarn & Pergantis 2000 [90]
MMA,DMA, AB, AC	Phenomenex C18, 150 x 2.0mm, 5 μm	25mM citric acid, 10 mM sodium pentanesulfonate, pH 2.4		B'Hymer *et al.* 1998 [91]
As(III), AB, AC, As(V), DMA, MMA TMA	Phenomenex C18, 300 x 3.9mm, 10 μBondclone Waters Bondapak C18 300 x 3.9 mm, 20μl	10mM propanesulfonate acid, 4mM malonic acid and 0.1% methanol 10mM methanesulfonic acid, 4mM malonic acid and 0.1% methanol 10mM methanesulfonic acid, 4mM malonic acid and 2% methanol	Urine	Le & Ma 1997 [92]
As(III), AB As(V), MMA p-ASA, 4-N PAA,DMA roxarsone	Isco Spherisorb 3μm C18 material, 150 x1mm	0.1% trifluoroacetic acid and 5-10% methanol in water. TBAH (1-5mM) 15-40 μL/min	Animal feed	Pergantis *et al.* 1997 [93]
As(III), AB As(V), AC DMA, MMA	Hamilton PRP1 resin based reverse phase, 250x 4.6mm	0.5 mM tetrabutylammonium phosphate, pH9	Natural water	Thomas & Sniatecki 1995 [94]
Roxarsone	PEP RPC HR 5/10 reverse phase	5% methanol-95% 10 mM orthophosphoric acid	Chicken tissue	Dean *et al.* 1994 [95]

Table 7-2. Continued.

Analyte	Column	Mobile Phase	Sample	Reference
As(III), AB As(V), DMA, MMA	Pierce RP-18 Spheri-10, Waters radial compression C18 μBondapak, Hamilton PRP-1, Pierce 5μm C18	5% methanol pH7,0.005 M TBAH 1mL/min	Dog fish	Beauchemin *et al.* 1989 [96]

*As(III)-arsenite, As(V)-arsenate, MMA-monomethylarsonate, DMA-dimethylarsinate, AB-arsenobetaine, AC-arsenocholine, TMA-tetramethylarsonium ion, TMAO-trimethylarsine oxide, roxarsone- 4-Hydroxy-3-nitrophenylarsonic acid, (p-ASA)-p-arsanilic acid, (4-NPAA)- 4-nitrophenylarsonic acid.

HPLC-ICP-MS Instrument Setup

The details of the HPLC and ICP-MS instrument have been described in Chapter 4. The typical liquid flow rate of 1 mL/min in HPLC is in good agreement with the optimum uptake rate of a Meinhard concentric nebulizer used in the ICP-MS sample introduction system. This makes HPLC-ICP-MS coupling simple. The column exit was directly connected to the Meinhard nebulizer (TR30) by a polytetrafluoroethylene (PTFE) tube, as shown in Figure 7-1.

HPLC Parameter Optimization

In this research, the parameters that influence both separation efficiencies and detection limits will be discussed in relation to optimization. The choices of HPLC separation conditions were based on the selection and optimization of ion-pairing reagent concentration, buffer concentration, methanol concentration, pH, and mobile phase flow rate. The organic solvent and flow rate effects on ICP-MS were considered.

Elution Peak Identification

In this research, four arsenic species (As(III), DMA, MMA, and As(V)) were separated on a reverse phase column with a mobile phase containing CTAB as the ion-pairing reagent, ammonium phosphate buffer, and methanol at an optimum condition. The chromatographic behaviors of arsenic species are based on their acid or base properties (pKa value) as shown in Table 7-3. The elution order was predicted from their pKa values and verified experimentally by injecting the four arsenic species individually. When the pH of phosphate buffer solution is 6.0, arsenite is present as neutral $HAsO_2$ (pKa=9.3), which is fully protonated and not retained by the column. Hence, As(III)

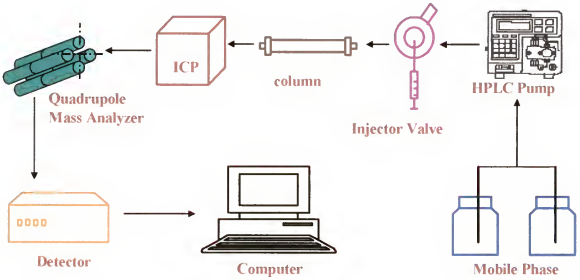

Figure 7-1. The schematic of HPLC-ICP-MS system.

elutes first with the void volume as shown in Figure 7-2 (a-d). DMA (pKa=6.2) is partially ionized at pH 6.0 and retained on the column a little longer than As(III), therefore it elutes a little later than As(III); MMA ($pKa_1=3.6$) and As(V) ($pKa_1=2.3$ and present as H_3AsO_4) are completely ionized and become anionic species, which react with hexadecyltrimethyl ammonium pairing cation and are retained longer on the column. However, As(V) elutes last due to its strong interaction with hexadecyltrimethyl ammonium pairing cation. Under the chromatographic conditions, the elution sequence is As(III), DMA, MMA, and As(V), respectively, as shown in Figure 7-2 (e).

Table 7-3. The formula and pKa value of arsenic species [27].

Compound	Formula	pKa
As(III)	O=As-OH	9.3
Dimethylarsinic acid (DMA)	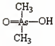 $O=\overset{CH_3}{\underset{CH_3}{As}}-OH$	6.2
Monomethylarsinic acid (MMA)	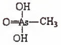 $O=\overset{OH}{\underset{OH}{As}}-CH_3$	3.6; 8.2
As(V)	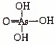 $O=\overset{OH}{\underset{OH}{As}}-OH$	2.3; 6.9; 11.4

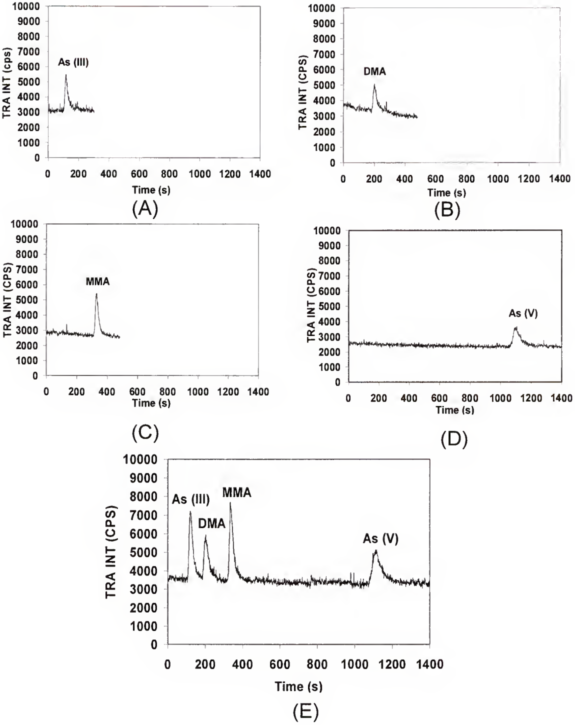

Figure 7-2. The elution sequence of As(III), DMA, MMA and As(V), respectively.

Effect of Equilibrated Time and Ion Paring Regent Concentration

In this research, the reverse phase mobile phase (98% ammonium phosphate buffer and 2% methanol) is polar and the stationary phase (silica-based bonded phase with C18 as ligand) is non-polar. Hexadecyltrimethyl ammonium bromide (CTAB) was used as the ion pairing reagent, which is a compound with a polar head (ammonium) and a non polar tail (hexadecyltrimethyl). All of the four arsenic compounds form anions. Hence, they can be separated by the anion ion pairing reagent (CTAB), which can form hexadecyltrimethyl ammonium cation. The ion pairing reagent (CTAB) was dissolved in the mobile phase, interacted with the stationary phase, and was strongly retained by the column after a period of time. Before CTAB dynamically coated on the column, the four arsenic species were not retained on the column completely and rinsed out quickly. With longer equilibration times, the retention time of MMA and As(V) got longer. Once the interaction between the ion pairing reagent and the column approached equilibrium, the retention time for four arsenic species did not change during the whole experiment. As shown in Figure 7-3, it took about 81 minutes for the retention times of the four arsenic species to stabilize for the 10 mM CTAB and 10 mM phosphate buffer condition. Therefore, the column was equilibrated with 10 mM CTAB and 10 mM phosphate buffer at 1 mL/min for 80 minutes before starting each day's chromatography runs.

The concentration of the ion pairing reagent, which is CTAB in the present research, affects the time for the column to achieve equilibrium. The higher the CTAB concentration, the sooner the column equilibrates. The concentration of the ion pairing reagent is typically in the range of 1 mM to 5 mM [97]. An increase in CTAB concentration would also increase the capacity factor, k', value. k' is given by

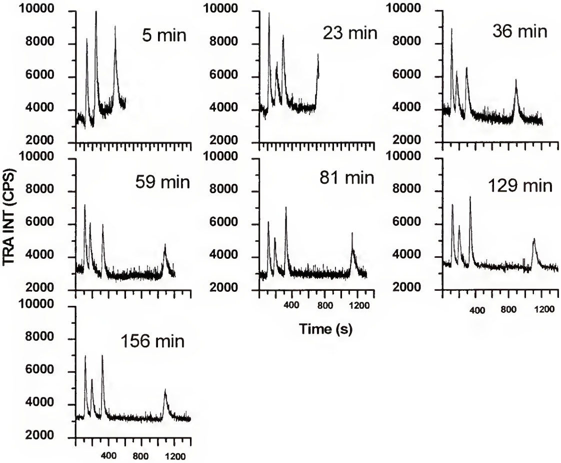

Figure 7-3. Effect of equilibrium time on arsenic species separation.

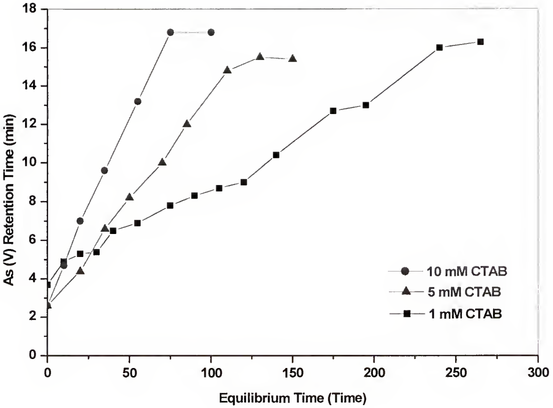

Figure 7-4. Effect of CTAB concentration on column equilibrium time.

$k' = (t_r - t_m) / t_m$, where t_r is the retention time of the arsenic species, in second, and t_m is the retention time of the void volume, in second [22].

As shown in Figure 7-4, it took 240 minutes to equilibrate the column with 1 mM CTAB; 130 minutes with 5 mM CTAB; but only 75 minutes with 10 mM CTAB holding all the other HPLC-ICP-MS conditions constant. After the column equilibrated, As(V) retention times were constant at approximately 16 minutes ± 0.17 minute, even at the different CTAB concentration conditions. Therefore, 10 mM CTAB concentration was chosen as the upper limit to equilibrate the column, and prevent clogging the sampler cone at the same time.

Effect of Methanol Concentration

The introduction of methanol into the phosphate mobile phase can affect the HPLC-ICP-MS system by achieving better separation and higher sensitivity. As shown in Figure 7-5, the addition of methanol (1% - 3% v/v) improved the resolution between DMA and MMA by decreasing the hydrophobic interaction between the C18 stationary phase and the CTAB. For the same 100 ppb arsenic solution, the signals of four arsenic species increased when 1%-2% v/v methanol was added into the mobile phase, but this decreased as the methanol concentration increased above 3% v/v. The influence of methanol concentration on the arsenic signal was further investigated by directly introducing it into the ICP-MS, which is shown in Figure 7-6. These results are similar with those from Demesmay group [85]. A small amount of methanol (1% - 2% v/v) can increase the sensitivity. This is due to the methanol improving the nebulization and transportation of the eluent aerosol into the ICP by reducing the aerosol particle size. Small amounts of methanol can also increase ionization efficiency. However, the use of

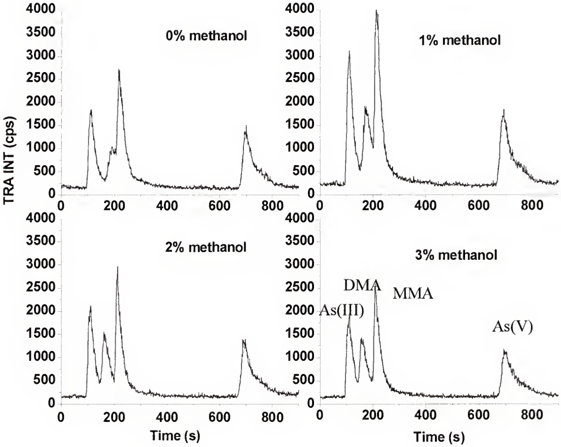

Figure 7-5. Effect of methanol concentration on arsenic species separation.

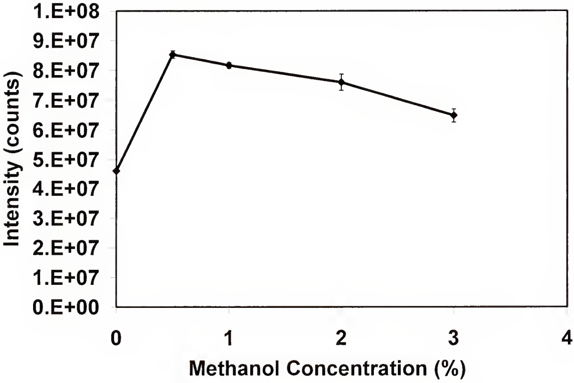

Figure 7-6. Effect of methanol concentration on arsenic signal of ICP-MS.

higher methanol concentration (> 3% v/v) is not advised. A higher organic solvent (methanol) concentration can cause ICP-MS problems: (a) decrease in the sensitivity due to the deterioration of the plasma property for the ionization of arsenic; (b) deposition of solid carbon on the sample and skimmer cones resulting in blocking the orifices; and (c) even extinction of the plasma.

Therefore, 2% v/v methanol concentration was chosen as the condition optimizing stability and sensitivity of the ICP-MS and separation efficiency of the HPLC. Most of the organic solvents (methanol and CTAB) were frozen and adhered to the inner wall of the spray chamber at 5°C, which was maintained by a chiller. With 2% v/v methanol, there was almost no carbon deposition on the skimmer cone and little clogging of the sampler cone of the ICP-MS over a period of 8 hours. The sample cone should be ultrasonically cleaned after 2-3 days of operation in order to maintain the high sensitivity of the ICP-MS. However, the lifetime of sampler cone is shorter when introducing methanol into the system.

Effect of Phosphate Buffer Concentration

Phosphate buffer has been used in many arsenic studies with either ammonium ion or sodium ion used as the counter ion. In this research, ammonium phosphate buffer was chosen since sodium is not desirable for use in an ICP-MS. Sodium phosphate buffer would decrease the sensitivity and increase the possibility of salt coating on the sampler cone. Ammonium phosphate had no effect on the ICP-MS signal.

As shown in Figure 7-7, the retention times of arsenic species shortened as the phosphate buffer concentration increased. For example, it took As(V) 29 minutes to elute completely with a 5 mM phosphate buffer condition; 19 minutes with a 10 mM phosphate

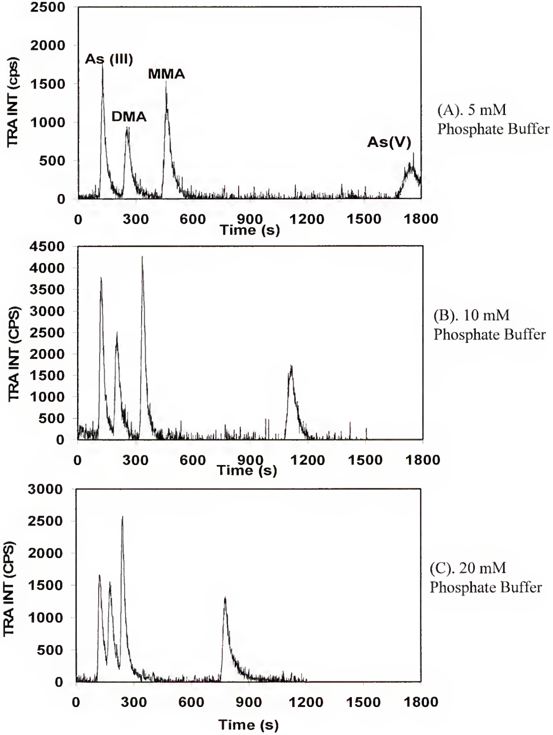

Figure 7-7. Effect of phosphate buffer concentration on arsenic species separation.

buffer condition; and only 13 minutes at a 20 mM phosphate buffer condition. This is due to the interaction of the ion pairing reagent and phosphate buffer in the mobile phase and their subsequent interactions with the stationary phase. The $H_2PO_4^-$ and HPO_4^{2-} anions should compete with As(V), DMA, and MMA anions in their interactions with CTAB. When the phosphate buffer concentration is increased, the pairing of $H_2PO_4^-$ and HPO_4^{2-} anions with hexadecyltrimethyl ammonium cation increased, and hence the pairing of As(V), DMA and MMA anions with hexadecyltrimethyl ammonium cation decreased. Thus the retention times of arsenic species decreased and were rapidly eluted from the column, but with poorer resolution.

Therefore, the mobile phase, which contained 98% v/v of 20 mM ammonium phosphate buffer and 10 mM CTAB with 2% v/v methanol, was suitable to HPLC-ICP-MS without any special precautions.

Effect of Phosphate Buffer pH

The pH of the mobile phase was also very important for the separation because the form of arsenic species in the mobile phase varied with pH. The use of a silica based column required a pH range of 2 to 8. At higher pHs (above the pKa value 6.2 of DMA), DMA is deprotonated, which could overlap with MMA. At pH values lower than 5.5, DMA was a neutral molecule which will elute with As(III) in the void volume. At a pH of 6.0, DMA was partly ionized so that it could be separated from the completely ionized MMA and As(V) and uncharged As(III). The separation of four arsenic species was investigated by using an ammonium phosphate buffer at different pH values. As shown in Figure 7-8, the retention times of As(V) and DMA became smaller as the phosphate buffer pH decreased. This is because the As(V) and DMA anions converted to neutral

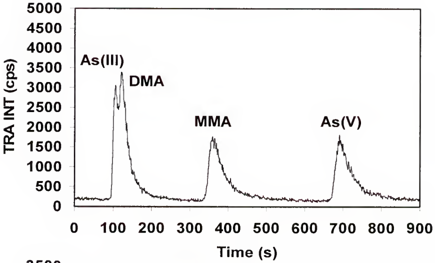

(A). pH= 5.0

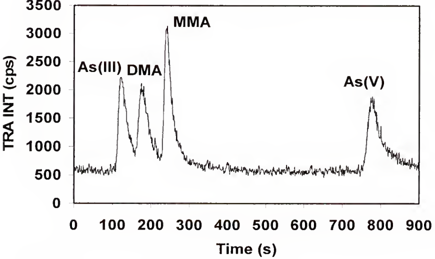

(B). pH= 6.0

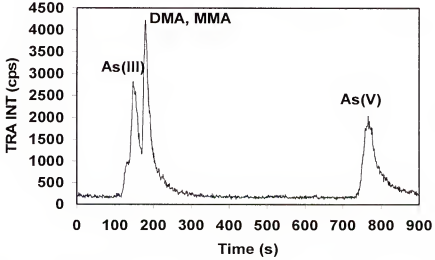

(C). pH= 7.0

Figure 7-8. Effect of phosphate buffer pH on arsenic species separation.

molecules. As a result, the ion pairs of the CTAB cation and arsenic anions decreased, and the capacity factor likewise decreased. The retention behavior of MMA was different from As(V) and DMA and the retention time of MMA increased with the decreasing pH. This can be explained by the stronger interaction between the MMA anion and CTAB cation at lower pH values; thus, MMA would be retained longer on the column. Therefore, a pH of 6.0 was chosen so that DMA could be better separated from As(III) and MMA.

Effect of Mobile Phase Flow Rate

The flow rate of the mobile phase affected both HPLC separation efficiency and ICP-MS sensitivity. As shown in Figure 7-9, the flow rate of 0.8 mL/min, 0.9 mL/min and 1.0 mL/min were compared. Lower flow rates resulted in longer retention times of arsenic species. The longer retention times would increase the number of theoretical plates hence achieving better resolution. However peak broadening and peak tailing also increased because arsenic species were retained on the column too long. There were no significant changes of ICP-MS signals relative to flow rates ranging from 0.8 mL/min to 1.0 mL/min. Therefore, the mobile phase flow rate was set at 1.0 mL/min so that the separation could be carried out in the shortest time and this flow rate was still compatible with ICP-MS optimum flow rate.

Gradient Elution

To optimize the HPLC-ICP-MS system, the influence of mobile phase (CTAB, phosphate buffer and methanol) concentration, pH, and flow rate were studied. As discussed in Section 7.3.4, the resolution improved as the phosphate buffer concentration decreased, but the retention time for all arsenic species increased. Gradient elution

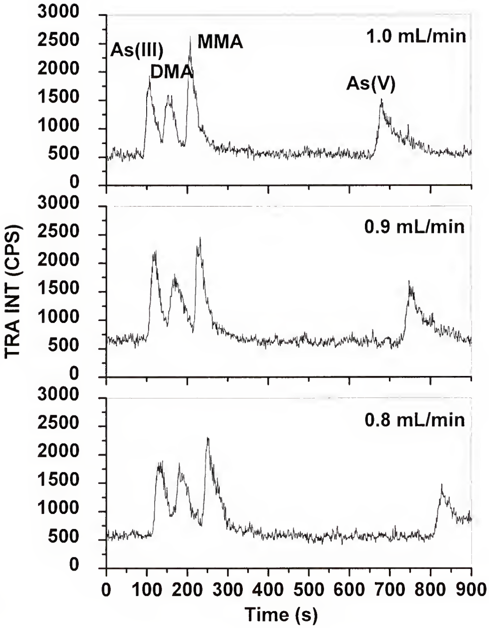

Figure 7-9. Effect of mobile phase flow rate on arsenic species separation.

method was evaluated by using a flow rate of 1 mL/min, 5 mM ammonium phosphate buffer in mobile phase A, and 30 mM ammonium phosphate buffer in mobile phase B. The gradient program was constant at 100% A for 5 minutes, then ramped to 100% B from 5 to 10 minutes, and held steady at 100% B for 5 minutes. The column had to be re-equilibrated for 2 minutes between each run. As shown in Figure 7-10, all of arsenic species were nearly baseline resolved within 15 minutes and reproducibility of retention times were good under this condition. This indicated that gradient elution could minimize arsenic species retention times and ensured better separation. The sloping baseline was significant because the impurity of arsenic in the ammonium phosphate buffer varied with different ammonium phosphate buffer concentrations. Therefore, the ICP-MS sensitivity varied over a chromatographic run. Gradient elution also introduced high concentration ammonium phosphate buffer into the ICP-MS which required a longer re-equilibration time to condition HPLC column. Therefore, an isocratic method was preferred in this research. This isocratic method provided a stabile baseline of ICP-MS signal throughout the entire elution of arsenic species, and a satisfactory separation in a shorter analysis time without re-equilibration of the column.

Spectroscopic Interference

Chloride or chloride containing reagents present in the sample matrix may react with the working gas, which is argon in this research, resulting in the formation of ${}^{40}Ar^{35}Cl^+$ (m/z = 75). The polyatomic argon chloride ion signal would interference with ${}^{75}As$ in ICP-MS analysis, leading an inaccurate result. In order to investigate the $ArCl^+$ effect in this research, sodium chloride solutions with concentrations ranging from 1 to 1000 ppm were analyzed by HPLC-ICP-MS, as shown in Figure 7-11. Up to a

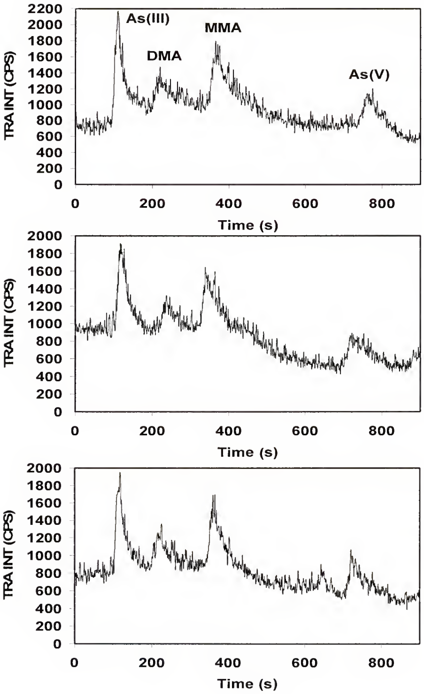

(A) Run No. 1

(B) Run No. 2

(C) Run No. 3

Figure 7-10. Gradient HPLC-ICP-MS chromatograms of four arsenic species.

concentration of 1000 ppm, no significant signal of $ArCl^+$ could be detected in a chromatographic run of 10 minutes. In addition, mobile phase was analyzed by HPLC-ICP-MS and no $ArCl^+$ peak was observed within 10 minutes under the optimized experiment conditions. These chromatograms were compared with the chromatogram of 1 ppm arsenic species standard at the same employed conditions.

New Column and Old Column Comparison

The lifetime of this Haisil 100 C18 silica based column is around 6 months with this employed experimental condition (CTAB as ion pairing reagent, ammonium phosphate buffer and 2% v/v methanol). The retention times of four arsenic species lengthened after using a new column for a period of time. As shown in Figure 7-12, for a standard solution containing As(III), DMA, MMA, and As(V) (each species 100 μg As L^{-1} (ppb)) under the same optimized conditions, the arsenic species peaks were sharper and the total analysis time was less than 10 minutes when the column was only used for a month. The peaks were broadened and the analysis time increased to 15 minutes when the column was used for more than 6 months. In the previous discussion, the same arsenic species with the same chromatographic condition occurred different chromatograms. The differences of chromatograms were due to using two different aged columns. However, this should not affect the optimization procedure.

Characteristics of HPLC-ICP-MS Method

The arsenic detection limit of the VG ICP-MS has been discussed in Section 6.1.4 and was 1.34 ppb. In September 2002, the length and position of the lens holder were changed and the sensitivity of this instrument was improved. The new arsenic calibration curve was based on mili-Q water, 0.1 ppb, 1 ppb, 10 ppb, and 100 ppb arsenic standard

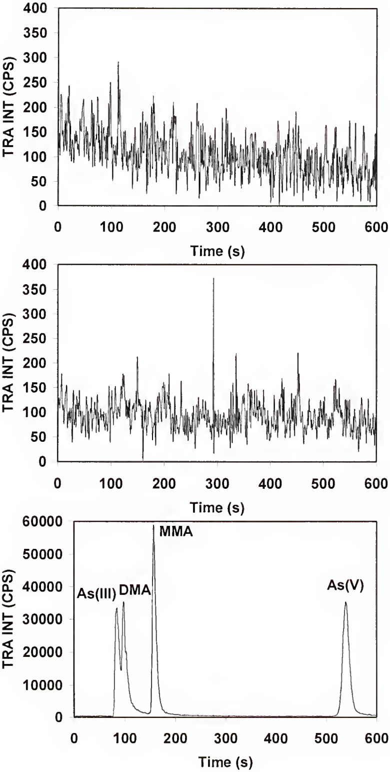

(A). 1000 ppm NaCl

(B). Mobile phase only.

(C). 1 ppm As(III), DMA, MMA and As(V) standard.

Figure 7-11. Spectroscopic interference comparison.

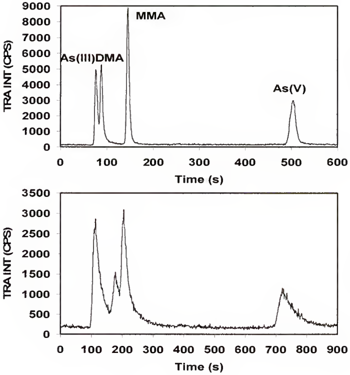

(A). New column within a month.

(B). Old column more than 6 month.

Figure 7-12. The chromatograms of arsenic species using different aged columns.

solution and then corresponding signals. The arsenic detection limit was calculated based on the concentration producing a signal equal to three times the standard deviation of the background noise (3σ) divided by the slope of the response curve for arsenic. The detection limit calibration curve is shown in Figure 7-13. The detection limit of arsenic is now 0.05 ppb.

The arsenic species detection limits of HPLC-ICP-MS were obtained by using a standard solution containing 100 ppb As(III), DMA, MMA, and As(V) and a 20 μL sample injection loop under the optimized conditions. The detection limit was calculated as three times the standard deviation of the background signal. Peak areas were used for quantification. The detection limits of arsenic species with HPLC-ICP-MS were 0.5, 0.4, 0.3 and 1.8 ppb of arsenic for As(III), DMA, MMA, and As(V), respectively.

The linearity study of the calibration curves was carried out by using arsenic standard concentrations of 0.1 ppm, 1 ppm and 10 ppm. The correlation coefficients were higher than 0.98 for all species shown in Figure 7-14.

Therefore, the detection limit and linearity of arsenic calibration curves indicated that the present HPLC-ICP-MS method would be suitable for speciation and determination As(III), DMA, MMA, and As(V) in environmental samples without any pre-conditioning requirement.

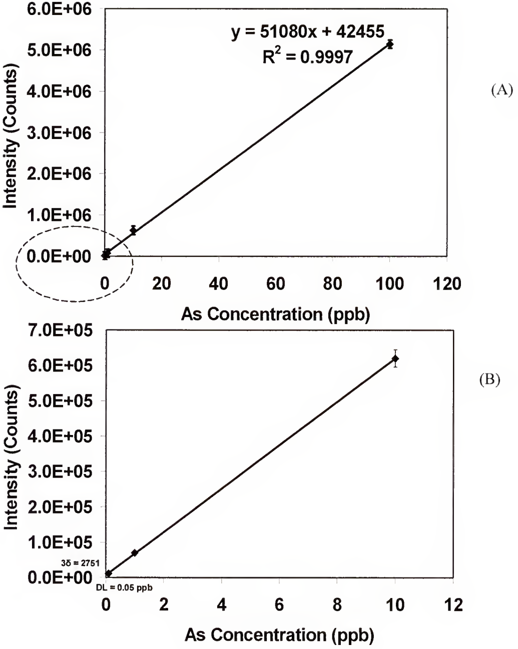

Figure 7-13. (A) Arsenic detection limit calibration curve of VG ICP-MS and (B) Expanded region (dashed).

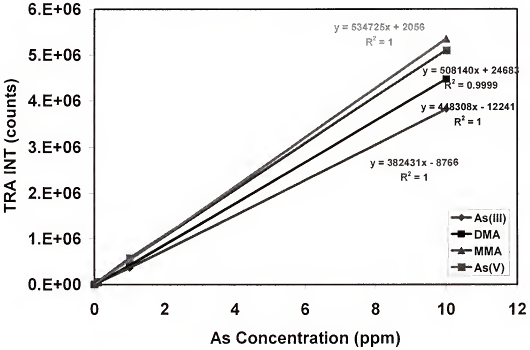

Figure 7-14. Calibration curves of As(III), DMA, MMA and As(V) with HPLC-ICP-MS.

CHAPTER 8
HPLC-ICP-MS APPLICATIONS

As discussed in Chapter 7, an ion-pair HPLC-ICP-MS method has been developed for arsenic species analysis with a mobile phase containing hexadecyltrimethyl ammonium bromide (CTAB) as the ion-pairing reagent, ammonium phosphate buffer and methanol at pH 6.0 on a reverse phased column (Haisil 100). This method resulted in low detection limits (0.5-1 $\mu g\ L^{-1}$), a wide linear range for calibration, and good reproducibility. Four arsenic species could be separated in 10 minutes with isocratic elution at the elution sequence of As(III), DMA, MMA and As(V) without interference from ArCl molecular ion. This HPLC-ICP-MS method has been successfully applied to determine arsenic species in human urine reference material (SRM2670), natural water reference material (1643d), and brake fern samples.

Human Urine

Arsenic contamination has been a global problem. There are numbers of ways that humans can be exposed to arsenic contamination. The principle exposure route is through the consumption of drinking water and all kinds of food that possess high arsenic levels. The different arsenic species, ingested by humans, affect the body differently. Inorganic arsenate is reduced to arsenite in the human body. Arsenite undergoes enzymatic methylation to MMA in the liver with S-adenosylmethionine (SAM) as a methyl group donor. MMA is further methylated to DMA. The arsenic enzymatic methylation is thought to reduce the arsenic toxicity [63]. Most of arsenic ultimately is excreted from the human body as urine. Thus, arsenic species in urine can be used as a biological monitor for occupational arsenic exposure and metabolism of arsenic in human body. Furthermore, urine has a relatively complex matrix and suitable arsenic concentration range. Therefore, the separation and determination capability in real sample application was verified in order to validate the accuracy of this HPLC-ICP-MS method for urine analysis. Despite the fact that there have been numerous recent publications on arsenic speciation, there is still no commercial standard reference material (SRM) available with certified concentration for individual arsenic species. The reference materials available for arsenic analysis in environmental and biological sample are only certified for total arsenic concentration. The accuracy of this HPLC-ICP-MS was carried out by determining the arsenic species present in SRM 2670 (Total Metal in Freeze-Dried Urine) from NIST (National Institute of Standards and Technology, Gaithersburg, MD) and comparing with the published results reported by other laboratories [71, 76, 87, 98-102].

SRM 2670 (normal and elevated levels) consists of freeze-dried urine in four 30 mL serum bottles with a certified total arsenic concentration. The normal level was not certified and the reference value was 60 $\mu g\ L^{-1}$. The elevated level was based on the normal human urine, which was spiked with arsenic at the certified value of 480 $\mu g\ L^{-1}$. The freeze-dried urine samples were reconstituted by the addition of 20 mL of mili-Q water to each bottle and filtered through 0.45 μm filter. Figure 8-1 shows the HPLC-ICP-MS chromatograms of urine reference material SRM 2670 normal level and elevated level, an adult, and a five-month-old infant urine samples. The main species detected in the normal and elevated levels of the SRM 2670 urine samples were As(III), DMA,

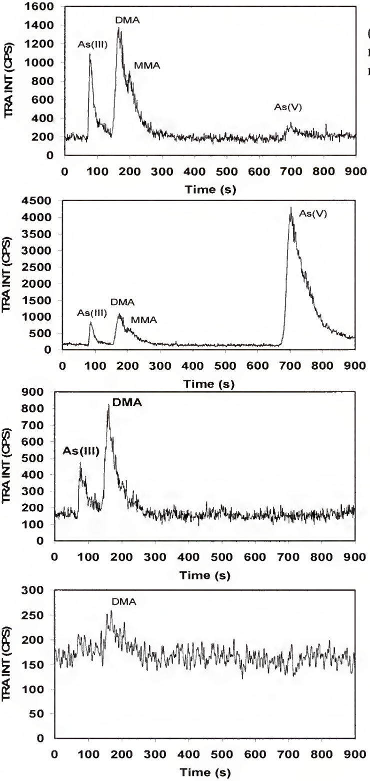

(A). Urine reference material SRM 2670 normal level

(B). Urine reference material SRM 2670 elevated level

(C). Adult Volunteer urine sample

(D). Infant Volunteer urine sample

Figure 8-1. Typical HPLC-ICP-MS chromatograms of SRM 2670 (normal and elevated level), adult and infant volunteer urine samples.

Table 8-1. Concentration comparison of arsenic species in SRM 2670 normal level samples of this HPLC-ICP-MS work and literature value. (μg L^{-1} As)

Species	DMA	MMA	As(III)	As(V)	AsB	Sum of species
Heitkemper *et al*. 1989[98]	46±4	9.9±1	53±4	0.8±0.5	ND	109±6
Sheppard *et al*. 1992 [87]	18±10	ND	29±4	ND	ND	47±11
Goessler *et al*. 1997 [99]	48±2	9.5±3	15±3	2.9±0.7	21±4	97±6
Le *et al*. 1998 [100]	49±5	11±3	ND	ND	ND	60±7
Le *et al*. 1998 [101]	48±2	7.4±0.7	ND	ND	ND	56±3
Tsalev *et al*. 1998 [102]	13±2	52±8	<2	<4	ND	65±10
Lindeman *et al*. 2000[71]	45±3	8±1	<4	5±3	22±3	80±9
Samanta *et al*. 2000[76]	31±1	12±2	ND	ND	15±0.3	58±2
This work	39±9	13±1	14±1	3±2	ND	68±7

*ND---Not determine.

Table 8-2. Experimentally determined concentrations of arsenic species in SRM 2670 elevated level, adult and infant urine samples by HPLC-ICP-MS. (μg L^{-1} As)

Species	DMA	MMA	As(III)	As(V)	AsB	Sum of species
Adult	29	ND	6	ND	ND	35
Infant	5	ND	ND	ND	ND	5
SRM 2670 (elevated level)	9	30	13	242	ND	293

Table 8-3. Sum of arsenic species concentration by HPLC-ICP-MS and the total arsenic concentration by solution introduction ICP-MS in SRM 2670 normal level and elevated level, adult and infant urine samples. (μg L^{-1} As)

	By HPLC-ICP-MS	By ICP-MS
SRM 2670 (normal level)	68	63
SRM 2670 (elevated level)	293	268
Adult	34	20
Infant	5	5

MMA and As(V), respectively. The concentration ratio of As(III), DMA, MMA and As(V) in the normal level was 1.1: 3.0: 1.0: 0.2. For the elevated level, the concentration ratio was 0.6: 2.2: 1.0: 18.2. This indicates the elevated level urine sample was spiked with either arsenate or arsenite, which oxidized to arsenate. The arsenic species present in the reference material SRM 2670 have been investigated by several other groups. Table 8-1 compared the results of arsenic species in urine reference material SRM 2670 by this HPLC-ICP-MS method with literature values from other research groups. DMA and MMA are major species which were detected by all of the research groups. As(V) could not be detected by some groups because of the low concentration. The different conclusions of As(III) and arsenobetaine are primarily due to the variation in analytical methods. Results obtained by this HPLC-ICP-MS method are in good agreement with results from most of other research groups. The sum concentration of all arsenic species (68 $\mu g\ L^{-1}$) is also comparable with the reference value of 60 $\mu g\ L^{-1}$ for total arsenic in normal level SRM 2670 provided by NIST. Therefore, this HPLC-ICP-MS method is reliable and SRM 2670 can be used as a quasi standard to validate arsenic speciation methods until commercial reference material is available.

The results for the adult volunteer and infant urine samples are listed in Table 8-2. The main species detected in the adult sample were As(III) and DMA. There is only a small amount of DMA present in the infant urine sample. These samples were also analyzed by direct introduction into ICP-MS without HPLC separation in order to determine the total arsenic concentration. Table 8-3 indicates good agreement between the sum concentration of all arsenic species by HPLC-ICP-MS and direct analysis with ICP-MS for the normal level SRM 2670, adult, and infant urine samples. For the elevated level SRM 2670 sample, the sum concentration of arsenic species (293μg L^{-1}) is in close agreement with the value from the ICP-MS (268 μg L^{-1}), but differed with the certified value (480 μg L^{-1}). This may be caused by the absorption of trace amount of arsenic in the storage bottle overtime. Generally, the total arsenic concentration in the urine of unexposed people ranges from 5 μg L^{-1} to 30 μg L^{-1} of arsenic [103]. The infant was five months old and fed mainly with breast milk, but there was still 5 μg L^{-1} of arsenic present in the subject's urine. Arsenic may either already existed in the infant's body or was transferred from the mother through breast milk. The adult urine sample contained 34 μg L^{-1} of arsenic, which is within the safe range for adult humans.

Natural Water Reference Material

SRM 1643d (Trace Elements in Water) is another standard reference material which has certified total arsenic concentration (56.02 ± 0.73 μg L^{-1}) from NIST. This standard material simulates the elemental composition in fresh water and originally consists of 250 mL filtered and acidified water in a polyethylene bottle. As shown in Figure 8.2, As(V) was the major component present in the SRM 1643d water sample. Neither organic arsenic DMA nor MMA was found in the standardized water sample. The total arsenic concentration was determined to be 84.6 μg L^{-1} by HPLC-ICP-MS and 106.2 μg L^{-1} by ICP-MS. The sample may have contained certain a small amount of As(III) with the fresh water sample, but overtime As(III) was oxidized to As(V). Acidification of the SRM 1643d water sample by nitric acid is another source of oxidation. Nitric acid was used initially to stabilize the trace elements at a concentration of 0.5 mol / L (equal to 3% w/w HNO_3 with a density of 1.016 g/mL at 22°C), resulting

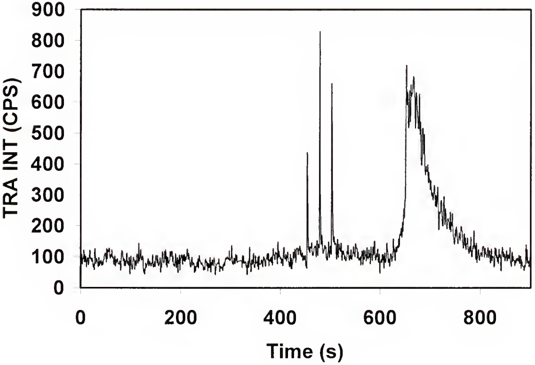

Figure 8-2. Typical HPLC-ICP-MS chromatogram of SRM 1643d water sample.

in a pH of 0.3 for the SRM 1643d sample. The permitted pH range for silicon based reverse phase column is from 2 to 8. There is a risk associated with running a strong acidic solution through such a Haisil 100 column.

The determination of arsenic species in an aquatic environment is also of prime importance to human health and has been carried out by scientists around the world. To date, no standard reference material with a certified arsenic species concentration in a real water sample is available. SRM 1643d can be used as a crude standard for arsenic speciation. However, more improvements are still needed. Hall Gwendy *et al.* tried to preserve natural water sample containing As(III) and As(V) species with 0.1 % HCl or 0.1 % HNO_3 [104]. This nature water treated with 0.1% HNO_3 may be used as another substitute standard for natural water analysis.

Analysis of Arsenic Species in Chinese brake fern

Chinese brake fern (*Pteris vittata L.)* is native to Asia, Africa and Australia, and is now widely adapted in warm regions of America. The fern was discovered to hyperaccumulate arsenic from an abandoned wood-treatment site in central Florida, which had been contaminated with preservatives containing chromium, copper and arsenic [2]. The total arsenic in the fronds of the fern was analyzed by graphite furnace atomic absorption spectroscopy (GFAAS). The Chinese brake fern from the contaminated site (18.8 – 1603 ppm As) contained 1442 - 7526 ppm arsenic and an uncontaminated site (0.47 – 7.56 ppm As) contained 11.8 – 64 ppm arsenic, however, other plants growing on normal soil only contained arsenic less than 3.6 ppm. Figure 8.3 shows a photo of Chinese brake fern grown on the University of Florida campus [105].

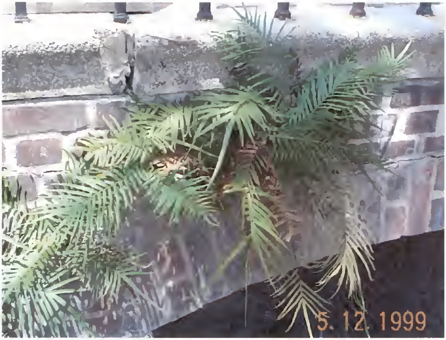

Figure 8-3. Photo of Chinese brake fern grown on the UF campus [105].

Chinese brake fern can effectively extract large amounts of arsenic from soil in a relatively short time and store it in the fronds. The fern is also hardy, versatile, and fast-growing. The arsenic hyperaccumulating property of the fern holds the potential to commercially and cost-effectively clean up thousands of soil and water sites which were contaminated by arsenic from natural or anthropogenic activities worldwide.

To fully evaluate the environmental impact of Chinese brake ferns, knowing only the total arsenic concentration in the fronds is insufficient. Therefore, the developed HPLC-ICP-MS method was employed to determine arsenic species in different parts of the fern. It was hoped that such speciation information could provide helpful information in understanding the mechanisms of arsenic accumulation, translocation, and detoxification in Chinese brake ferns.

Chinese brake Fern Root Exudate

Chinese brake fern cultivation and root exudate collection

All of the Chinese brake fern samples used in this research was grown in a greenhouse. The spores of the Chinese brake fern were germinated in an arsenic free soil mixture for three months. Then the fern plants with 5-6 fronds were transported to a controlled hydroponic system with a relatively constant temperature of 23 – 28 ºC, humidity of 70%, and equal amounts of artificial light. It took approximately two weeks for the Chinese brake fern plant to grow new roots.

The Chinese brake fern roots were washed free of soil by tap and deionized waters, respectively. Then the ferns were transferred to 20% strength Hoagland nutrition solutions, which were spiked with different levels of arsenic species. The solution were buffered by 5 mM MES (2-2(N-morpholino) ethanesulfonic acid) at pH 6.0. After two days, the fern roots were washed again with tap water, deionized water and phosphate buffer to assure arsenic desorbed from the root free space. After washing with tap and deionized waters again, each fern plant was placed in 150 mL deionized water (sterilized) to collect root exudate for six hours. The root exudate solution was filtered immediately by a 0.45 μM filter and then analyzed immediately by the HPLC-ICP-MS method, or stored under -20 °C for future analysis.

Chinese brake fern roots treated with different levels As(V) solution

In this experiment, Chinese brake fern roots were treated with 1.5 ppm, 15 ppm, and 150 ppm As(V) solution. The results are shown in Figure 8-4 and further comparison with arsenic cartridge-GFAAS analysis was shown in Table 8-4. When the fern roots were treated with As(V), the predominant arsenic species in the fern root exudate remained As(V), ranging from 83% to 100% of the total arsenic concentration (Figure 8-4). As(III) was presented in some cases ranging from 0% to 17% of the total arsenic concentration. This indicated As(V) is the main species in the fern root while some of the As(V) was reduced to As(III) by the roots. This plant survived in the solution containing up to 150 ppm As(V). The total arsenic concentration in root exudates ranged from 1405 ppb to 2955 ppb for a 150 ppm treatment, corresponding to 1 - 2% of the original treatment solution. This indicated that the fern root was not the principal location for arsenic storage by this plant.

HPLC-ICP-MS and GFAAS method comparison

As(V) and As(III) were separated by using an arsenic separation cartridge (Metal Soft Center, Highland Park, NJ) in the Ma's laboratory. This disposable cartridge will retain As(V) and allow As(III) to pass through to the filtrate [106]. Then As(III)

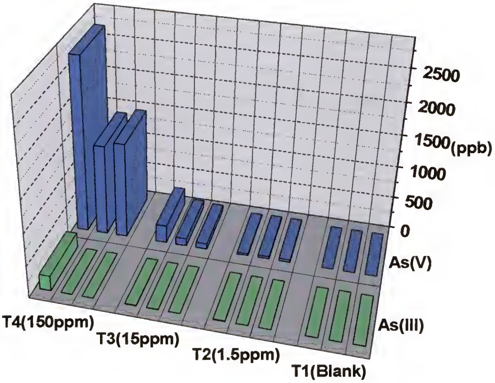

Figure 8-4. Concentrations of As(III) and As(V) in Chinese brake fern root exudates. Roots were treated with 1.5 ppm, 15 ppm, and 150 ppm As(V) solution.

concentration was determined by using GFAAS (graphite furnace atomic absorption spectrometer) (Perkin Elmer SIMMA 6000, Perkin-Elmer Corp, Norwalk, CT) to analyze the total arsenic in the filtrate.

The same fern root exudate samples were analyzed at the same time by this HPLC-ICP-MS method and the arsenic cartridge GFAAS; the concentrations of As(III) and As(V) are shown in Table 8-4. These results further verify the accuracy of the developed HPLC-ICP-MS method. As shown in Table 8-4, the sum of As(III) and As(V) concentrations determined by HPLC-ICP-MS and the total arsenic concentration determined by arsenic cartridge GFAAS, were in good agreement for the majority of the fern root exudate samples. However, the As(III) concentrations were slightly different. In some cases, the arsenic cartridge-GFAAS method gave As(III) concentrations ranging from 0.8 % to 5.9 % of the total arsenic concentration. However, HPLC-ICP-MS results showed that there was no As(III) present. This is possible since the cartridge retains only As(V), which means all species other than As(V) will pass through the column and be counted as As(III). Therefore, it is expected that cartridge-GFAAS method may overestimate As(III) concentration if As(V) in the fern sample is present as complex form and hence passes through column. The average recovery of As(III) was 98% using the cartridge, with arsenic concentrations less than 500 $\mu g\ L^{-1}$. The sensitivity of this GFAAS method was adequate to analyze total arsenic in most fern samples. However, DMA and MMA could not be determined by this arsenic cartridge-GFAAS method since this cartridge does not remove organic arsenic. Therefore, HPLC-ICP-MS becomes an important analytical technique for arsenic speciation in Chinese brake fern.

Table 8-4. Concentrations of arsenic species in Chinese brake fern root exudates determined by HPLC-ICP-MS and arsenic cartridge GFAAS. (ppb)

	HPLC-ICP-MS				Arsenic cartridge GFAAS			
	As(III)	As(V)	Total As	As(III)/total As *100	As(III)	As(V)	Total As	As(III)/total As *100
T1-1(0ppm)	0	0	0		1		2	
T1-2	0	0	0		0		1	
T1-3	0	0	0		0		2	
T2-1(1.5ppm)	0	38	38	0	1		50	3
T2-2	0	38	38	0	3		48	6
T2-3	6	29	35	17	6		44	14
T3-1(15ppm)	0	84	84	0	2		97	2
T3-2	2	118	120	2	10		170	6
T3-3	6	276	282	2	11		287	4
T4-1(150ppm)	0	1483	1483	0	12		1430	1
T4-2	0	1405	1405	0	30		1340	2
T4-3	234	2721	2955	7	389		2810	14

*As(III)/total As *100 ------- (As(III) concentration / total arsenic concentration) * 100

Chinese brake fern roots treated with 15 ppm As(III), DMA, MMA, or As(V) solutions

In this experiment, Chinese brake fern roots were treated separately with 15 ppm As(III), DMA, MMA, or As(V) solutions. The results are shown in Figure 8-5 and summarized in Table 8-5 for comparison purposes. For the control with no treatment applied, the only species present in the root exudate was As(V) at a low level of 2 ppb to 7 ppb. When the Chinese brake fern roots were treated with As(III), the main arsenic species in the Chinese brake fern root exudate was As(V) ranging from 97% to 100% of the total arsenic concentration. As(III) was detected in some cases ranging from 0% to 3% of the total arsenic concentration when treated with As(V) solutions, which is consistent with experiments in Section 8.3.1.2. Such results indicate that oxidation of As(III) to As(V) occurred in or outside of the roots, which cannot be verified in this experiment. Though the root exudate was collected with minimum contact hours (i.e. 6 hour), to minimize microbial-mediated arsenic oxidation in the solution, such a process is still possible. Approximately 76% -87% of DMA was detected in the root exudate when the sample was treated with DMA. Additionally, there was no MMA present with such treatments. A typical chromatogram is shown in Figure 8-6 (C). When the fern was treated with MMA, MMA was the main species ranging from 18% to 56% of the total arsenic concentration. However, DMA was present when the fern was treated with 15 ppm MMA, as shown in Figure 8-6 (B). The concentration of DMA was far above the detection limit of the HPLC-ICP-MS method and ranged from 8% to 22% of the total arsenic concentration. The original 15 ppm MMA treatment solution was also analyzed to verify that there was no DMA contamination as shown in Figure 8-6 (A). This is the first time that MMA has been shown experimentally to convert to DMA in the Chinese brake

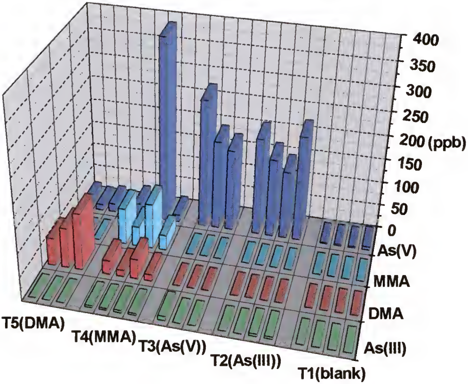

Figure 8-5. Concentrations of four arsenic species in Chinese brake fern root exudates. The roots were treated separately with 15 ppm As(III), DMA, MMA, or As(V) solutions.

Table 8-5. Concentrations of four arsenic species and total arsenic concentration in Chinese brake fern root exudates. The roots were treated separately with 15 ppm As(III), DMA, MMA, or As(V) solutions.

	As(III)		DMA		MMA		As(V)		Total(ppb)
	C(ppb)	%	C(ppb)	%	C(ppb)	%	C(ppb)	%	
R1-1(Blank)*	0	0	0	0	0	0	7	100	7
R1-2	0	0	0	0	0	0	3	100	3
R1-3	0	0	0	0	0	0	3	100	3
R1-3	0	0	0	0	0	0	2	100	2
R2-1(As(III))	5	2	0	0	0	0	221	98	226
R2-2	5	3	0	0	0	0	143	97	147
R2-3	0	0	0	0	0	0	165	100	165
R2-4	0	0	0	0	0	0	205	100	205
R3-1(As(V))	0	0	0	0	0	0	173	100	173
R3-2	0	0	0	0	0	0	188	100	188
R3-3	9	3	0	0	0	0	271	97	280
R4-1(MMA)	4	6	14	22	32	50	15	23	64
R4-2	5	1	42	8	95	18	386	73	528
R4-3	4	5	13	14	42	46	32	36	91
R4-4	4	3	29	21	77	56	27	20	136
R5-1(DMA)	0	0	120	87	0	0	18	13	138
R5-2	0	0	84	87	0	0	12	13	96
R5-3	0	0	58	76	0	0	19	24	77

*R1-1 ------ Root exudate blank sample No.1

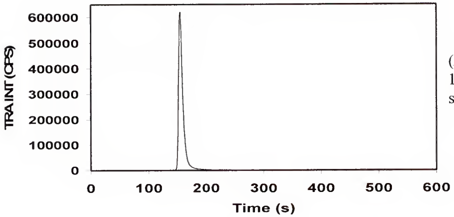

(A) Original 15 ppm MMA solution

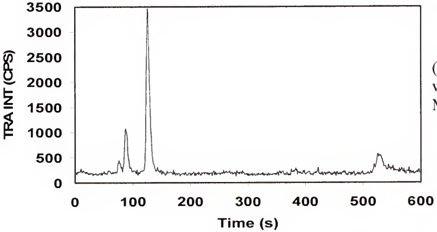

(B) Root exudate with 15 ppm MMA treatment

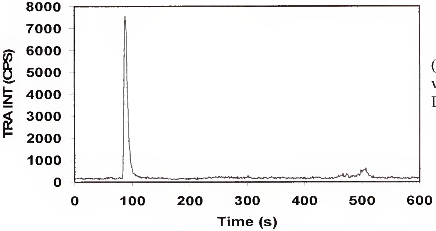

(C) Root exudate with 15 ppm DMA treatment

Figure 8-6. Typical chromatograms of arsenic species (A) original 15 ppm MMA treatment solution and Chinese brake fern root exudates with (B) 15 ppm MMA treatment; (C) 15 ppm DMA treatment.

fern. Odanaka *et al.* [107] also found the same phenomenon in rice plants with GC/MID/MS-HG/HCT (gas chromatography with a multiple ion detection mass spectrometry and hydride generation-heptane cold trap). This indicates that Chinese brake fern root can convert MMA to DMA by methylation.

Chinese brake Fern Xylem Sap

Chinese brake fern xylem sap collection

The Chinese brake fern cultivation in this experiment was the same as the procedure described in Section 8.3.1.1. For this study, Chinese brake fern with similar size and age were selected. After the roots were washed free of soil by tap and deionized waters, the ferns were transported to a 20% strength Hoagland nutrition solution for one week. Prior to harvesting, the ferns were transferred to a new 20% strength Hoagland nutrition solution, which was spiked with different levels MMA or DMA, and grown for three days. One or two fronds of similar size were cut from the fern and placed immediately into a pressure chamber for xylem sap collection. Xylem sap was forced to be excreted from the cut of the frond rachis by nitrogen gas in the pressure chamber. Approximately 0.7 mL to 1 mL of xylem sap was collected from each frond with a micropipette and was stored at -86 °C for future analysis.

Chinese brake fern treated with 10 ppm or 50 ppm DMA or MMA solutions and xylem sap sample analysis

The role of xylem sap in the fern is to transport arsenic from the roots to the fronds. In this experiment, the fern roots were treated separately with 10 ppm or 50 ppm DMA or MMA solutions. The results are shown in Figure 8-7 and summarized in Table 8-6 for comparison. For the control with no treatment, approximately 70% to 89% of the total arsenic concentration in the xylem sap was present as As(III) and 10% to 25% was

As(V). It is important to note that As(V) was the only species in the root exudate for the Chinese brake fern without any treatment. This is in good agreement with previous research concerning the conversion of As(V) to As(III) in the plant [108]. Inorganic arsenic is the predominant form of arsenic in xylem sap. There was only a small amount of MMA present, ranging from 1% to 7% of the total arsenic. Furthermore, no DMA was detected. As shown in Table 8-6, the total arsenic concentration in xylem sap can increase up to 344 ppm with 50 ppm DMA treatment, which was approximately seven times greater than the solution concentration. This further verifies the unique characteristics of arsenic hyperaccumulation in Chinese brake fern.

When the Chinese brake fern roots were treated with either 10 ppm or 50 ppm DMA, the predominant arsenic species in the xylem sap was DMA. DMA ranged from 78% to 100% of the total arsenic concentration, and there was no MMA present, as indicated in the typical chromatogram shown in Figure 8-8 (B). MMA remained the primary species ranging from 79% to 95% of the total arsenic concentration when treated with either 10 ppm or 50 ppm MMA. Furthermore, DMA was also discovered in xylem sap with either 10 ppm or 50 ppm MMA treatment, as the typical chromatogram shown in Figure 8-8 (A). The concentration of DMA was far above the detection limit of this HPLC-ICP-MS method and ranged from 2% to 5% of the total arsenic concentration. This is in agreement with the conversion of MMA to DMA in Chinese brake fern root exudate discussed in Section 8.3.1.4.

In summary, the discovery of methylation of MMA to DMA in Chinese brake fern root exudate and xylem sap suggests a pathway of arsenic species transformation in the fern. The cause and conditions of the methylation will be subject to further studies.

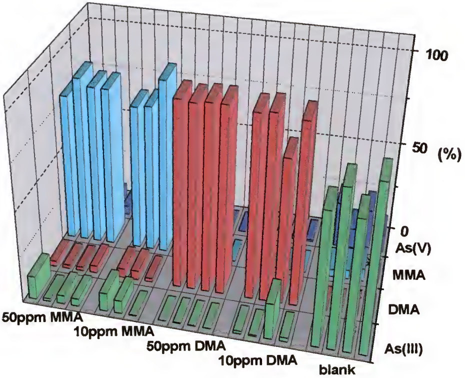

Figure. 8-7. Concentrations of four arsenic species in Chinese brake fern xylem sap. The roots were treated separately with 10 ppm or 50 ppm DMA or MMA solutions.

Table 8-6. Concentrations of four arsenic species and total arsenic concentration in Chinese brake fern xylem sap. The roots were treated separately with 10 ppm or 50 ppm DMA or DMA solutions.

	As(III)		DMA		MMA		As(V)		
Blank	C(ppm)	%	C(ppm)	%	C(ppm)	%	C(ppm)	%	Total(ppm)
S1-1*	1.0	89	0	0	0.015	1	0.12	10	1.2
S1-2	0.29	70	0	0	0.031	7	0.093	23	0.41
S1-3	0.055	84	0	0	0.003	5	0.007	11	0.066
S1-4	0.14	72	0	0	0.007	4	0.047	25	0.19
10ppm DMA									
S2-1	0.17	2	7.7	97	0	0	0.093	1	8.0
S2-2	0.36	20	1.4	78	0	0	0.042	2	1.8
S2-3	0.032	1	4.4	99	0	0	0.024	1	4.4
S2-4	0.068	2	4.3	98	0	0	0.011	0	4.4
50ppm DMA									
S3-1	0.091	0	65	100	0	0	0.23	0	65
S3-2	0.083	0	38	100	0	0	0.055	0	38
S3-3	0.11	0	30	99	0	0	0.058	0	31
S3-4	0.11	0	344	100	0	0	0.043	0	344
10ppm MMA									
S4-1	0.14	0	0.87	2	44	95	1.53	3	47
S4-2	0.52	7	0.40	5	5.9	80	0.54	7	7.3
S4-3	0.33	10	0.16	5	2.7	79	0.21	6	3.4
50ppm MMA									
S5-1	1.3	4	1.4	4	29	87	1.8	5	33
S5-2	0.43	5	0.15	2	8.3	87	0.71	7	9.6
S5-3	0.29	1	0.35	2	18	90	1.3	6	21
S5-4	1.2	13	0.31	3	7.2	80	0.32	4	9.0

*S1-1 ------- Xylem sap sample Blank No.1

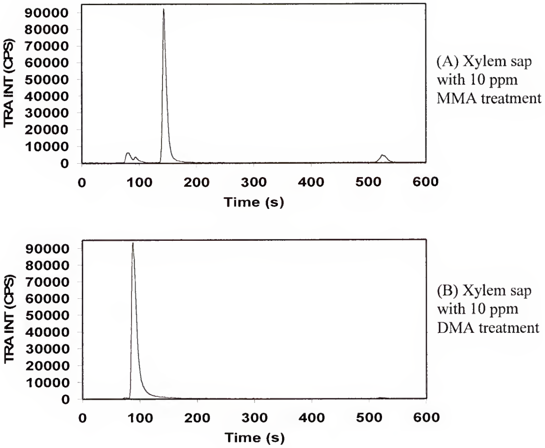

Figure 8-8. Typical chromatograms of arsenic species in Chinese brake fern xylem sap with (A) 10 ppm MMA treatment; (B) 10 ppm DMA treatment.

CHAPTER 9
CONCLUSIONS AND FUTURE DIRECTIONS

Conclusions

Both CE-ICP-MS and HPLC-ICP-MS are powerful techniques for trace elemental speciation analysis, which make use of the excellent separation potential of CE or HPLC and the superior element-selective detection capability of ICP-MS.

In this research, a modified concentric Meinhard nebulizer and an interface were developed and used for coupling CE with ICP-MS. The interface was inexpensive, flexible and universal. It was easily installed and removed and moreover used in combination with different types of ICP mass spectrometers. This CE-ICP-MS system was used to determine arsenite (As(III)) and arsenate (As(V)) in laboratory created sample under optimized conditions. However, CE-ICP-MS has disadvantages including low liquid flow rate ranging from several hundred nL/min to several μL/min, and the requirement of a special interface for ICP-MS sample introduction.

Compared with CE-ICP-MS, HPLC is more suitable coupled with ICP-MS. This is because the liquid flow rate of HPLC, which is 1 mL/min typically in the range of 0.1-10 mL/min, is consistent with the requirement of the ICP-MS nebulizer sample uptake rate (0.5-1.0 mL/min). Ion-pair reverse phase HPLC-ICP-MS was used to separate and determine arsenite (As(III)), dimethyl arsenic acid (DMA), monomethyl arsenic (MMA), and arsenate (As(V)) in various sample matrices. The separation was performed on a reverse phase C18 column (Haisil 100) by using a mobile phase containing 10 mM hexadecyltrimethyl ammonium bromide (CTAB) as an ion-pairing reagent, 20 mM ammonium phosphate buffer, and 2% methanol at pH 6.0. There was no available standard reference material (SRM) with certified concentration for individual arsenic species. This method was validated by determining the arsenic species present in SRM 2670 (Total metal in freeze-dried urine) from NIST (National Institute of Standards and Technology) and compared with the results reported by other research groups. This optimized HPLC-ICP-MS method was also applied to determine arsenic species in several parts of Chinese brake fern and provided helpful information to better understand the mechanisms of arsenic accumulation, translocation and detoxification in Chinese brake fern.

Future Directions

Despite the fact that a number of papers have been published concerning arsenic speciation within recent years, there is still no ideal method to separate and determine arsenic species due to instrumental limitation. The problems include uncertainty related to identifying chromatography peaks due to a lack of chromatographic standards and the similar physical and chemical properties of arsenic compounds; there is difficulty of quantitative analysis because of no commercially available arsenic speciation certified standard. A possible solution to the uncertainty in the future could be the use of HPLC-ICP-MS and electrospray tandem mass spectrometry (ES MS-MS) in sequence for arsenic speciation [87].

The current HPLC-ICP-MS method also suffers from long analysis time, an organic solvent effect, and the incapability to separate all arsenic species in one run. A narrow-bore column can be used to short analysis time and less introduction of organic solvent. The future work may also focus on developing a membrane interface between HPLC and ICP-MS nebulizer to block the organic solvent, and using platinum sample cone and skimmer cone in the ICP-MS to extend the lifetime of sample cone and skimmer cone.

The sample preparation procedure can also affect the separation resolution and sensitivity of HPLC-ICP-MS system. A method, which can efficiently extract arsenic species and maintain the original species information of environmental and biological samples, needs to be developed in the future.

In the present research, this HPLC-ICP-MS method has been applied for arsenic speciation in urine, water, and Chinese brake fern. It can be further employed to environmental and biological samples such as soil, seawater and ground water, different kinds of plants, seafood, animal components, etc.

Elemental speciation has become increasingly important in different research and industry fields, such as environmental control, food science, pharmaceutical and clinical analysis. HPLC-ICP-MS will play an important role in not only the speciation of arsenic but also the determination of numerous elemental species such as Al, As, Cd, Cr, Fe, I, Hg, Se, Sn, P, Pb, Pt, Sb, etc, in the environmental, geological, and biological fields.

APPENDIX
ABBREVIATIONS

ICP: Inductively Coupled Plasma
MS: Mass Spectrometry
CE: Capillary Electrophoresis
HPLC: High Performance Liquid Chromatography
As(III):Arsenite
As(V): Arsenate
DMA: Dimethyl Arsenic Acid
MMA: Monomethyl Arsenic
CTAB: Hexadecyltrimethyl Ammonium Bromide
SRM: Standard Reference Material
NIST: National Institute of Standard and Technology
ICP-AES: Inductively Coupled Plasma Atomic Emission Spectrometry
MCS: Multi-channel Scaler
ETV: Electrothermal Vaporization
LA: Laser Ablation
HG: Hydride Generation
GC: Gas Chromatography
SFC: Supercritical Fluid Chromatography
DIN: Direct Injection Nebulizer
USN: Ultrasonic Nebulizer
MCN: Micro-concentric Nebulizer
HEN: High Efficiency Nebulizer
OCN: Oscillating Capillary Nebulizer
DIHEN: Direct Injection High Efficiency Nebulizer
PTFE: Polytetrafluoroethylene
DC: Direct Current
RF: Radio Frequency
TRA: Time Resolved Acquisition
EOF: Electroosmotic Flow
MIP: Microwave Induced Plasma
GFAAS: Graphite Furnace Atomic Absorption Spectrometry
ESI: Electrospray Ionization
CCA: Chromated Copper Arsenic
EPA: Environmental Protection Agency
OSHA: Occupational Safety and Health Administration
PEL: Permissible Exposure Limit
TTAB: Tetradecyltrimethyl Ammonium Bromide

TBAH: Tetrabutylammonium Hydroxide
TBAP: Tetrabutylammonium Phosphate
GC/MID/MS-HG/HCT: Gas Chromatography with A Multiple Ion Detection Mass Spectrometry and Hydride Generation-heptane Cold Trap
ES MS-MS: Electrospray Tandem Mass Spectrometry

REFERENCES

1. Smith, A. H.; Lings, E. O.; Rahman, M. *Bulletin of the World Health Organization*, **2000**, 78, 9, 1093-1103.

2. Ma, L. Q.; Komart, K. M.; Tu, C.; Zhang, W.; Cai, Y.; Kennelley, E. *Nature*, **2001**, 409, 579.

3. Montaser, A., Ed. *Inductively Coupled Plasma Mass Spectrometry*; Wiley-Vch: New York, **1998.**

4. *VG PlasmaQuad System Manual*; VG Elemental: Danvers, MA, **1988.**

5. Montaser, A.; Golightly, D.W., Ed. *Inductively Coupled Plasma In Analytical Atomic Spectrometry*; Wiley-Vch: New York, **1992**.

6. Baker, S. A.; Bi, M.; Aucelio, R. Q.; Smith, B. W.; Winefordner, J. D. *J. Anal. At Spectrom.* **1999**, 14, 19-26.

7. Yang, C. L.; Chen, R. X.; Wang, X. R. 5th National Conference on Atomic Spectrometry, **1996**, Wuhan, China.

8. Nakazato, T.; Tao, H.; Taniguchi, T.; Isshiki, K. *Talanta.* **2002**, 58, 121-132.

9. Bouyssiere, B.; Szpunar, J.; Lobinski, R. *Spectrochim. Acta Part B.* **2002**, 57, 805-828.

10. Vela, N. P.; Caruso, J. A. *J. Chromatogr.* **1993**, 641, 337-345.

11. The Meinhard nebulizer, http://www.meinhard.com/nebulizers.html, accessed March 16, 2003.

12. Kniseley, R. N.; Amenson, H.; Butler, C. C.; Fassel, V. A. *Appl. Spectrosc.* **1974**, 28, 285-286.

13. Clifford, R. H.; Sohal, P.; Liu, H.; Montaser, A. *Spectrochim. Acta Part B.* **1992**, 47, 1107-1122.

14. Liu, Y.; Lopez-Avila, V.; Zhu, J. J.; Weiderin, D. R.; Beckert, W. F. *Anal. Chem.* **1995**, 67, 2020-2025.

15. Huang, M.; Lehn, S. A.; Andrews, E. J.; Hieftje, G. M. *Spectrochim. Acta Part B.* **1997**, 52, 1173-1193.

16. Camilleri, P., Ed. *Capillary Electrophoresis-Theory and Practice*; CRC Press: Boca Raton, FL, **1993.**

17. *Dionex Capillary Electrophoresis System I Operator's Manual*; Dionex Corporation: Sunnyvale, CA, **1990.**

18. Mei, E.; Ichihashi, H.; Gu, W.; Yamasaki, S. *Anal. Chem.* **1997**, 69, 2187-2192.

19. Michalke, B.; Lustig, S.; Schramel, P. *Electrophoresis*. **1997**, 18, 196-201.

20. Barnes, R.M. *Fresenius J. Anal. Chem.* **1998,** 361, 246-251.

21. Michalke, B.; Schramel, P.; kettrup, A. *Fresenius J. Anal. Chem.* **1999**, 363, 456-459.

22. Brown, P. R.; Hartwick, R. A. *High Performance Liquid Chromatography*; John Wiley & Sons Inc: New York, **1989.**

23. *SpectraSystem Gradient Pumps Reference Manual*; Thermo Separation Products Inc: Fremont, CA, **1994.**

24. Megarbane, B.; Borron, S.W.; Trout, H.; Hantson, P.; Jaeger, A.; Krencrker, E.; Bismuth, C.; Baud, F.J. *Intensive Care Med.* **2001**, 27, 1370-1378.

25. Timerbaev, A.R. *Talanta*. **2000**, 52, 573-606.

26. Li, Y.; Xue, H. *Anal. Chim. Acta*. **2001**, 448, 121-134.

27. Kot, A.; Namiesnik, J.; *Trends Analy. Chem.* **2000**, 19, 69-79.

28. David, R. L., Ed. *CRC Handbook Of Chemistry And Physics*, CRC Press: Boca Raton, FL, **1994**.

29. Centennial, Ed. *The Merck Index, eleventh edition*, Merch & Co., Inc: Whitehouse Station, NJ, **1989**.

30. Francesconi, K. A.; Tanggaard, R.; McKenzie, C.J.; Goessler, W. *Clin. Chem.* **2002**, 48, 92-101.

31. Matus, R. Baby Gator to Tear Down Playground *in The Gainesville Sun*: Gainesville, FL, March 22, **2001**, 1A.

32. Environmental Protection Agency, http://www.epa.gov/, accessed March 16, 2003.

33. Olesik, J. W.; Kinzer, J. A.; Olesik, S. V. *Anal. Chem.* 1995, *67*, 1-12.

34. Lu, Q.; Bird, S. M.; Barnes, R. M. *Anal. Chem*. **1995**, 67, 2949-2956.

35. Michalke, B.; Schramel, P. *Fresenius J. Anal. Chem*. **1997,** 357, 594-599.

36. Majidi, V.; Miller-Ihli, N.J. *Analyst*. **1998**, 123, 803-808.

37. Rocha, M.S.da; Soldado, A.B.; Blanco-Gonzalez, E.; Sanz-medal, A. *J. Anal. At. Spectrom*. **2000**, 15, 513-518.

38. Kinzer, J.A.; Olesik, S.V.; Olesik, S.V. *Anal. Chem*. **1996**, 68, 3250-3257.

39. Sutton, K. L.; B'Hymer, C.; Caruso, J. A. *J. Anal. At. Spectrom*. **1998,** 13, 885-891.

40. Stewart, I.I.; Olesik, J.W. *J. Chromatog. A*. **2000**, 872, 227-246.

41. Magnuson, M.L.; Creed, J. T.; Brockhoff, C.A. *J. Anal. At. Spectrom*. **1997**, 12, 689-695.

42. Tangen, A.; Trones, R.; Greibrokk, T.; Lund, W. *J. Anal. At. Spectrom*. **1997**, 12, 667-670.

43. Taylor, K. A.; Sharp, B. L. ; Lewis, D. J.; Crews, H. M. *J. Anal. At. Spectrom*. **1998**, 13, 1095-1100.

44. Holderbeke, M. V.; Zhao, Y.; Vanhaecke, F.; Moens, L.; Dams, R.; Sandra, P. *J. Anal. At. Spectrom*. **1999**, 14, 229-234.

45. Schaumloffel, D.; Prange, A. *Fresenius J. Anal. Chem*. **1999**, 364, 452-456.

46. Day, J.A.; Sutton, K.L. Soman, R. S.; Caruso, J. A. *Analyst*. **2000**, 125, 819-823.

47. Lee, T.; Jiang, S. *Anal. Chim. Acta*. **2000**, 413, 197-205.

48. Tangen, A.; Lund, W.; Josefsson, B.; Borg, H. *J. Chromatog. A*. **1998,** 826, 87-94.

49. Bendahl, L.; Gammelgaard, B.; Jons, O.; Farver, O.; Hansen, S. H. *J. Anal. At. Spectrom*. **2000**, 16, 38-42.

50. Baker, S. A.; Miller-Ihli, N. J. *Appl. Spectrosc*. **1999,** 53, 471-478.

51. Lu, Q.; Barnes, R. M. *Microchem. J.* **1996**, 54, 129-143.

52. Kirlew, P. W.; Caruso, J. A. *Appl. Spectros*. **1998**, 52, 770-772.

53. B'Hymer, C.; Sutton, R. M. C.; Sutton, K. L.; Caruso, J. A. *Anal. Commun.* **1999**, 36, 349-353.

54. Majidi, V.; Quarnstrom, J.; Tu, Q.; Frech, W.; Thomassen, Y. *J. Anal. At. Spectrom.* **1999**, 14, 1933-1935.

55. Li, J.; Umemura, T.; Odake, T.; Tsunoda, K. *Anal. Chem.***2001**, 73, 5992-5999.

56. Alvarez-Llamas, G.; Fernandez, de la Campa M.R.; Sanz-Medel, A. *Anal. Chim. Acta*. **2001**, 448, 105-119.

57. Alvarez-Llamas, G.; Fernandez,de la Campa M.R.; Fernandez, M. L.; Sanz-Medel, A. *J. Anal. At. Spectrom.* **2002**, 17, 655-661.

58. Michalke, B.; Schramel, P. *J. Chromatogr.* A. **1996**, 750, 51-62.

59. Hieftje, G. M. *J. Anal. At. Spectrom.* **1992**, 7, 783-790.

60. Hieftje, G. M. *J. Anal. At. Spectrom.* **1996**, 11, 613-621.

61. Thompson, J.J.; Houk, R.S. *Anal. Chem.* **1986**, 58, 2541.

62. Raab, A,; Hansen, H. R.; Zhuang, L.; Feldmann, J. *Talanta.* **2002**, 58, 67-76.

63. Suzuki, K.T.; Mandal, B.K.; Ogra, Y. *Talanta.* **2002**, 58, 111-119.

64. Brisbin, J.A.; B'Hymer, C.; Caruso, J. A. *Talanta.* **2002**, 58, 133-145.

65. Abedin, M. J.; Cresser, M. S.; Meharg, A. A.; Feldmann, J.; Cotter-Howells, J. *Sci. Environ. Technol.* **2002**, 36, 962-968.

66. McSheehy, S.; Szpunar, J.; Lobinski, R.; Haldys, V.; Tortajada, J.; Edmonds, J. *Anal. Chem.* **2002**, 74, 2370-2378.

67. Caruso, J. A.; Heitkemper, D. T.; B'Hymer, C. *Analyst.* **2001**, 126, 136-140.

68. Vassileva, E.; Becker, A.; Broekaert, J. A.C. *Anal. Chim. Acta.* **2001**, 441, 135-146.

69. Heitkemper, D.T.; Vela, N.P.; Stewart K.R.; Westphal C.S. *J. Anal. At. Spectrom.* **2001**, 16, 299-306.

70. Yehl, P.M.; Gurleyuk, H.; Tyson, J.F.; Uden, P.C. *Analyst.* **2001**, 126, 1511-1518.

71. Lindemann, T.; Prange, A.; Dannecker, W.; Neidhart, B. *Fresenius J. Anal. Chem.* **2000**, 368, 214-220.

72. Bissen, M.; Frimmel, F.H. *Fresenius J. Anal. Chem.* **2000**, 367, 51-55.

73. Chatterjee, A. *Talanta.* **2000**, 51, 303-314.

74. Gomez-Ariza, J.L.;Sanchez-Rodas, D.; Giraldez, I.; Morales, E. *Analyst.* **2000**, 125, 401-407.

75. Madsen, A.D.; Goessler, W.; Pedersen, S.; Francesconi, K.A. *J. Anal. At. Spectrom.* **2000**, 15, 657-662.

76. Samanta, G.; Chowdhury, U.K.; Mandal, B.K.; Chakraborti, D.; Sekaran, N. C.; Tokunaga, H.; Ando, M. *Microchemical Journal,* **2000**, 65, 113-127.

77. Londesborough, S.; Mattusch, J.; Wenrich, R. *Fresenius J. Anal. Chem.* **1999**, 363, 577-581.

78. Jackson, B.P.; Miller, W.P. *J. Anal. At. Spectrom.* **1998**, 13, 1107-1112.

79. Kavanagh, P.; Farago, M.E.; Thornton, I.; Goessler, W.; Kuehnelt, D.; Schlagenhaufen, C.; Irgolic, K.J. *Analyst.* **1998**, 123, 27-29.

80. Geiszinger, A.; Goessler, W.; Kuehnelt, D.; Francesconi, K.; Kosmus, W. *Environ. Sci. Technol.* **1998**, 32, 2238-2243.

81. Goessler, W.; Kuehnelt, D.; Schlagenhaufen, C.; Slejkovec, Z.; Irgolic, K.J. *J. Anal. At. Spectrom.* **1998,** 13, 183-187.

82. Broeck, K.V.d.; Vandecasteele, C.; Geuns, J. M.C. *Anal. Chim. Acta.* **1998,** 361, 101-111.

83. Thomas, P.; Finnie, J.K.; Williams, J.G. *J. Anal. At. Spectrom.* **1997**, 13, 1107-1112.

84. Branch, S.; Ebdon, L.; Oneill, P. *J. Anal. At. Spectrom.* **1994,** 9, 33-37.

85. Demesmay, C.; Olle, M.; Porthault, M. *Fresenius J. Anal. Chem.* **1994**, 348, 205-210.

86. Larsen, E.H.; Pritzl G.; Hansen, S.H. *J. Anal. At. Spectrom.* **1993**, 8, 1075-1084.

87. Sheppard, B.S.; Caruso, J.A.; Heitkemper, D.T.; Wolnik, K.A. *Analyst.* **1992**, 117, 971-975.

88. McSheehy,S.; Pohl, P.; Lobinski, R.; Szpunar, J. *Anal. Chim. Acta.* **2001**, 440, 3-16.

89. McSheehy,S.; Pohl, P.; Lobinski, R.; Szpunar, J. *Analyst.* **2001**, 126, 1055-1062.

90. Wangkarn, S.; Pergantis, S. A. *J. Anal. At. Spectrom.* **2000**, 15, 627-633.

91. B'Hymer, C.; Sutton, K. L.; Caruso, J. A. *J. Anal. At. Spectrom.* **1998**, 13, 855-858.

92. Le, X. C.; Ma, M. *J. Chromatogr. A.* **1997**, 764, 55-64.

93. Pergantis, S. A.; Heithmar, E. H.; Hinners, T. A. *Analyst.* **1997**, 122, 1063-1068.

94. Thomas, P.; Sniatecki, K. *J. Anal. At. Spectrom.* **1995**, 10, 615-618.

95. Dean, J. R.; Ebdon, L.; Foulkes, M. E.; Crews, H. M.; Massey, R. C. *J. Anal. At. Spectrom.* **1994**, 9, 615-618.

96. Beauchemin, D.; Siu, K. W. M.; Mclaren, J. W.; Berman, S.S. *J. Anal. At. Spectrom.* **1989**, 4, 285-289.

97. Sutton, K. L.; Caruso, J. A. *J. of Chromatogr. A.* **1999,** 856, 243-258.

98. Heitkemper, D.; Creed, J.; Crauso, J. *J. Anal. At. Spectrom.* **1989**, 4, 279-283.

99. Goessler, W.; Kuehnelt, D.; Irgolic, K. J. Determination of arsenic compounds in human urine by HPLC-ICP-MS in: Abernathy, C. O.; Calderon, R. L.; Chappell, W. R. (Eds). *Arsenic Exposure and Health Effects*, Chapman and Hall, New York, **1997**, 33-44.

100. Le, X. C.; Ma, M. *Anal. Chem.***1998**, 70, 1926-1933.

101. Ma, M.; Le, X. C. *Clin. Chem.* **1998**, 44, 539-550.

102. Tsalev, D.; Sperling, M.; Welz, B. *Analyst.* **1998**, 123, 1703-1710.

103. Hakala, E.; Pyy, L. *J. Anal. At. Spectrom.* **1992**, 7, 191-196.

104. Hall Gwendy, E. M.; Pelchat, J.C.; Gauthier, G. *J. Anal. At. Spectrom.* **1999**, 14, 205-213.

105. Ma, L. Q., http://lqma.ifas.ufl.edu/FERN.HTML, accessed March 16, 2003.

106. Meng, X.; Wang, W. *Third International Conference on Arsenic Exposure and Health Effects*, **1998**, San Diego, CA.

107. Odanaka, Y.; Tsuchiya, N.; Matano, O.; Goto, S. *J. Agric. Food Chem.* **1985**, 33, 757-763.

108. Zhang, W.; Cai, Y.; Yu, C.; Ma, L. Q. *Sci. Total Environ.* **2002**, 300, 167-177.

BIOGRAPHICAL SKETCH

Ruixue Chen was born on January 9, 1974 in Nanyang, China, to Yongzheng Chen and Zhiying Wang. Her family moved from Nanyang (north side of China) to Xiamen (south side of China) in 1986. She received her Bachelor of Science degree in chemistry in July 1995 from Xiamen University, China. After graduation, she worked in the Chinese Animal and Plant Quarantine Service in Xiamen from July 1995 to December 1998. She started graduate school at the University of Florida in January 1999 and joined Dr. James D. Winefordner's research group. She received her Doctor of Philosophy in analytical chemistry from University of Florida in May 2003. She married Chenglong Yang in 1997 and had a lovely son, Edward, in 2001.

I certify that I have read this study and that in my opinion it conforms to acceptable standards of scholarly presentation and is fully adequate, in scope and quality, as a dissertation for the degree of Doctor of Philosophy.

James D. Winefordner, Chairman
Graduate Research Professor of Chemistry

I certify that I have read this study and that in my opinion it conforms to acceptable standards of scholarly presentation and is fully adequate, in scope and quality, as a dissertation for the degree of Doctor of Philosophy.

Willard W. Harrison
Professor of Chemistry

I certify that I have read this study and that in my opinion it conforms to acceptable standards of scholarly presentation and is fully adequate, in scope and quality, as a dissertation for the degree of Doctor of Philosophy.

Weihong Tan
Associate Professor of Chemistry

I certify that I have read this study and that in my opinion it conforms to acceptable standards of scholarly presentation and is fully adequate, in scope and quality, as a dissertation for the degree of Doctor of Philosophy.

David E. Richardson
Professor of Chemistry

I certify that I have read this study and that in my opinion it conforms to acceptable standards of scholarly presentation and is fully adequate, in scope and quality, as a dissertation for the degree of Doctor of Philosophy.

Lena Q. Ma
Associate Professor of Soil and Water
Science

This dissertation was submitted to the Graduate Faculty of the Department of Chemistry in the College of Liberal Arts and Sciences and to the Graduate School and was accepted as partial fulfillment of the requirements for the degree of Doctor of Philosophy.

May 2003

Dean, Graduate School